

1

AD-A172 376

DTIC FILE COPY

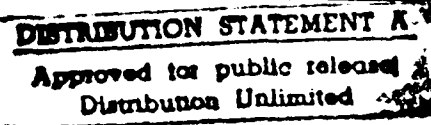


AN EXPERIMENTAL INVESTIGATION OF A CIRCULAR  
THRUST AUGMENTING EJECTOR  
THESIS

AFIT/GAE/AA/86M-3

Generoso C. Uhuad

Captain USAF



DTIC  
ELECTED  
OCT 2 1986

S D

DEPARTMENT OF THE AIR FORCE  
AIR UNIVERSITY  
**AIR FORCE INSTITUTE OF TECHNOLOGY**

Wright-Patterson Air Force Base, Ohio

86 10 01 210

AFIT/GAE/AA/86M-3

AN EXPERIMENTAL INVESTIGATION OF A CIRCULAR  
THRUST AUGMENTING EJECTOR  
THESIS

AFIT/GAE/AA/86M-3

Generoso C. Uhuad

Captain USAF

DTIC  
ELECTED  
OCT 2 1986  
S D  
B

Approved for public release; distribution unlimited

AFIT/GAE/AA/86M-3

AN EXPERIMENTAL INVESTIGATION OF A CIRCULAR  
THRUST AUGMENTING EJECTOR

THESIS

Presented to the Faculty of the School of Engineering of the  
Air Force Institute of Technology  
In Partial Fulfillment of the  
Requirements for the Degree of  
Master of Science

Generoso C. Uhuad, B.S. Engr  
Captain      U.S. Air Force

Graduate Aeronautical Engineering  
December 1985

Approved for public release; distribution unlimited

## PREFACE

The purpose of this investigation was to determine the effects of primary nozzle injection angle and height on the thrust augmentation of a 4.4 in diameter circular ejector. Also investigated were the effects of diffuser boundary layer control, inlet cross flow and alternating primary jet injection angles on thrust augmentation. This study was essentially a continuation of the works conducted in 1980 by Capt Reznick, USAF, in 1981 by Capt Unnever, USAF, and 1983 by Capt Lewis, U.S. Army.

I would like to acknowledge several individuals who provided valuable support, guidance, criticisms and assistance during the conduct of this study.

- Dr. M. Franke, my thesis advisor, for his guidance and encouragement.
- Dr. W. Elrod and Capt W. Cox, members of the Reading Committee.
- Messrs. N. Yardich, S. Coates, L. Cannon and H. Linnville for their tireless laboratory assistance.
- Mr Joseph Martin from the Flight Dynamics Laboratory, for his advice and technical assistance.
- Mr J. Tiffany from the AFIT Fabrication Shop for his suggestions and dedication to supporting the test article modifications.

My special thanks to my wife Cheryl, and sons Ryan and Randy, for their sacrifices and support during the conduct of this study.

Accession No.	<i>[Signature]</i>
NTIS GRAIL	
DTIC TAB	
Unannounced	
SAC/AFIT	
By	
PLS	
Approved	
Dist	
A-1	



## TABLE OF CONTENTS

	Page
Preface .....	i
Table of Contents .....	ii
List of Figures .....	iv
List of Tables .....	vii
List of Symbols .....	viii
Abstract .....	ix
I. Introduction .....	1
Background .....	1
Objectives .....	5
Scope of Experimental Work .....	6
II. Facility Description .....	7
III. Ejector Description .....	13
IV. Experimental Procedures .....	24
V. Results and Discussions .....	26
a. Baseline Verification .....	26
b. Effects of Injection Angle and Height .....	28
c. Effects of Alternating Nozzle Injection Angles ...	43
d. Effects of Diffuser Suction and Blowing .....	52
e. Effects of Inlet Cross Flow .....	65
f. Effects of Pt/Pa on Thrust Augmentation .....	76
VI. Conclusions .....	81
VII. Recommendations .....	83
VIII. Bibliography .....	84
IX. Appendix .....	85

X. Vita .....

89

## LIST OF FIGURES

Figure	Title	Page
1	Center Blowing Thrust Augmentor Ejector .....	3
2	Wall Blowing Thrust Augmentor Ejector .....	3
3	Ejector Test Stand .....	8
4	Automatic Data Acquisition System.....	10
5	Cross Flow Fan .....	11
6	Circular Ejector With Discrete Circumferential Nozzles .....	14
7	Ejector Cross Section .....	15
8	Nozzle Mounting System.....	16
9	Variable Height and Injection Angle.....	16
10	Variable Height-Constant Alpha Adjusting Method .....	19
11	Variable Alpha-Constant Height Adjusting Method .....	19
12	Nozzle Numbering System.....	20
13	Alternating Nozzle Arrangement .....	20
14	Diffuser Suction Hole Modification.....	22
15	Diffuser Blowing Hole Modification.....	23
16	Thrust Augmentation Ratio Verification.....	27
17	Effect of Nozzle Height on Thrust Augmentation (Nozzle Location 2) .....	29
18	Effect of Nozzle Height on Thrust Augmentation (Nozzle Location 3) .....	30
19	Effect of Nozzle Height on Exit Velocity Profile (Nozzle Location 2) .....	31

20	Effect of Nozzle Height on Three-Dimensional Exit Velocity .....	32
21	Effect of Nozzle Height on Mass Augmentation Ratio .....	36
22	Effect of Injection Angle on Thrust Augmentation (Location 2).....	37
23	Effect of Injection Angle on Exit Velocity Profile .....	38
24	Effect of Injection Angle on Three-Dimensional Exit Velocity .....	40
25	Comparison of Thrust Augmentation-Constant Nozzle Height vs Variable Nozzle Height and Injection Angle .....	41
26	Effect of Alternating Injection Angles on Thrust Augmentation (Location 2) .....	44
27	Effect of Alternating Injection Angles on Thrust Augmentation (Location 1) .....	45
28	Effect of Alternating Injection Angles on Three-Dimensional Exit Velocity .....	46
29	Effect of Alternating Injection Angles on Mass Augmentation .....	50
30	Effect of Rear Diffuser Suction on Thrust Augmentation .....	53
31	Effect of Front Diffuser Suction on Thrust Augmentation .....	54
32	Effect of Rear Diffuser Suction on Three- Dimensional Exit Velocity .....	55
33	Effect of Front Diffuser Suction on Three- Dimensional Exit Velocity .....	56

34	Effect of Rear Diffuser Suction on Three-Dimensional Exit Velocity (With Flow Separation).....	60
35	Effect of Diffuser Blowing on Thrust Augmentation .....	63
36	Effect of Diffuser Blowing on Exit Velocity Profiles.....	64
37	Cross Wind Velocity Profile.....	66
38	Cross Wind Effect on Thrust Augmentation .....	67
39	Cross Wind Effect on Exit Velocity Profile.....	68
40	Three-Dimensional Plot of Exit Velocity With Cross Wind.....	69
41	Velocity Profiles at the Inlet Exit Plane.....	71
42	Inlet Flow Deflector Plate.....	72
43	Effect of Deflector Plate on Thrust Augmentation.....	73
44	Effect of Deflector Plate on Exit Velocity Profiles.....	74
45	Effect of Pt/Pa on Thrust Augmentation Ratio (h = 0.25 in) .....	77
46	Effect of Nozzle Location on Exit Velocity Profile (Pt/Pa = 1.027).....	78
47	Effect of Nozzle Location on Mass Augmentation Ratio (Pt/Pa = 1.027).....	79
48	Effect of Nozzle Location on Three-Dimensional Exit Velocity (Pt/Pa = 1.027).....	80
A-1	Procedure for Varying Nozzle h at a Fixed Value of $\alpha$ .....	87
A-2	Procedure for Varying Nozzle $\alpha$ at a Fixed Value of h .....	88

LIST OF TABLES

Table Number	Title	Page
I	Summary of Nozzle Locations, Theta ( $\Theta$ ), Injection Angles and Heights .....	17

## LIST OF SYMBOLS

A	Area ( $\text{in}^2$ )
$A_0$	Primary Nozzle Area ( $\text{in}^2$ )
$A_1$	Inlet Area ( $\text{in}^2$ )
$A_2$	Mixing Chamber Cross Sectional Area ( $\text{in}^2$ )
$A_3$	Diffuser Exit Area ( $\text{in}^2$ )
$F_i$	Isentropic Thrust (lbf)
$F_m$	Measured Net Thrust (lbf)
h	Nozzle Height (in), Ref Figure 8
$h_p$	Nozzle Height at $\alpha_p$ (in)
M	Mass Augmentation Ratio
$\dot{m}_e$	Mass Flow Rate at the Ejector Exit Plane (lbm/sec)
$\dot{m}_1$	Primary Air Mass Flow Rate (lbm/sec)
$\dot{m}_2$	Secondary Air Mass Flow Rate (lbm/sec)
$\Phi$	Thrust Augmentation Ratio
$\Phi_p$	Peak Thrust Augmentation Ratio
$\Theta$	Primary Nozzle Exit Location (deg)
$\alpha$	Primary Nozzle Injection Angle (deg)
$\alpha_p$	Injection Angle Corresponding to the Peak Thrust Augmentation (deg)
$\alpha_o$	Injection Angle of Odd Numbered Nozzles (deg)
$\alpha_e$	Injection Angle of Even Numbered Nozzles (deg)
$\psi$	Deflector Plate Angle (deg)

## ABSTRACT

A 4.4 in diameter circular thrust augmentor ejector was tested to investigate the effects on thrust augmentation ratio of the primary nozzle injection angle and height, alternating primary jet injection angle, diffuser boundary layer control, inlet cross flow velocity and primary-nozzle-pressure-to-ambient-pressure ratio.

The results showed that the primary nozzle jet injection angle and height are both critical in the establishment of a smooth attached flow at the ejector inlet and both parameters influence the maximum thrust augmentation ratio. The use of alternating primary jet injection angles to enhance primary and secondary flow mixing did not increase the thrust augmentation ratio above that which was obtained using a uniform injection pattern. The lower thrust augmentation ratio was caused by the inability of the alternating jet arrangement to establish and maintain a smooth attached flow around the inlet.

For the diffuser geometry that was tested, diffuser boundary layer control using either blowing or suction, did not provide any improvement in thrust augmentation over the case without control. The results of the tests showed that the decrease in thrust augmentation ratio at injection angles slightly above or below the injection angle where maximum thrust augmentation ratio occurred was caused primarily by departures from the smooth attached flow at the inlet surface area and not due to flow separation emanating from the diffuser.

The presence of a small cross flow velocity component at the ejector inlet increased thrust augmentation and did not cause a diffuser stall. The cross flow improved mixing and also introduced asymmetry on the exit velocity profile. The addition of a deflector plate in front of the ejector inlet to modify the direction of the cross flow relative to the ejector centerline did not provide an advantage over the configuration without the deflector plate. The results

suggest that the increase in thrust augmentation caused by a small amount of cross flow may provide an advantage for V/STOL aircraft in a hovering mode.

Finally, at low primary nozzle exit velocities (low  $P_t/P_a$ ), the thrust and mass augmentation ratios increased as nozzle location was moved further out along the inlet surface. The lower primary jet velocities allowed the flow to turn along and remain attached to the curved inlet surface at higher nozzle locations (higher  $\Theta$ ). As a result, the effective mixing chamber length increased as nozzle location increased along the surface of the inlet thereby allowing an improvement in the flow mixing and thrust augmentation.

## I. INTRODUCTION

### BACKGROUND

Current interest in the design and development of aircraft with V/STOL capability continue to stimulate various studies on the methods of improving the performance, particularly the thrust available from existing turbofan and turbojet engines. The need to improve propulsion systems' thrust to weight ratios for V/STOL applications is dramatized by existing airplanes such as the AV-8A/B Harrier and other experimental designs which have limited range when compared to non-V/STOL capable aircraft of comparable take off gross weights. For the AV-8 aircraft, lift for vertical take off or landing is obtained by direct engine thrust vectoring, usually at high engine throttle settings which leads to high fuel consumption rates, thereby limiting operational radius or endurance.

One method of increasing available thrust from a jet engine is through thrust augmentation utilizing thrust augmenting ejectors. This method provides considerable promise of improving V/STOL aircraft range and endurance when effectively integrated in the design by reducing the fuel weight fraction required during the transition and hovering phases of the flight. Two distinct approaches to the utilization of ejectors exist. The first approach is to use high aspect ratio low thrust performance ejectors for lift enhancement by inducing supercirculation around lifting surfaces such as wings. The second approach is to augment the thrust available from the propulsive unit directly through a viscous interaction between the primary jet exhaust and the surrounding air and vectoring the thrust to generate a vertical component that can be used to augment the wing lift.

A typical ejector is shown in Figure 1. It consists of a primary nozzle and a shroud surrounding the primary nozzle. The shroud consists

of an inlet or a bellmouth, a constant area mixing duct and a diffuser section. The primary nozzle is used to inject a low mass high velocity jet into the mixing chamber and induce thrust augmentation through a turbulent mixing of the primary air with the entrained secondary air. The mixing process results in the flow in the ejector exit plane of low momentum air with considerably higher mass flow rate than the primary air flow rate. The effect is similar to that of a high by-pass ratio turbofan engine where a large flow of low momentum air is used to generate considerably higher thrust than a turbojet engine. The mixing and entrainment process also causes a static pressure change on the shroud inner walls which generates a net lip thrust. In aircraft applications, the primary jet may be provided by the engine compressor bleed air or by the hot exhaust gases.

Numerous investigations have been conducted on ejectors since the publication of Von Karman's classical paper on the subject (Ref 4). Studies have been conducted on the effect on thrust and mass augmentation of ejector shroud geometric parameters such as diffuser area ratio, primary nozzle to exit area ratio, inlet area ratio, mixing chamber length, for both rectangular and circular configurations. Figure 2 illustrates a wall blowing ejector. This method relies on the establishment of a smooth attached flow on the inlet surface and the remainder of the diffuser wall to form the favorable pressure distribution that is essential in the generation of the net lip thrust that augments the primary nozzle thrust. Alperin and Wu (Ref 8) reported augmentation ratios as high as 2.0 for two-dimensional ejectors with primary air blowing near the inlet walls. Reznick and Franke (Ref 2) extended the concept of wall blowing to circular ejectors and reported augmentation ratios as high as 2.07 utilizing "hook" type discrete circumferential nozzles.

Bevilaqua (Ref 6) investigated hypermixing nozzles in a two-dimensional center blowing ejector and reported improvements in thrust augmentation (2.0)

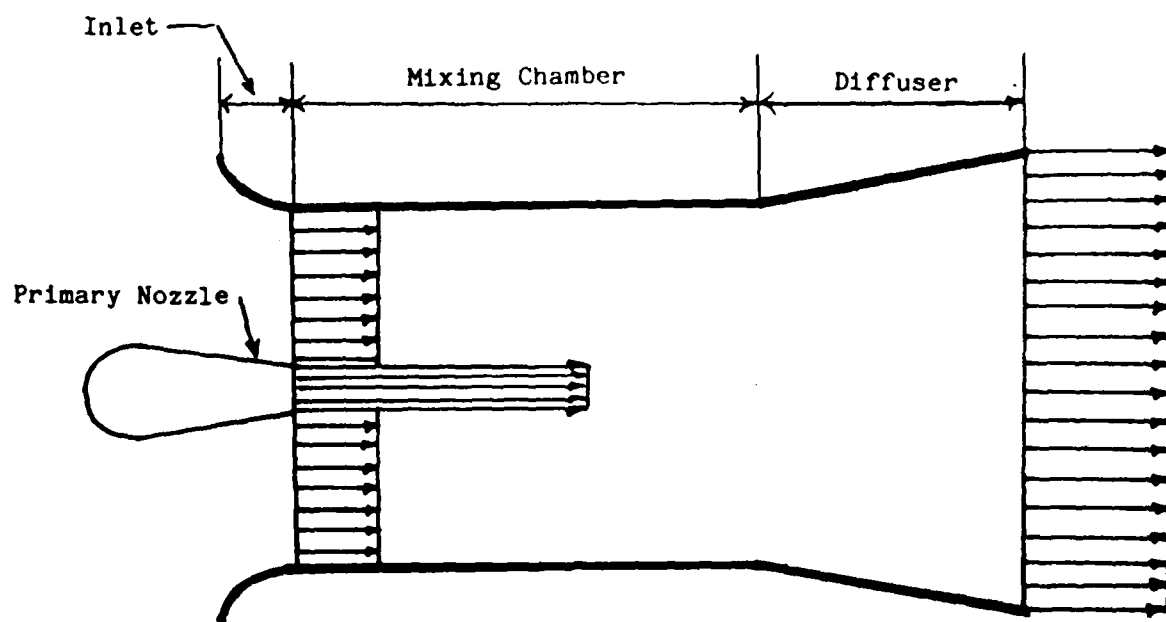


Figure 1 . Center Blowing Thrust Augmentor Ejector

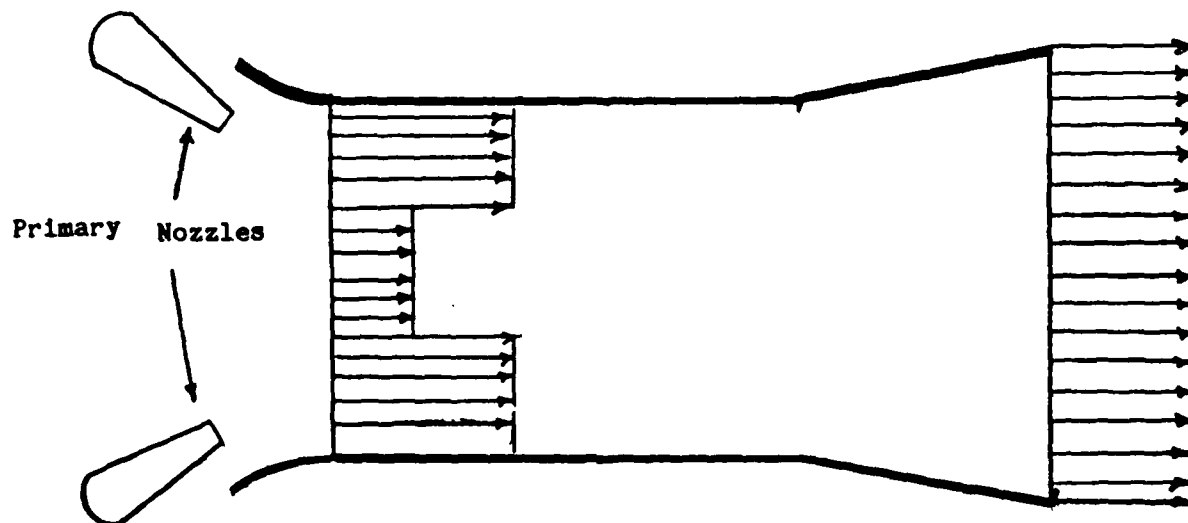


Figure 2 . Wall Blowing Thrust Augmentor Ejector

and mass augmentation. A hypermixing nozzle consists of a series of small discrete nozzles with alternating angles of blowing. This blowing pattern induces the formation of streamwise vortices emanating from the adjoining sides of the nozzles. The vortices enhance turbulence and encourage a more complete mixing in the mixing chamber and diffuser sections, creating a more uniform exit flow thereby improving thrust and mass augmentation. With uniform flow forming early upstream of the diffuser exit plane, the diffuser length can be shortened, resulting in savings in the ejector weight. In Ref 2 and 3, various primary jet flow patterns using various nozzle configurations and combinations thereof to enhance mixing and thrust augmentation for circular ejectors were investigated. The results showed lower thrust augmentation ratios relative to that obtained using discrete circumferential nozzles with uniform injection angles. It was concluded that nozzle modifications that are made to improve flow mixing which also introduce protruberances to the flow and increase the nozzle wetted perimeter will negate gains made in thrust augmentation due to an accompanying increase in drag losses.

## OBJECTIVES

The goal of this study was to continue the investigations conducted in Ref 1, 2 and 3 on the various parameters affecting the thrust augmentation of a circular ejector. Of specific interest were the development of a detailed understanding of the relationships between primary jet injection angle and nozzle height to thrust augmentation ratio, the inlet flow mechanism affecting the maximum thrust augmentation ratio and the decrease of thrust augmentation below the maximum value. Also investigated were the effectiveness of boundary layer control in the diffuser section in maintaining a high thrust augmentation, the effect of a hypermixing primary jet pattern on thrust augmentation, the sensitivity of the ejector device to inlet cross flow and the effect of nozzle location on thrust augmentation. The specific objectives of this study were as follows:

1. Determine the independent effects of primary nozzle injection angle and height on thrust and mass augmentation.
2. Determine the effect of an alternating primary jet injection pattern on thrust and mass augmentation.
3. Determine the effectiveness of diffuser blowing and suction in maintaining a high thrust augmentation.
4. Examine the effect of a cross flow component of velocity at the inlet face on thrust augmentation.
5. Determine the effect of primary-nozzle-pressure-to-ambient-pressure ratio on thrust and mass augmentation.

## SCOPE OF EXPERIMENTAL WORK

An existing 4.4 inch diameter circular ejector with eight discrete "hook" type circumferential nozzles blowing near the inlet wall was tested in an automated thrust augmentor test facility. The locations of the eight primary nozzles as well as their injection angles and heights were varied to determine the configuration that provided the highest thrust augmentation and improved mixing.

Diffuser wall blowing and suction were investigated by modifying the diffuser to provide plenum chambers and blowing and suction holes at two diffuser locations. Wall suction was first examined using suction holes distributed circumferentially at two locations along the diffuser wall. Blowing effects were studied utilizing tangential blowing holes distributed circumferentially near the diffuser exit plane.

The effect of crosswind on thrust augmentation was examined by using a constant-speed fan located in front of and below the ejector inlet. The fan provided the freestream velocity entering the inlet with a component perpendicular to the ejector centerline. An inlet flow deflector plate was also used to vary the direction of the cross flow relative to the centerline.

Data on net thrust, exit velocity profiles, thrust and mass augmentation ratios were acquired and reduced using the AFIT thrust augmentor test rig.

## II. FACILITY DESCRIPTION

The test was conducted using a thrust augmentor test stand which was developed (Ref 1) in order to automate the acquisition and processing of ejector test data. The system was very flexible and was designed to allow a rapid investigation of various parameters affecting ejector performance. The system consisted of the ejector test stand, pendulum, test article and the system instrumentation which included the transducers and their interface equipment and the Data Acquisition System(HP 3052A). A detailed description of the test facility is provided in Ref 1 and is briefly summarized in this section.

Figure 3 shows the ejector test stand with the pendulum and the ejector apparatus. The stand consisted of three vertical I beam legs bolted to the floor for rigidity and to damp out vibrations which may affect ejector operation. Two of the adjacent legs were connected by a cross beam. A calibrated horizontal slide connected the center of the cross beam to the third rear upright. The horizontal slide was graduated and was used to index the position of the exit velocity probe drive system frame which was adjusted manually, depending on the requirements of the test. The slide also provided a mounting point for the exit probe total pressure transducer.

Figure 3 also shows the Tee pendulum and ejector combination. The pendulum hangs between two vertical column members mounted on top of the two adjacent uprights. The Tee was held in place by bearings and was free to rotate on a plane parallel to the axis of the horizontal slide. The ejector apparatus was attached to the bottom of the pendulum. The pendulum was fabricated from a 4 in diameter steel pipe and was used to supply the primary air flow from the 100 psi supply line to the 8 primary nozzles mounted on the ejector inlet. An L section beam, mounted horizontally, connected the two

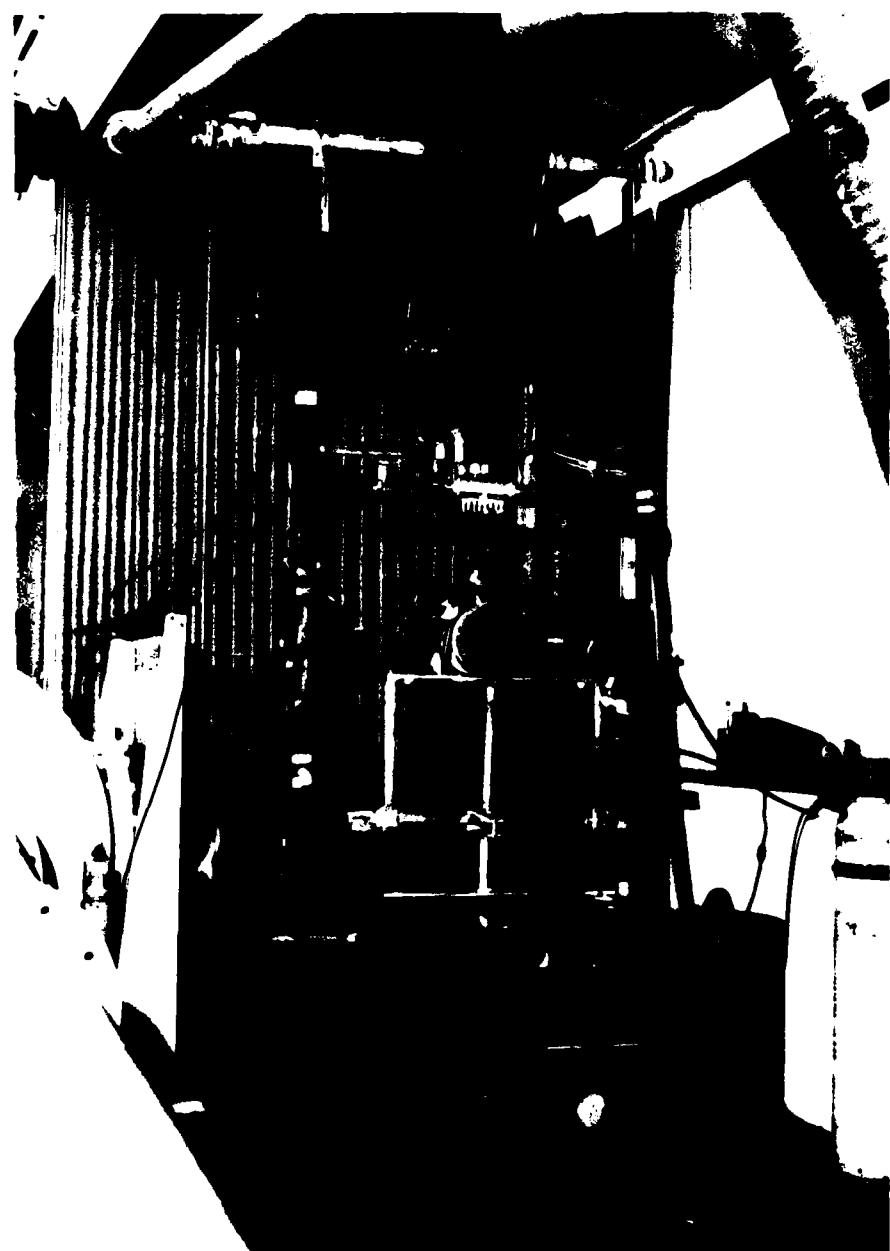


Figure 2. Ejector Test Stand

vertical column members above the ejector attachment point. The cantilever load cell used to measure thrust was bolted to the cross member. On the pendulum Tee, upstream of the bearing location, a dome valve was installed in the primary air supply line to facilitate the fine adjustment of the primary pressure in the nozzles. It also allowed a rapid and convenient shut off point for the primary air supply. On the vertical section of the pendulum Tee, midway between the ejector and the top, a flowmeter using an orifice with pipe flange taps was installed. A pressure transducer was installed upstream of the orifice to measure the orifice inlet static pressure. A differential transducer installed across the flange measured the pressure drop across the orifice. Both pressure data were used to calculate the mass flow according to the method recommended in Ref 9.

A detailed description of the system transducers and their interfaces and the transducer calibration process is provided in Ref 1. The Automatic Data Acquisition System shown in Figure 4 was the heart of the ejector test system. It included the table top computer (HP 9845), two floppy disk drives (HP 9885M), an automatic channel scanner (HP 709) and a digital voltmeter (HP 3455A). It was responsible for controlling all of the utility and operating software required to coordinate the operation of the exit plane drive system, scanivalve positioner, pressure transducers and the load cell. The automatic scanner was controlled and reconfigured internally by the computer and was used to select the appropriate channel to be monitored. The digital voltmeter displayed the input and output voltages of the selected channel.

For the cross flow test, a single speed fan mounted on a pedestal was installed in front of and below the ejector centerline, Figure 5. The direction of blowing was perpendicular to the ejector centerline.

In this study, the same pressure transducers used in Ref 1 were utilized



Figure 4. Automatic Arts Acquisition System

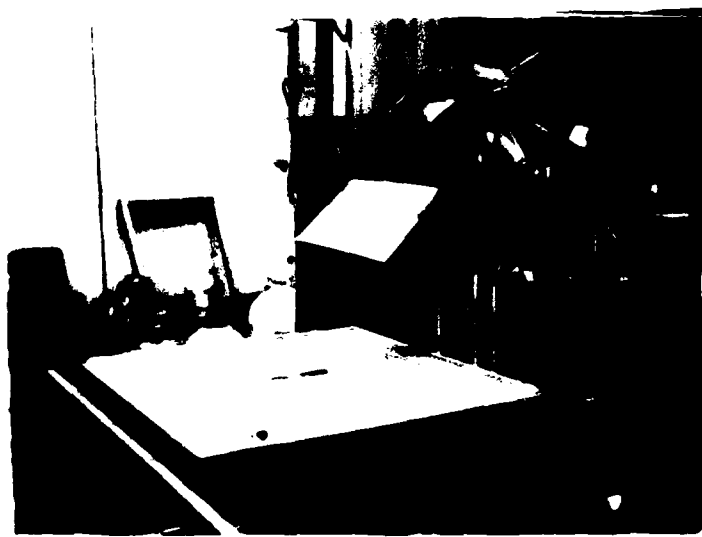


Figure 5. Cross Flow Fan

with the exception that the ambient pressure transducer data were not used in the data reduction process and that the scanivalve used to measure the 8 primary nozzle total pressures was used as a single channel pressure transducer. The ambient pressure transducer was located in the control room and did not represent the true ambient pressure condition in the vicinity of the ejector. The barometric pressure readings obtained using the mercury barometer were used in the data reduction process.

### III. EJECTOR DESCRIPTION

The circular ejector with the eight discrete circumferential nozzles, Figure 6, selected for this experiment was tested by Lewis, Unnever and Reznick (Ref 1, 2 and 3 respectively) and was found to provide the highest thrust augmentation compared to the other nozzle configurations that were tested. Figure 7 shows a sketch of the ejector cross section. The inlet diameter was 4.0 in. The diffuser section consisted of two conic sections that were separated by flanges provided at the ends of each section. The diffuser geometry remained fixed throughout the study while the primary nozzle parameters were varied. The diffuser area ratio,  $A_3/A_2$ , was 1.88 and the primary nozzle area ratio,  $A_2/A_0$ , was 32. The eight discrete circumferential nozzles were similar to those tested in Ref 1 and 2. Each nozzle was attached to the inlet through a special bracket, Figure 8, designed to permit an adjustment in the nozzle location, injection angle and height. The injection angle,  $\alpha$ , was measured between the primary jet and the ejector centerline. Nozzle height,  $h$ , was measured as the vertical distance between the nozzle chin and the inlet surface. Nozzle location on the bracket was defined as the location of the front nozzle leg pivot point. The angle,  $\Theta$ , was measured between a line perpendicular to the ejector centerline (passing through the inlet center) and a line connecting the nozzle exit with the inlet center.

The injection angle was varied in large increments by changing the nozzle location. Small changes in  $\alpha$  and  $h$  were made by pivoting the nozzle about the front leg pivot point. To obtain the desired value of  $\alpha$ , the nozzle height was adjusted to a value corresponding to the desired angle using an appropriate feeler gage. The nozzle locations, chin heights and the corresponding injection angles are summarized in Table I. In the front leg pivoting method of varying the injection angle, a small change in  $\alpha$  was usually accompanied by a small change in  $h$  as shown in Figure 9. This

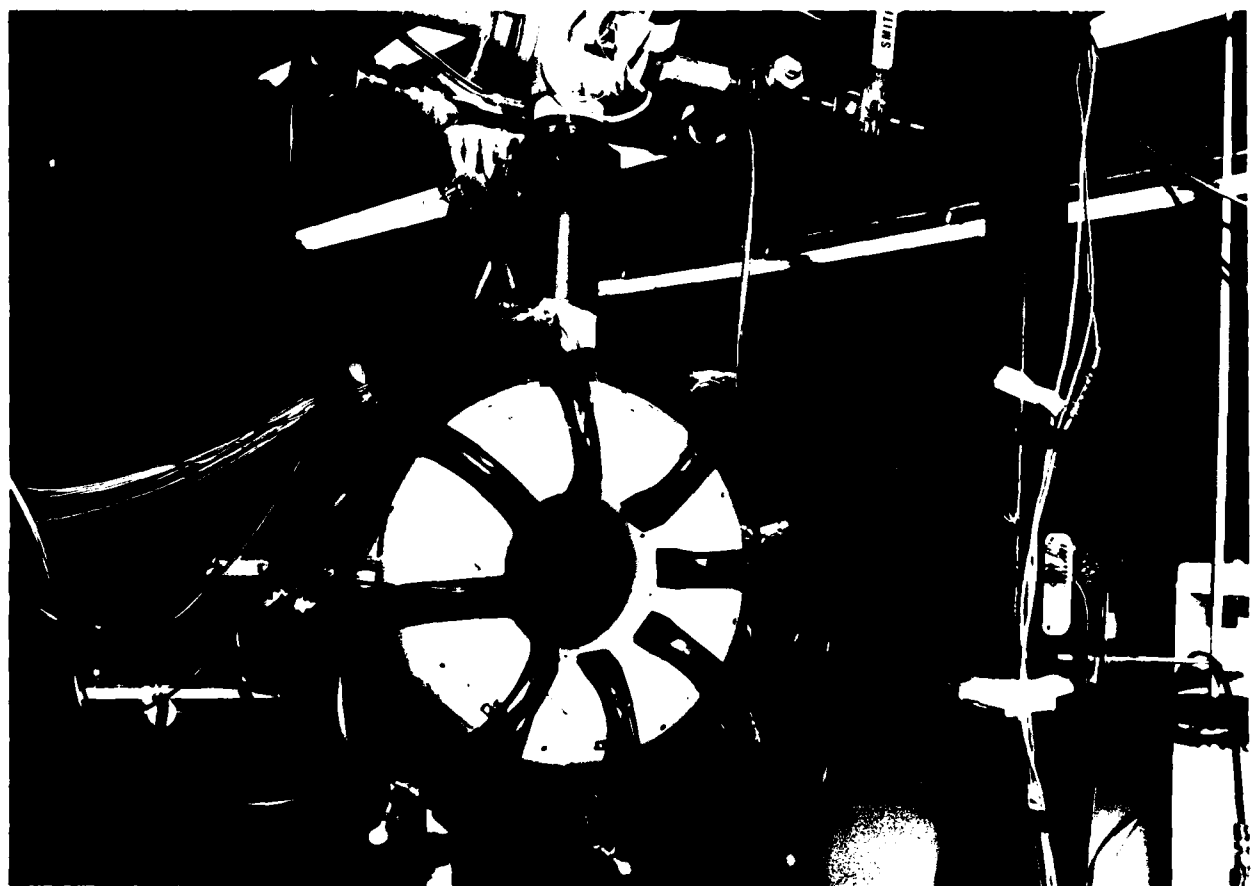


Figure 6. Circular Injector With Linear-to-Circumferential Load.

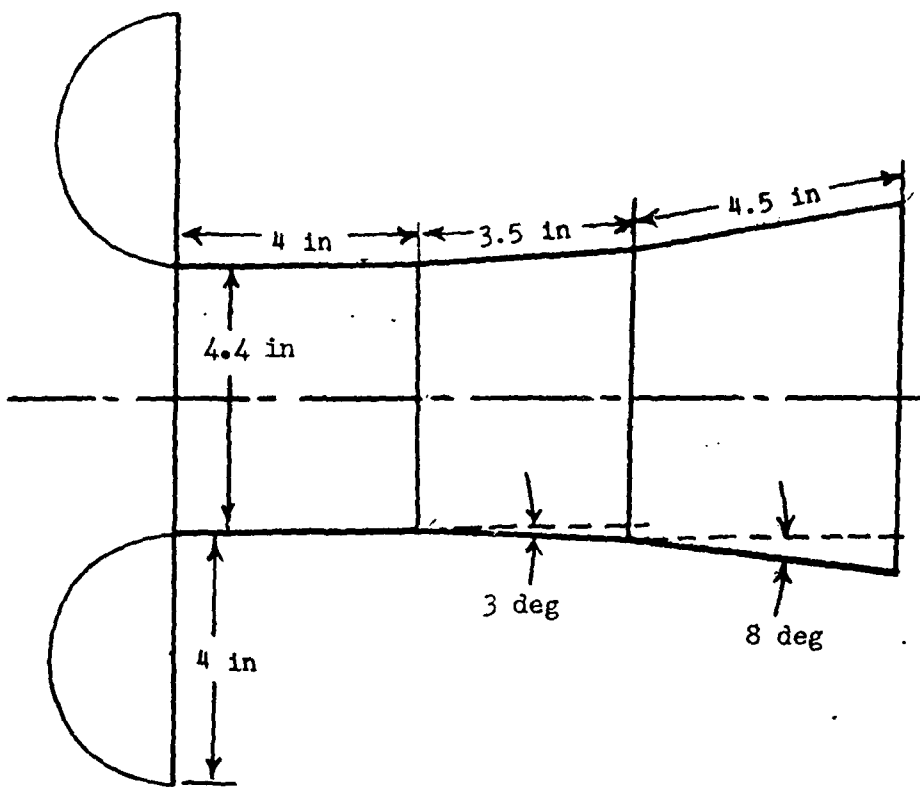


Figure 7. Ejector Cross Section

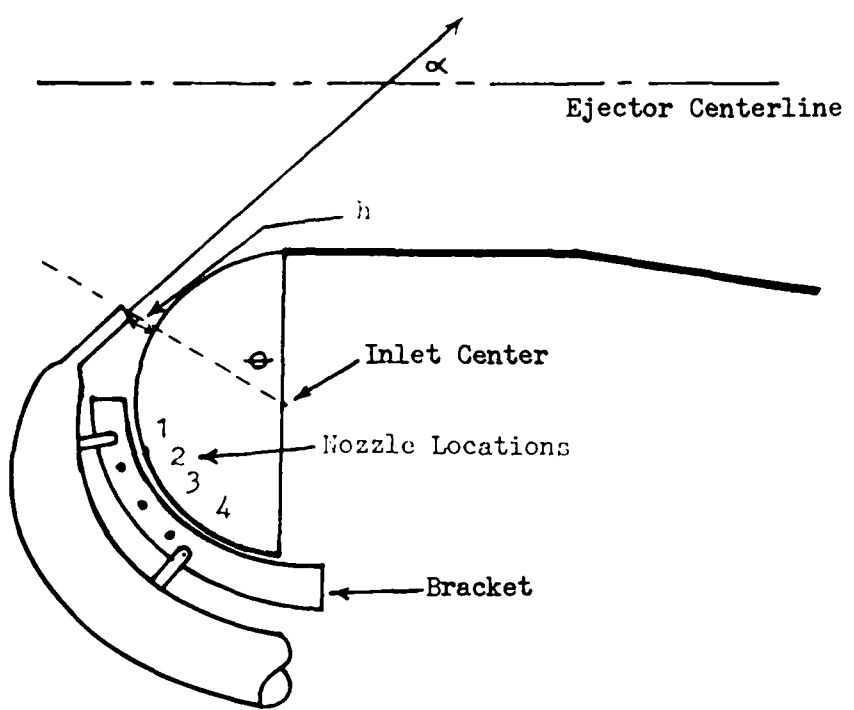


Figure 8. Nozzle Mounting System

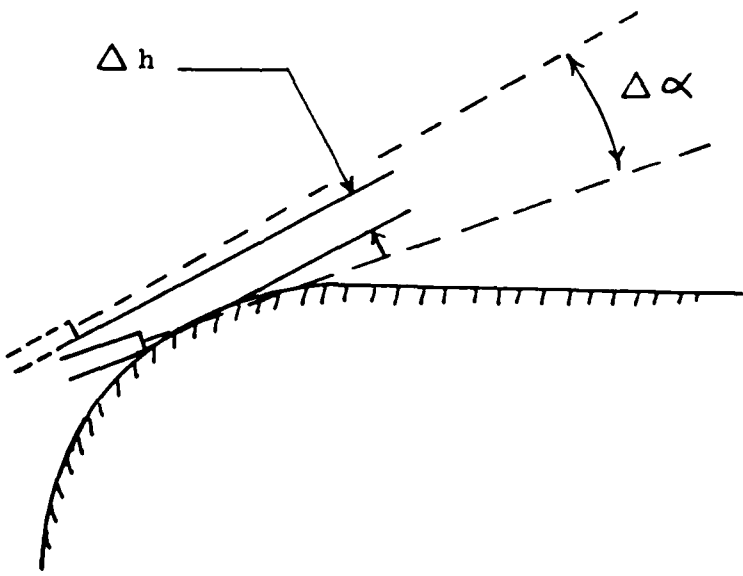


Figure 9. Variable Height and Injection Angle

Table I. Summary of Nozzle Location, Theta ( $\Theta$ ), Injection Angle ( $\alpha$ ) and Height (h)

	Location 1	Location 2	Location 3	Location 4
	$\Theta = 30$ deg	$\Theta = 41$ deg	$\Theta = 56$ deg	$\Theta = 71$ deg
Height (in)	Injection Angle (deg)			
0.000	13	25	38	52
0.063	14	26	39	53
0.125	16	27	40	54
0.188	17	29	42	56
0.250	20	32	45	59
0.313	21	34	46	60

technique of varying  $\alpha$  was used in Ref 1 and 2 and the results showed the combined effects of height and injection angle on thrust augmentation ratio. This approach was quite satisfactory in the investigations of ejector shroud geometric parameters such as area ratios, diffusion angles, etc, where the injection angles were kept constant while the shroud geometric parameters were varied.

In order to study the independent effects of nozzle height and injection angle on thrust augmentation, a deviation from the pivot method of varying the injection angle was necessary. Figure 10 illustrates a typical template used to vary  $h$  while keeping the value of  $\alpha$  and nozzle location fixed. The template edge along the constant  $\Theta$  line was marked in 0.125 in increments. The constant  $\alpha$  lines (parallel lines), scribed on the template starting on the constant  $\Theta$  edge represented the primary jet direction at various values of  $h$ .

The same type of templates used in the constant  $\alpha$ -variable  $h$  tests were used in the constant  $h$ -variable  $\alpha$  tests. As shown in Figure 11, at a fixed value of  $h$ , radial lines corresponding to different values of  $\alpha$  were scribed on the template. The radial lines were used as a guide to fix the direction of the primary jet and were varied at 5 deg increments. Except for the constant  $\alpha$ -variable  $h$  and constant  $h$ -variable  $\alpha$  experiments, all of the remaining experiments in this study were conducted using the front leg pivoting method of adjusting  $\alpha$ . A detailed description of the procedures used to set the primary nozzle height at a fixed  $\alpha$  or the injection angle at a fixed  $h$  is provided in the Appendix.

For the alternating injection angle test, the nozzle numbering system shown in Figure 12 was used. Figure 13 shows an illustration of the nozzles distributed around the primary nozzle exit plane. In this arrangement, all even numbered nozzles were fixed at one injection angle while those of the odd numbered nozzles were varied. This allowed the formation of an alternating jet

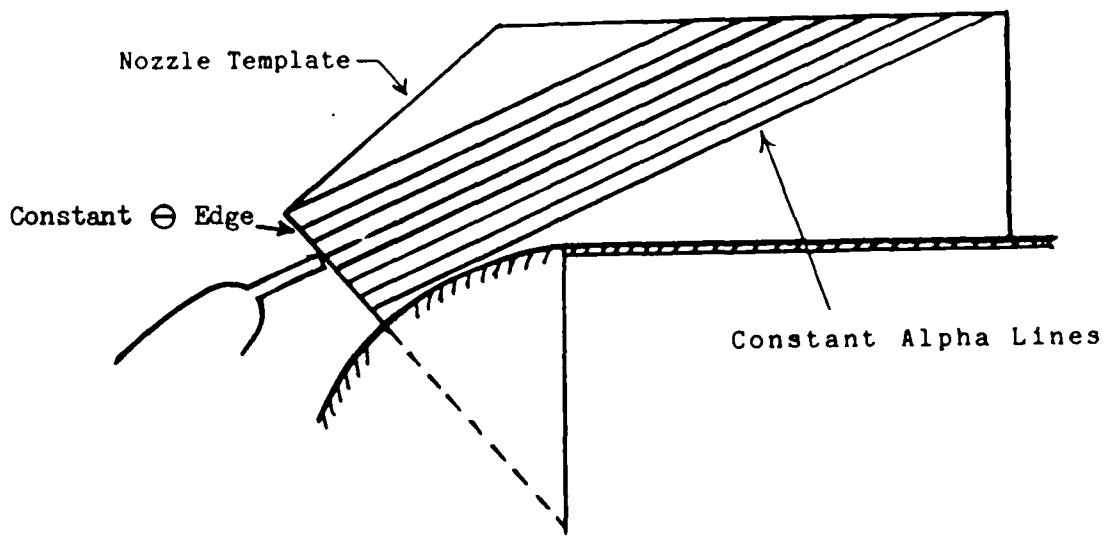


Figure 10. Variable Height, Constant Alpha Adjusting Method

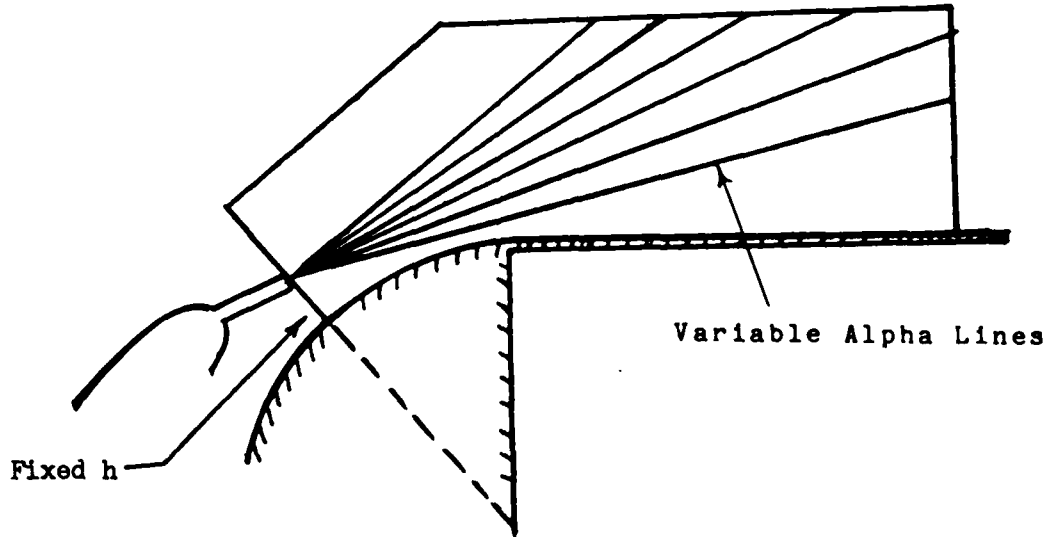
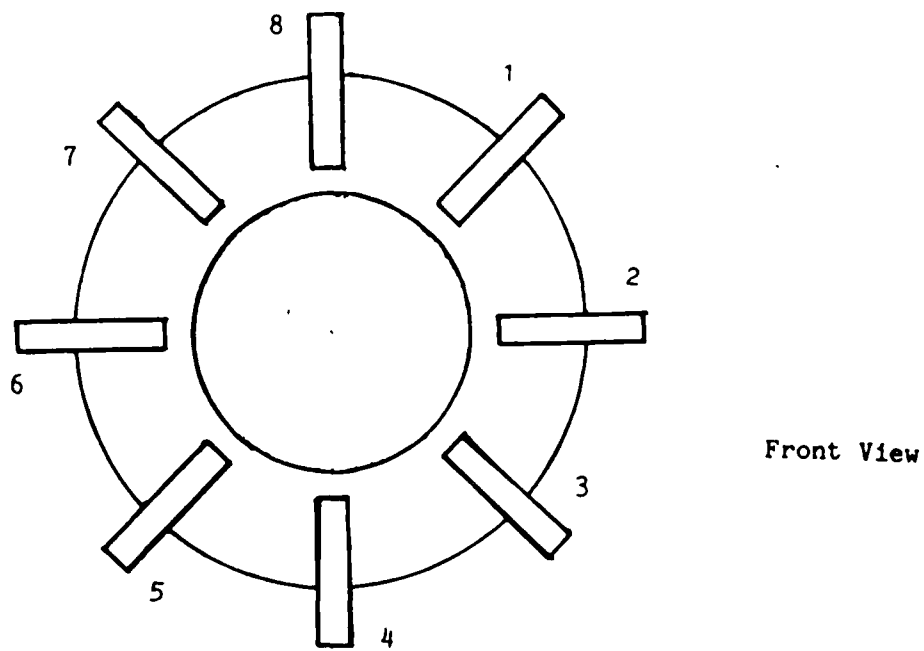
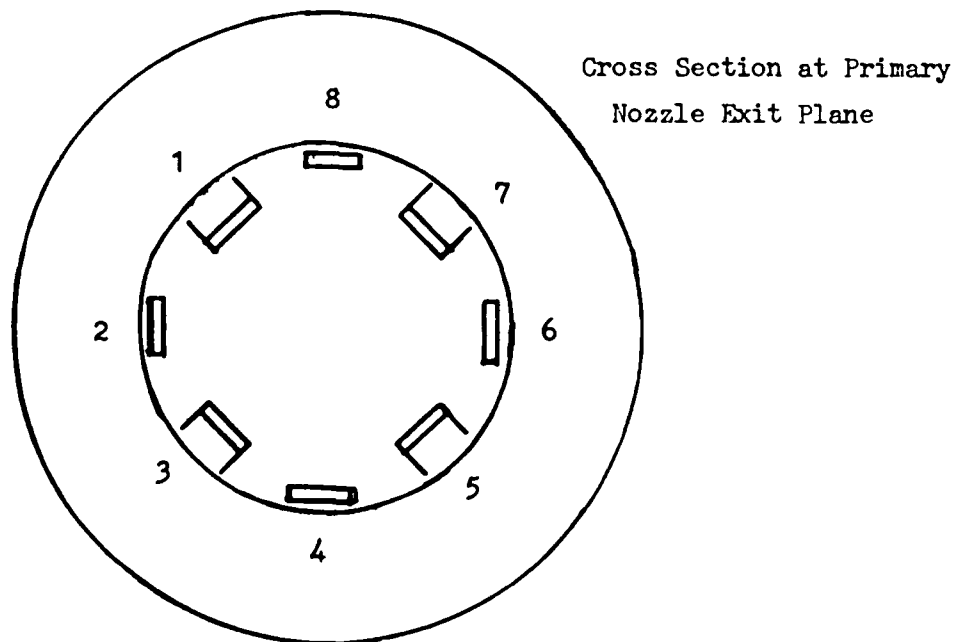


Figure 11. Variable Alpha-Constant Height Adjusting Method



Front View

Figure 12. Nozzle Numbering System



Cross Section at Primary  
Nozzle Exit Plane

Figure 13. Alternating Nozzle Arrangement

in the vicinity of the inlet and mixing chamber without an increase in the nozzle wetted perimeter.

For the diffuser boundary layer test, the diffuser sections were modified to provide two plenum chambers that were used to channel air circumferentially around the diffuser for blowing or suction. The modifications are illustrated in Figure 14. Two sets of holes were provided for the suction experiments. The front and rear sets were located 7.75 in and 4.25 in from the diffuser exit plane respectively. For the blowing test, the rear suction holes were sealed and blowing holes distributed circumferentially around the inner wall were drilled along a perimeter located approximately 4 in from the ejector exit plane. Figure 15 shows the modifications made on the rear diffuser section for the blowing experiments. A detailed discussion of the blowing and suction hole dimensions are provided in the Appendix.

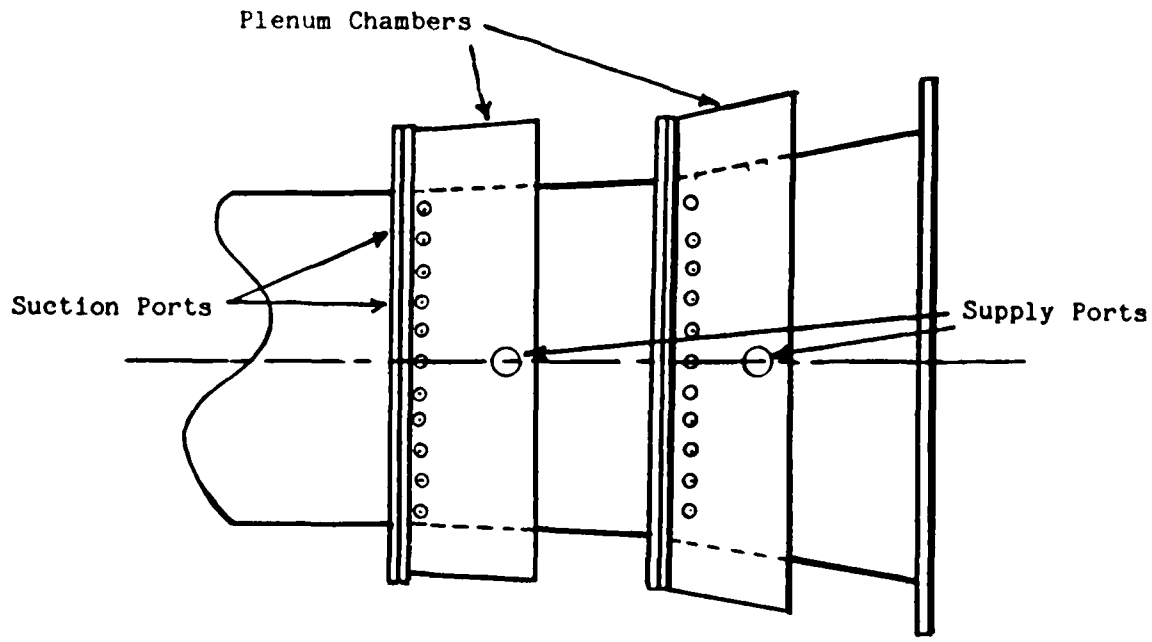


Figure 14. Diffuser Suction Hole Modification

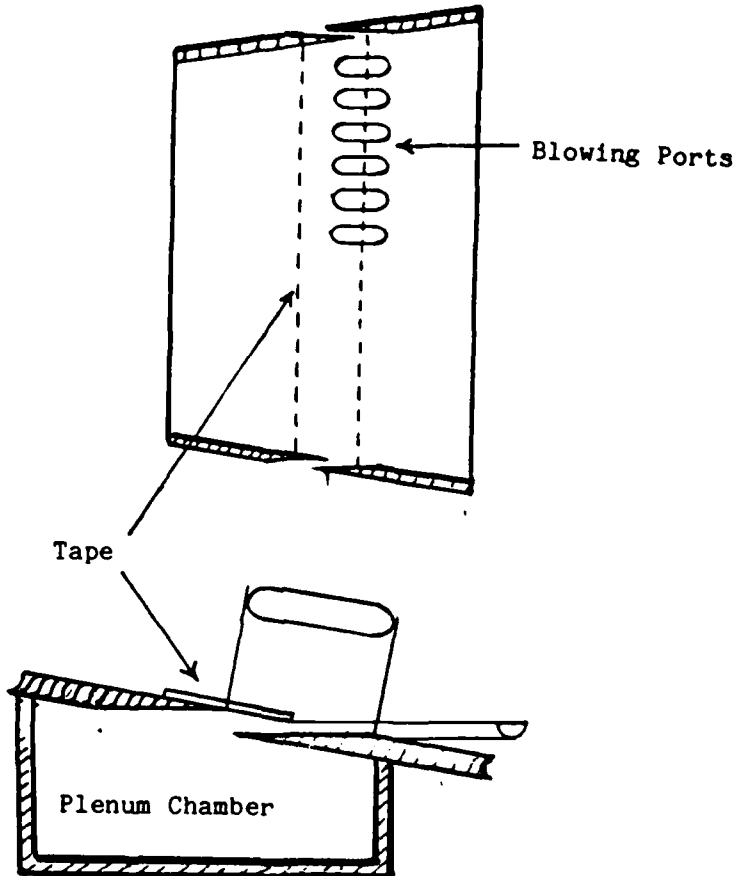


Figure 15. Diffuser Blowing Hole Modification

#### IV. EXPERIMENTAL PROCEDURES

Thrust augmentation ratio was calculated using the relation:

$$\Phi = F_m / F_i \quad (1)$$

where  $F_m$  is the net thrust measured by the cantilever load cell and  $F_i$  is the isentropic thrust. The isentropic thrust of the eight primary nozzles was calculated from the relation:

$$F_i = 7 A Pa ((P_t/P_a)^{285} - 1) \quad (2)$$

where  $P_a$  is the ambient pressure,  $P_t$  is the total pressure in the primary nozzles and  $A$  is the cross sectional area of the nozzles. Equation 2 is a measure of the ideal performance of the primary nozzles when allowed to discharge to ambient pressure conditions in the absence of the ejector shroud. In this study, the primary nozzle total-pressure-to-ambient-pressure ratio was equal to or less than 1.14. At this low ratios, the primary nozzle total pressure was approximately equal to the static pressure. This same ratio was used in Ref 1 and was found to introduce errors of no more than 1% of the isentropic thrust.

Mass augmentation ratio was calculated using the relation:

$$M = \dot{m}_2 / \dot{m}_1 \quad (3)$$

$$\dot{m}_2 = \dot{m}_e - \dot{m}_1 \quad (4)$$

where  $\dot{m}_e$  is the total mass flow rate at the diffuser exit,  $\dot{m}_2$  is the secondary mass flow rate and  $\dot{m}_1$  is the primary mass flow rate, measured using the

flowmeter with a 1 in diameter orifice described in Ref 1.

For tests where three-dimensional exit velocity distributions were measured, mass flow at the diffuser exit plane was measured using the relation:

$$\dot{m}_e = \rho \sum A_i V_i \quad (5)$$

where  $A_i$  is the area of an element of the exit plane grid and  $V_i$  is the velocity measured at the element. The maximum measured velocity at the diffuser exit was approximately 125 fps. Flow was assumed incompressible and density was calculated using the measured values of ambient temperature and pressure.

For short tests where the full three-dimensional exit velocity plots were not obtained,  $\dot{m}_e$  was calculated using the approximation used in Ref 1. In this procedure, the exit plane was divided into 6 annuli. A two-dimensional velocity distribution was measured along a vertical line passing through the center of the diffuser exit area. The two values of velocity corresponding to a particular annulus were averaged and assumed constant throughout that area. Mass flow through the annulus was then computed. The total mass flow at the exit plane was the summation of the calculated mass flow through the 6 annuli.

## V. RESULTS AND DISCUSSIONS

### a. Baseline Verification

In order to validate the data obtained in this study and to establish a baseline against which the results of the primary nozzle parameter variation tests can be compared, some initial tests were conducted to duplicate the configuration and test conditions used in Ref 3. The results are shown in Figure 16 which shows a comparison of the effect of injection angle on thrust augmentation ratio. The results were generally in agreement. The trend in the curves were similar in that peaks in thrust augmentation ratio occurred at certain values of  $\alpha$ . For a given nozzle location, augmentation ratio increased as  $\alpha$  was varied up to  $\alpha_p$ . Beyond  $\alpha_p$ , a further increase in  $\alpha$  resulted in a decrease in thrust augmentation. Also, the values of  $\phi_p$  decreased as the nozzle location was moved further out on the inlet surface ( $\Theta$  increased).

Similar trends in  $\phi$  have been reported by other investigators. The differences in  $\alpha_p$  and the values of  $\phi_p$  are attributed to differences in test technique and instrumentation. Also, the nozzles tested in Ref 3 had the brackets located at a slightly different point ( $\Theta = 6$  deg less) than those tested in this study. As a result, the injection angles where the peak thrust augmentation ratios were occurring were generally lower than those obtained in this study.

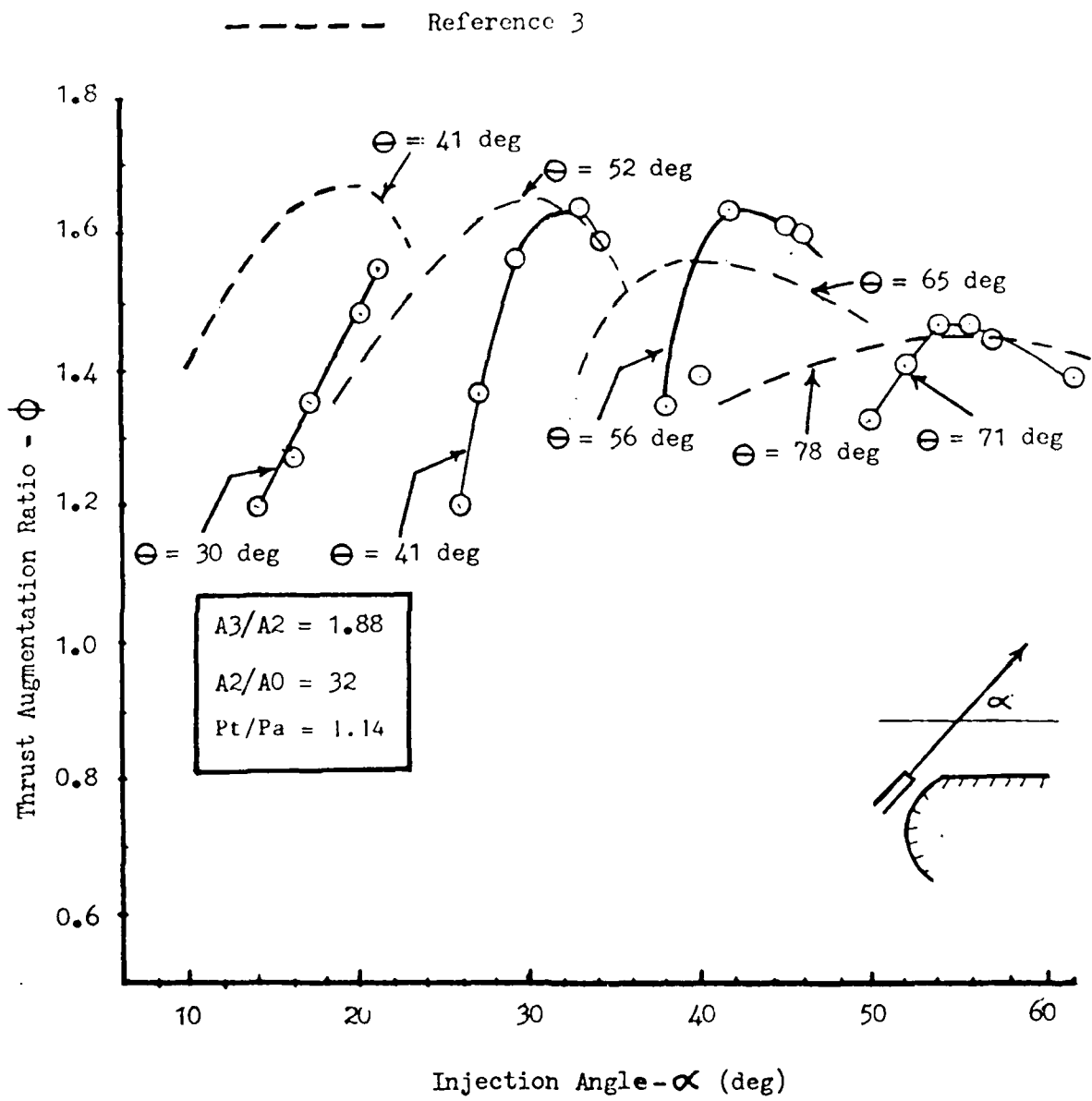


Figure 16. Thrust Augmentation Ratio Verification

b. Effect of Nozzle Height and Injection Angle

This experiment concentrated on the determination of the separate effects of the primary nozzle injection angle and height on thrust augmentation by varying the primary nozzle injection angle independently from the height. The results are discussed in the following paragraphs.

Height Effect

Figure 17 shows the effect of  $h$  on  $\Phi$  at  $\alpha = 25$  deg and  $\Theta = 41$  deg. Thrust augmentation ratio increased as  $h$  increased from 0.125 in to 0.375 in. Peak augmentation occurred at 0.375 in. Beyond this height,  $\Phi$  began to gradually decrease as height was increased up to 0.875 in. An injection angle of 25 deg was initially chosen to ensure that the test was conducted away from the very sensitive peak thrust augmentation region noted in Figure 16.

Figure 18 shows the effect of  $h$  on  $\Phi$  at  $\Theta = 56$  deg and  $\alpha = 41$  deg. Again, the trend was similar to that shown in Figure 17. Figure 19 shows a comparison of the exit velocity profiles for 3 injection heights (0.125, 0.375 and 0.875 in) and  $\Theta = 41$  deg. The profiles for  $h = 0.125$  in and 0.375 in showed high velocities near the wall. The peak velocity for  $h = 0.125$  in was slightly higher than that at 0.375 in and both profiles exhibited no wall separation. An improvement in the mixing also occurred as the height was increased to 0.375 in as evidenced by the disappearance of the low velocity region at the center. The profile for  $h = 0.875$  in had a high peak velocity at the center and separation was beginning to occur at the wall.

Figures 20A to 20E show the three dimensional plots of the exit velocities at various primary nozzle heights. At  $h = 0.125$  in, the plot had a deep cup shaped profile with thin high walls, which confirmed the existence of high velocities near the diffuser wall. At  $h = 0.375$  in, the peak wall velocities were slightly lower and the low velocity region near the center began to

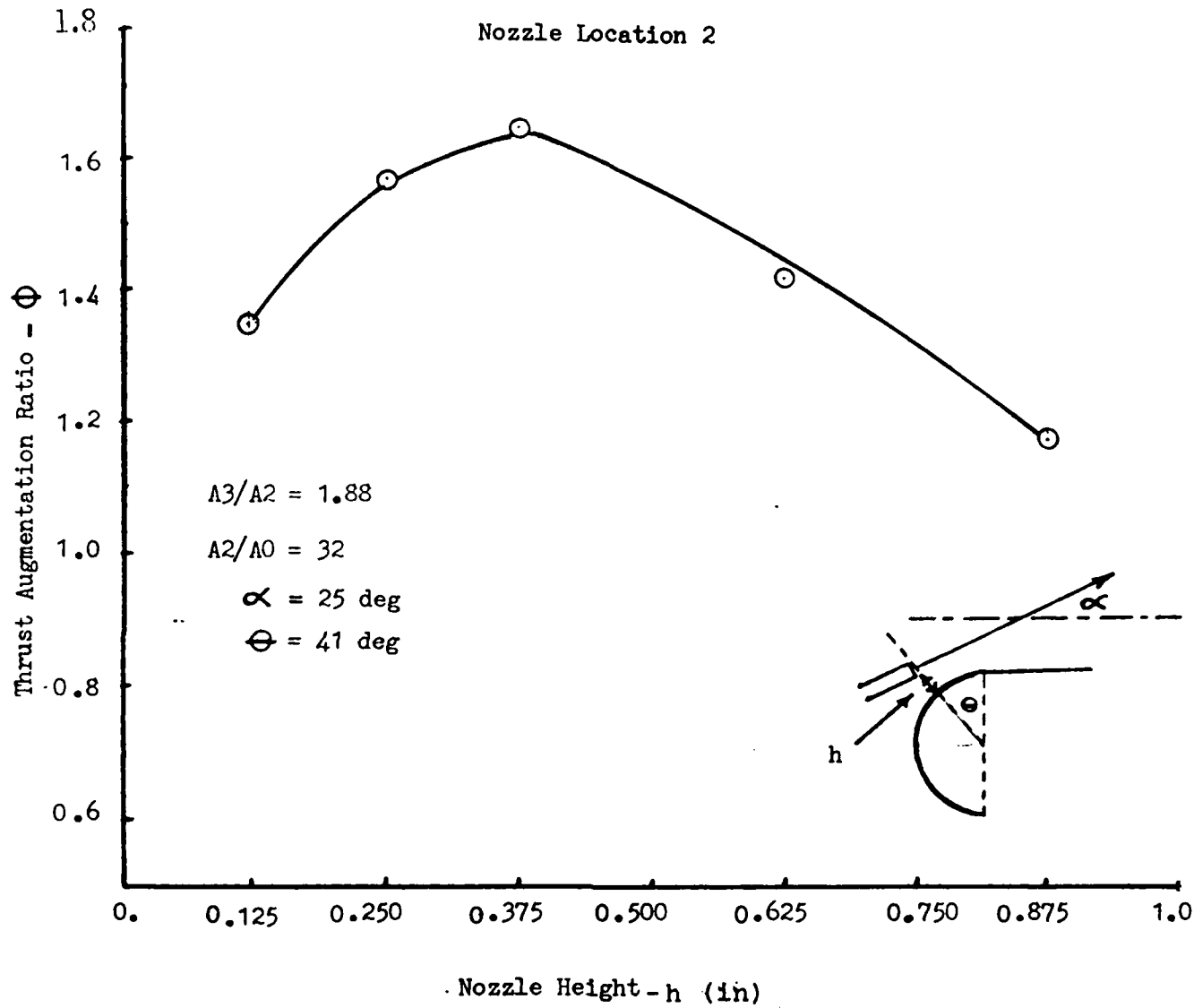


Figure 17. Effect of Nozzle Height on Thrust Augmentation (Location 2)

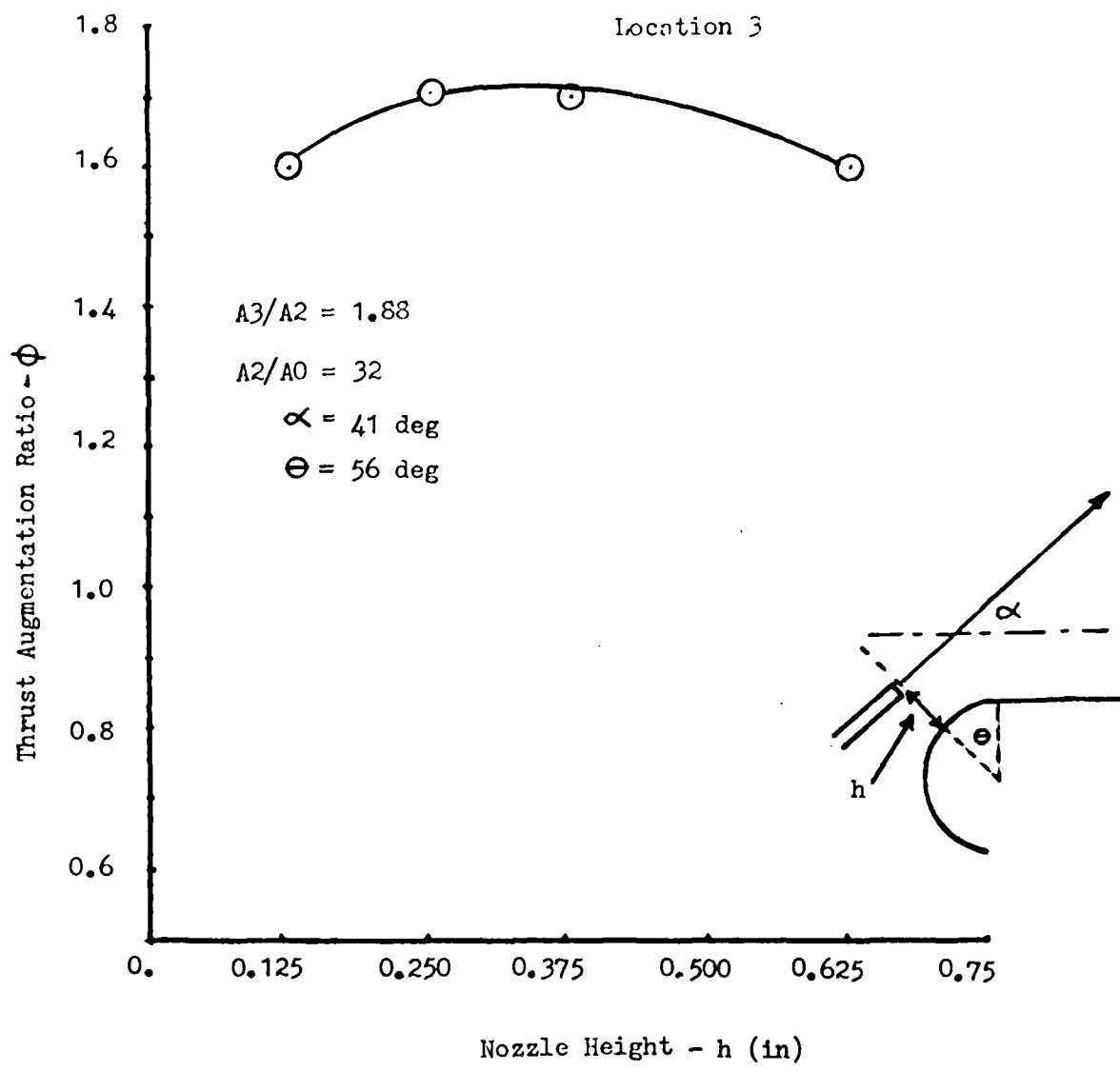


Figure 18. Effect of Nozzle Height on Thrust Augmentation (Location 3)

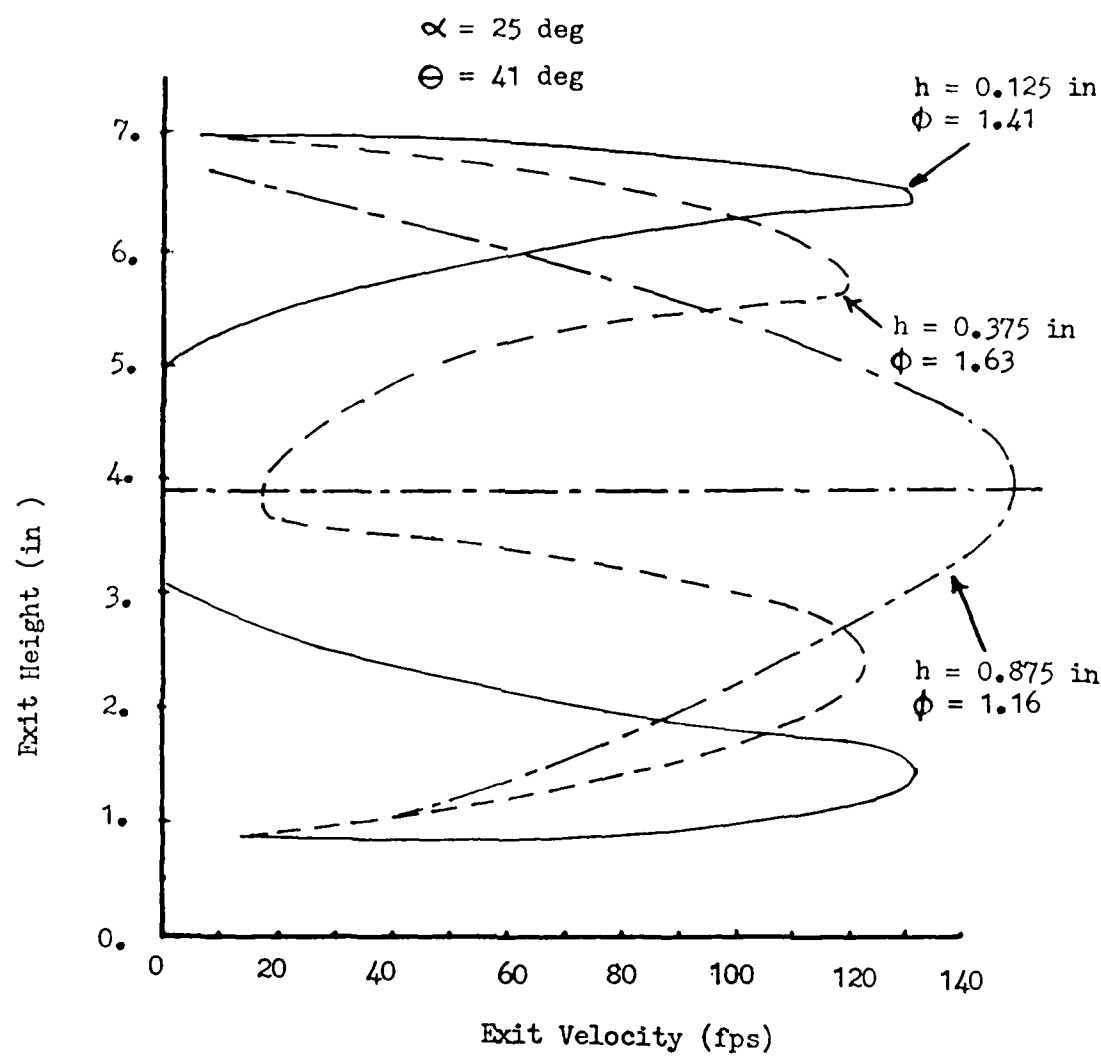


Figure 19. Effect of Nozzle Height on Exit Velocity Profile (Location 2)

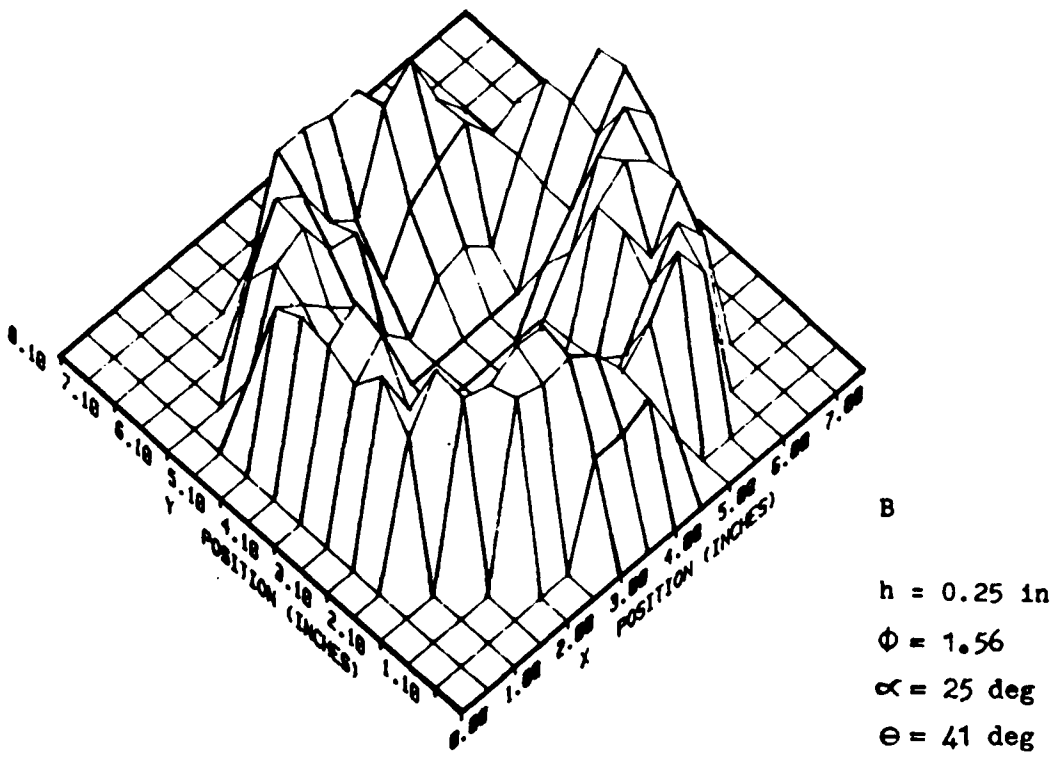
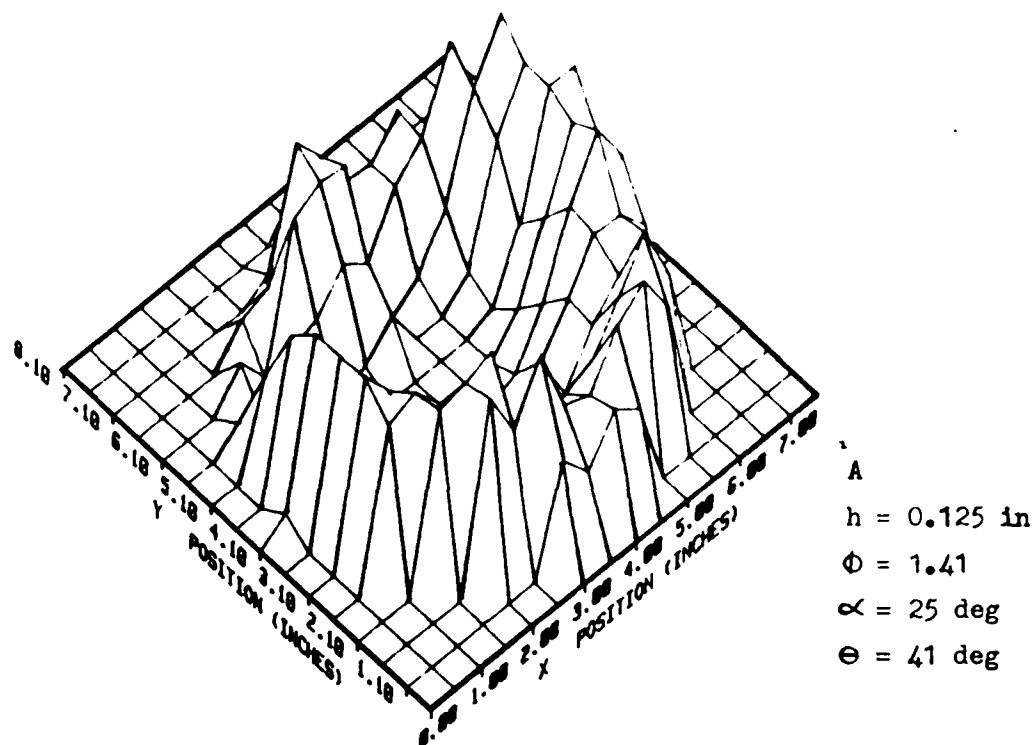
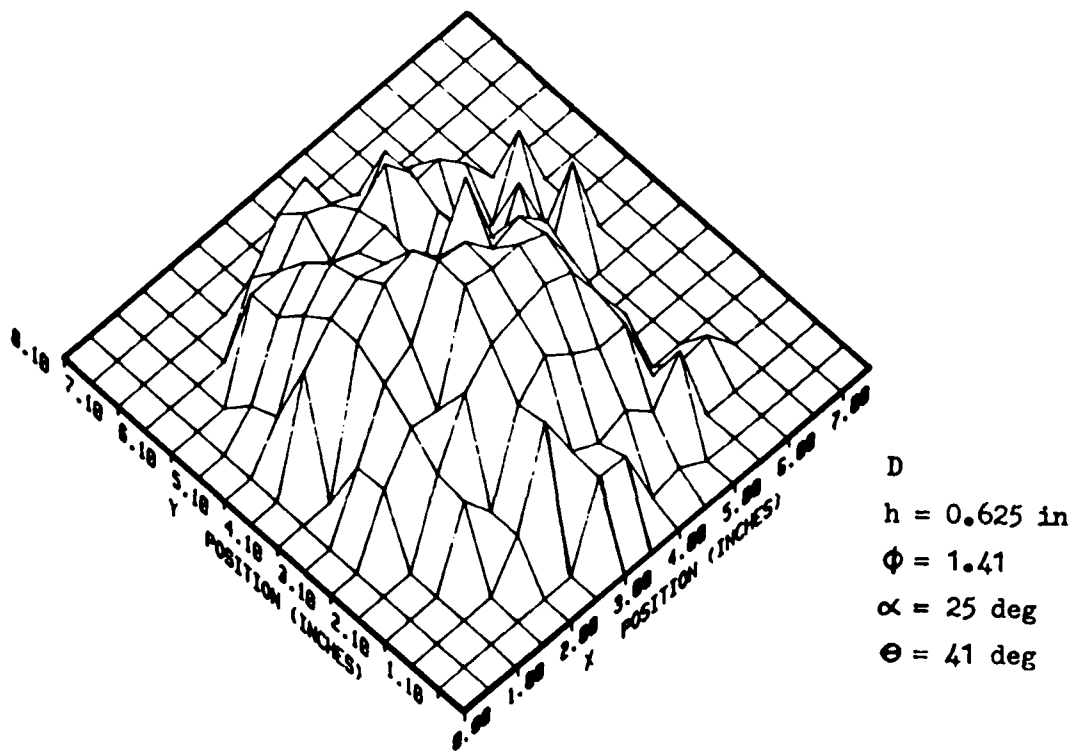
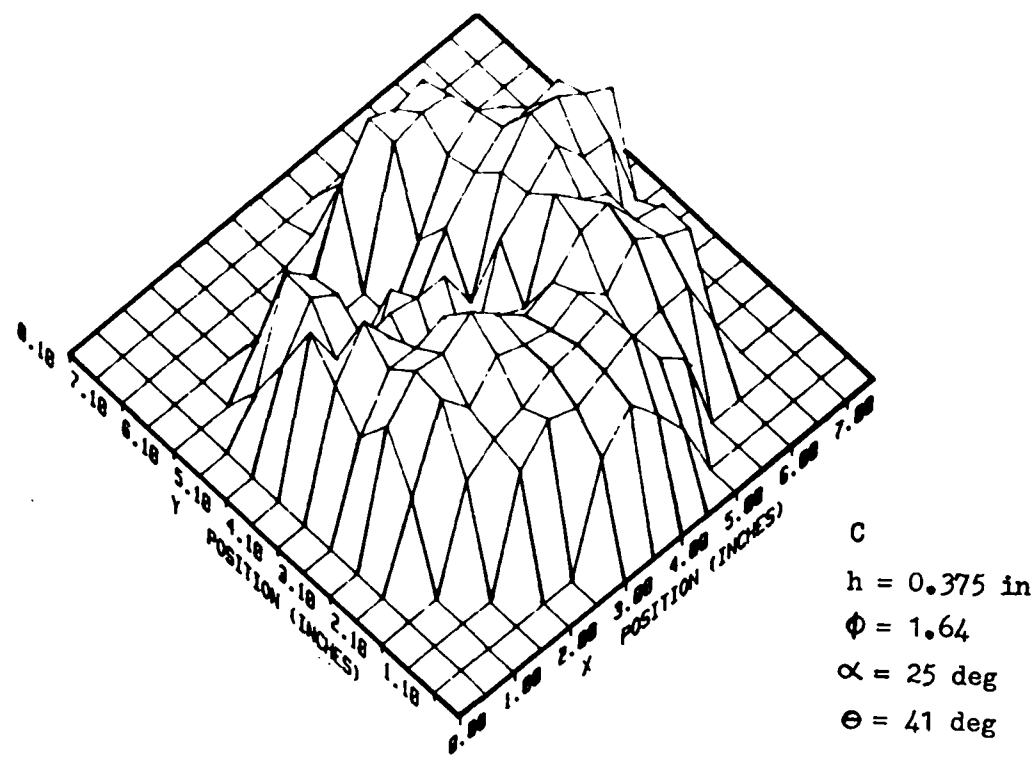


Figure 20. Effect of Nozzle Height on Three-Dimensional Exit Velocity



**Figure 20.** Effect of Nozzle Height on Three-Dimensional Exit Velocity  
(Continued)

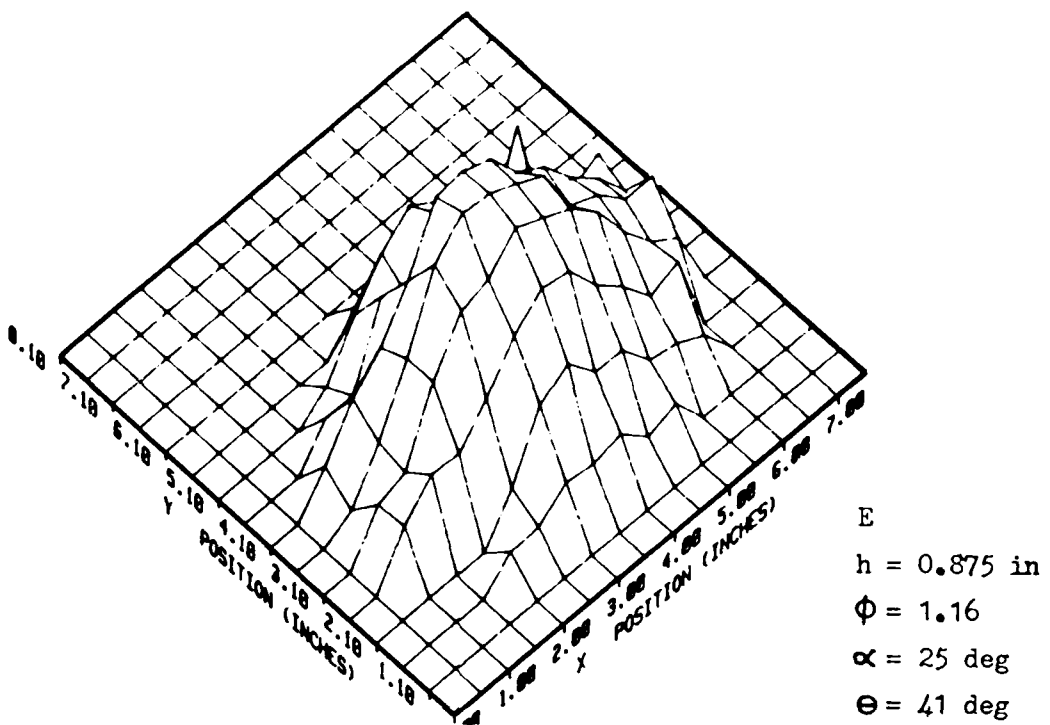


Figure 20. Effect of Nozzle Height on Three-Dimensional Exit Velocity  
(Continued)

exhibit improved mixing. At  $h = 0.625$  in, partial separation started to occur on some areas at the exit plane. At  $h = 0.875$  in, flow was totally separated around the perimeter of the exit plane. Figure 21 shows a comparison of the mass augmentation ratio at the heights tested in Figure 17. The peak mass augmentation also occurred at a height of 0.375 in.

The results of this test show that the primary nozzle height, independent of the injection angle, exerts a strong influence on thrust augmentation ratio. As shown in Figure 19, at heights below  $h_p$ , a lower thrust augmentation occurs due to incomplete mixing of the flow reaching the exit plane as well as due to the presence of high peak velocities near the walls which cause high frictional losses. At nozzle heights above  $h_p$ , the primary flow may fail to reattach on the inlet and mixing chamber surfaces resulting in localized flow separation which then propagates downstream to the diffuser area. Separated flow on the ejector inner walls results in a decrease in mass augmentation and also causes changes to the wall static pressure resulting in a reduction of the net lip thrust and a lower thrust augmentation.

#### Injection Angle Effect

For this test, height was fixed at 0.375 in, which was the height that provided the peak thrust and mass augmentation ratio obtained in Figures 17 and 21. The value of  $\Theta$  was fixed at 41 deg and  $\alpha$  was varied at 5 deg increments from 20 to 35 deg.

Figure 22 shows the results of this experiment. Augmentation ratio increased as the injection angle increased up to 30 degrees. Beyond 30 deg, augmentation began to fall. The angle where augmentation ratio peaked was close to the angle where peak augmentation ratio was observed in Refs 1, 2 and 3. Figure 23 shows a comparison of the exit velocity profiles for  $\alpha = 20, 30$  and 35 deg. At  $\alpha = 20$  deg, the profile showed high peak velocities near the wall and a large low velocity region at the center. At  $\alpha = 30$  deg, the wall

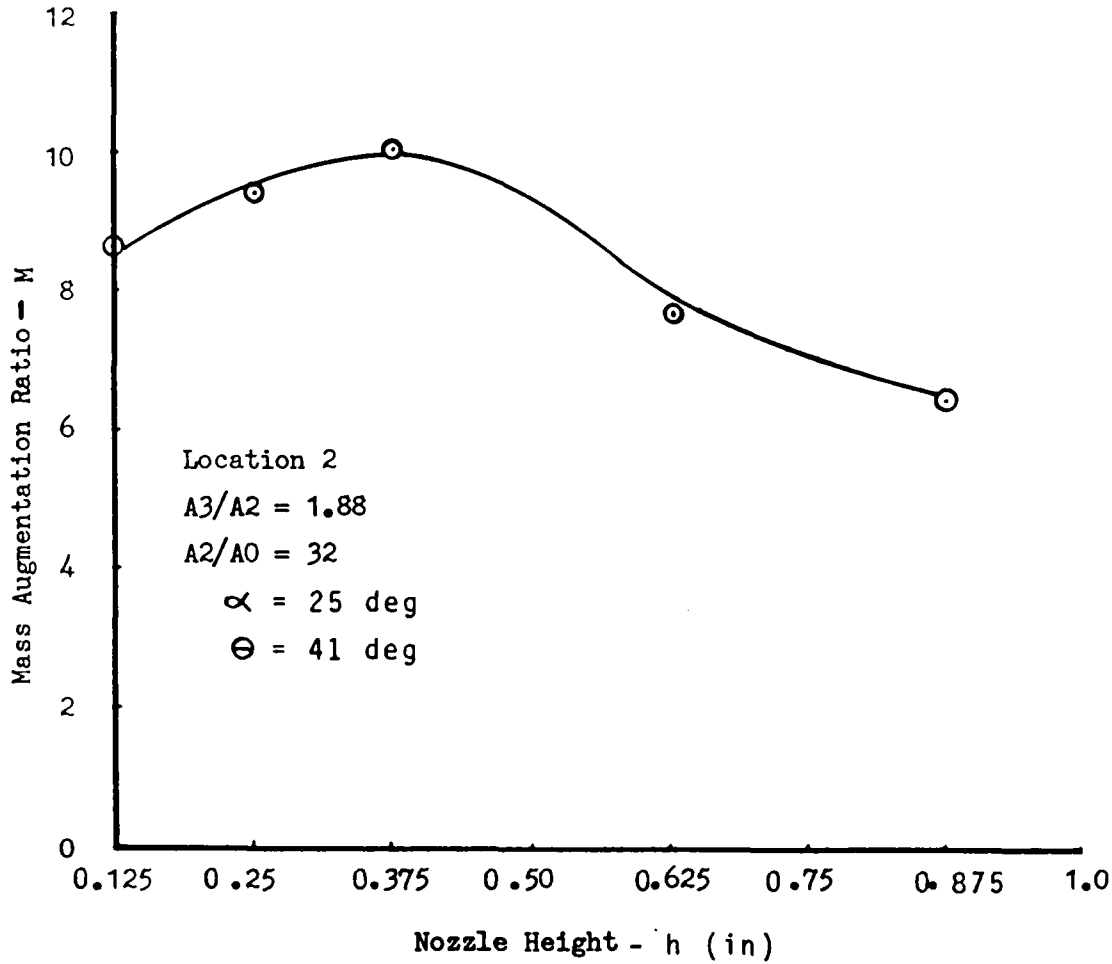


Figure 21. Effect of Nozzle Height on Mass Augmentation Ratio

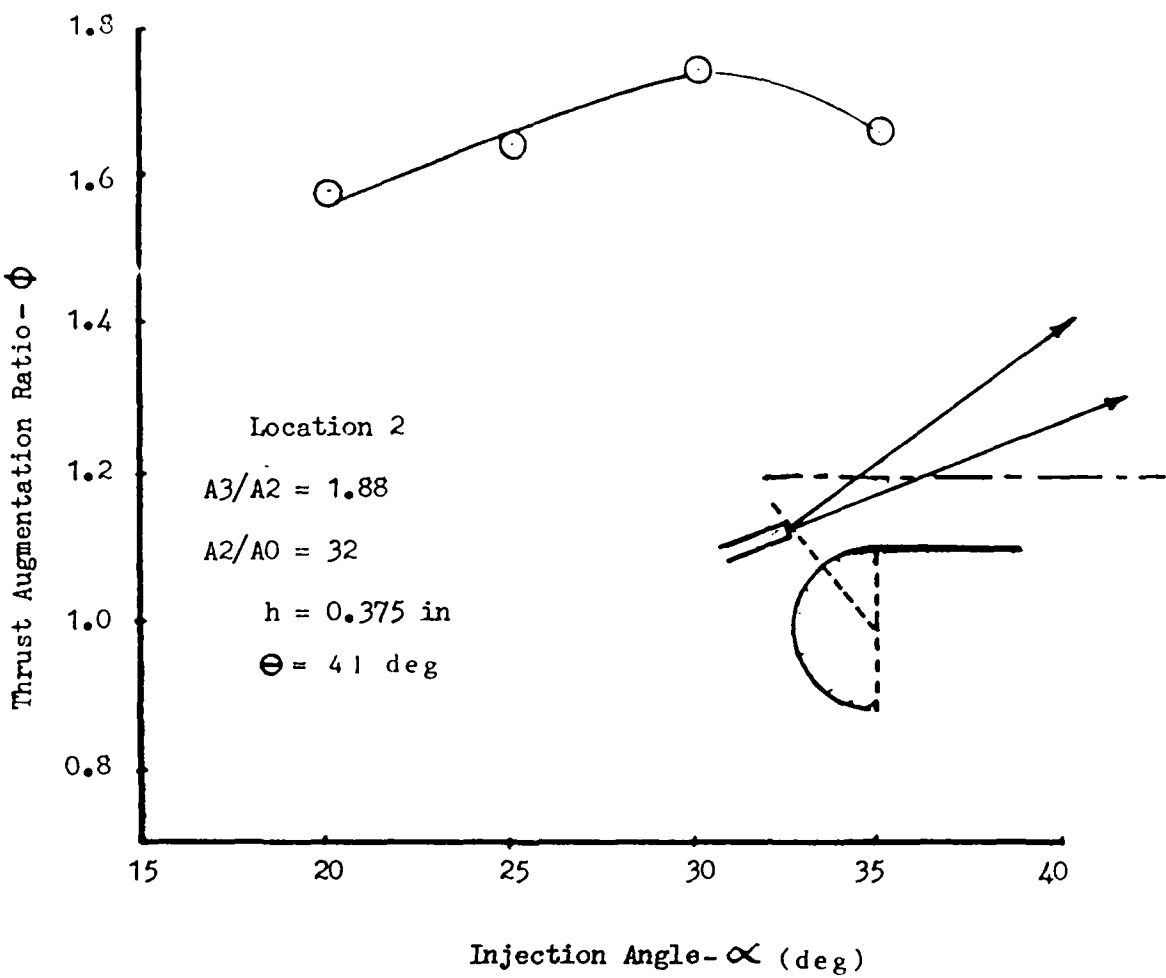


Figure 22. Effect of Injection Angle on Thrust Augmentation (Location 2)

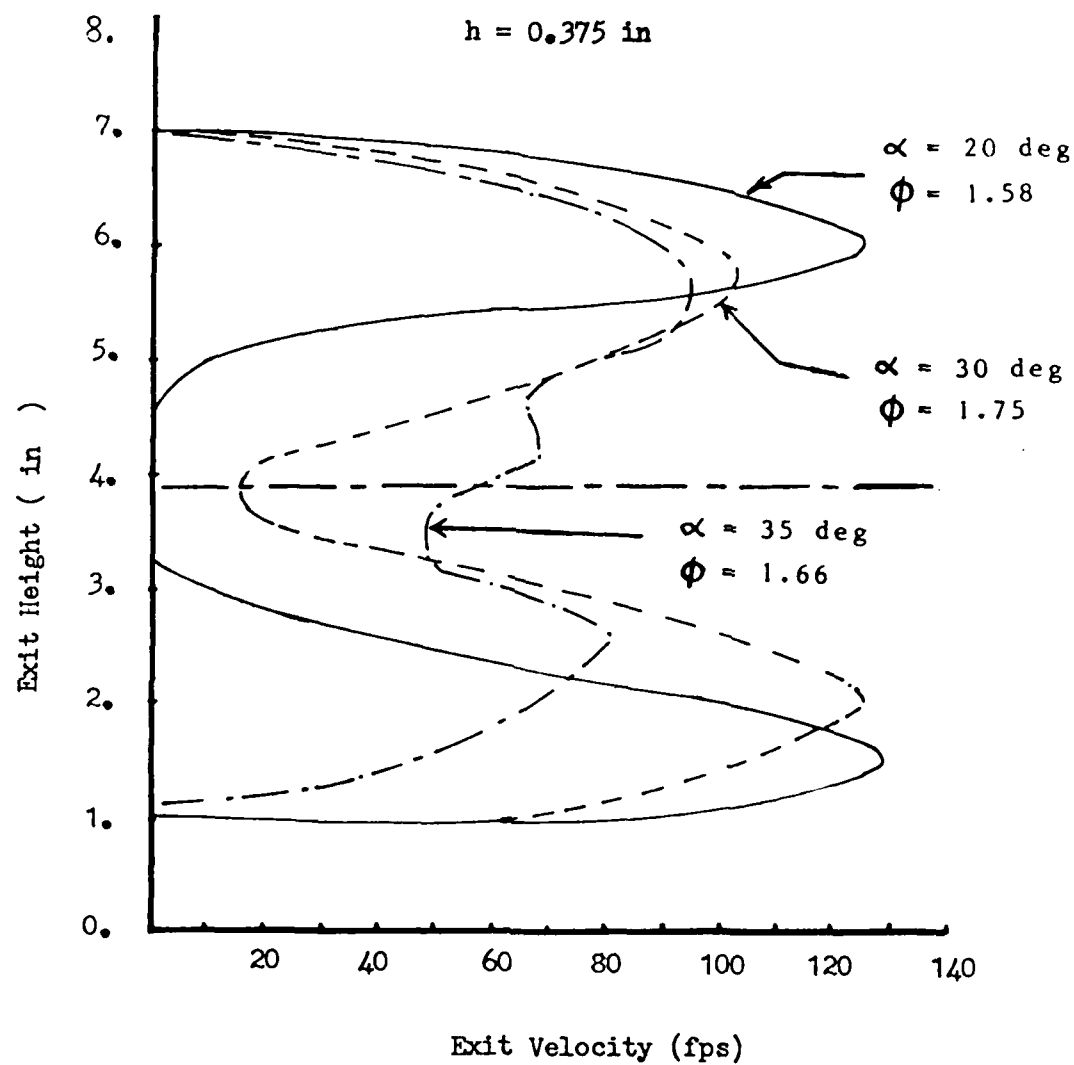
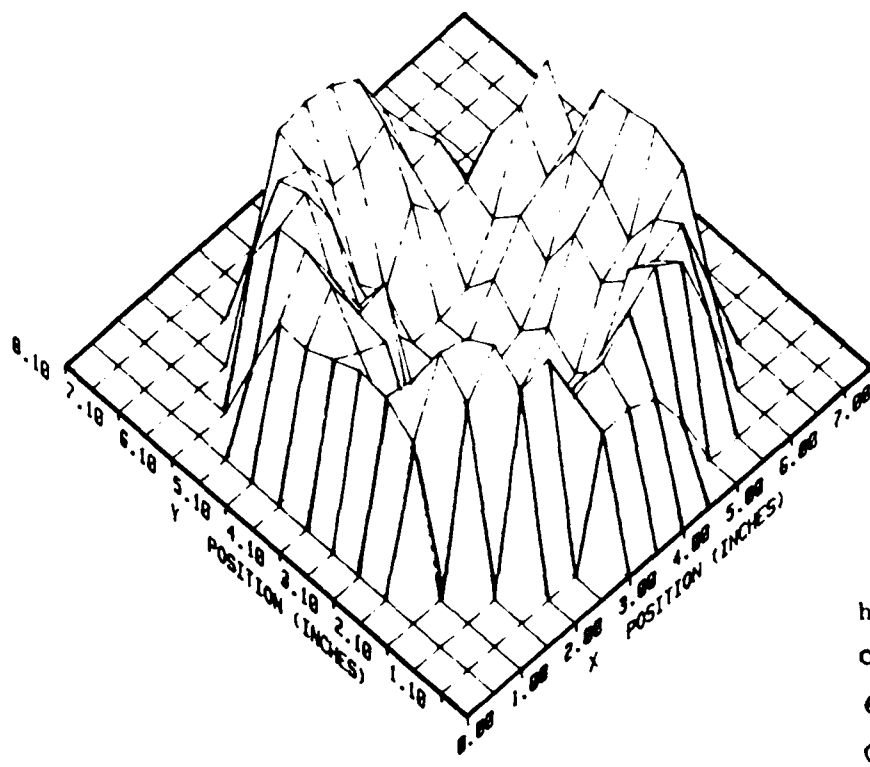


Figure 23. Effect of Injection Angle on Exit Velocity Profile

peak velocities were slight lower than that at  $\alpha = 20$  deg and the center region began to exhibit improved mixing. At  $\alpha = 35$  deg, the peak wall velocity was considerably lower than that at 30 deg, the center region showed a considerably more uniform profile but also began to exhibit separation on the lower wall. Figure 24 shows the three-dimensional plots of the exit velocity for  $\alpha = 20$  and 30 deg. The plots were similar to those shown in Figures 20B and 20C. At  $\alpha = 20$  deg, a deep cup shaped profile with high wall velocities was obtained. At  $\alpha = 30$  deg, the unmixed region near the center has disappeared.

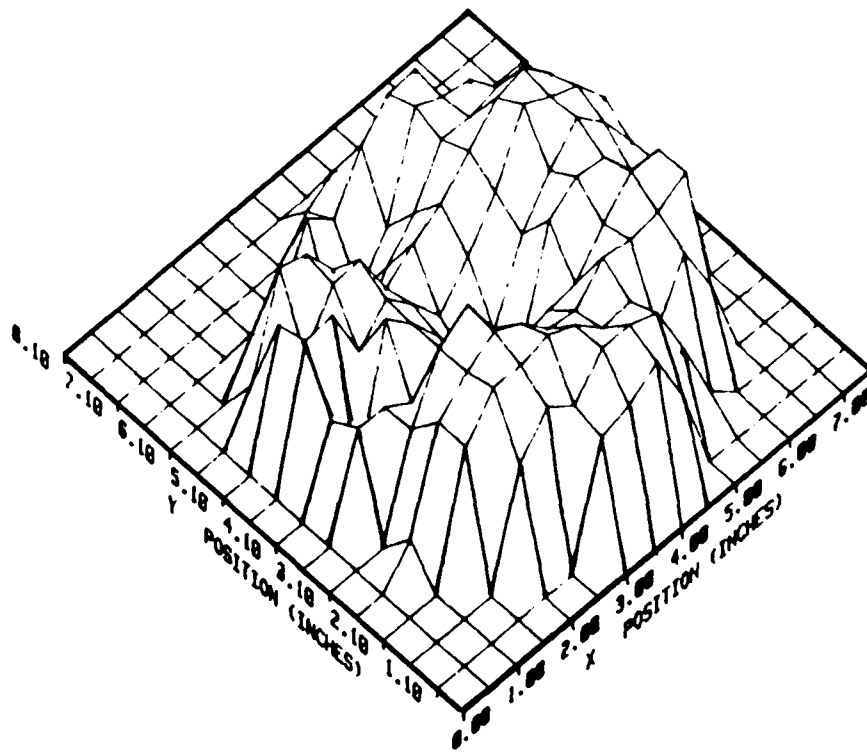
The results of these tests have shown that the effect of injection angle was similar to the effect of height on thrust augmentation. The decrease in  $\Phi$  below  $\alpha_p$  was caused by frictional losses and incomplete mixing as shown by the high wall velocities and the large low velocity region at the center of the exit velocity profiles. Above  $\alpha_p$ , decrease in  $\Phi$  is attributed to the failure of the primary jet to reattach and maintain a Coanda flow which then resulted in local flow separation which propagated downstream to the diffuser section. The amount of decrease in  $\Phi$  from  $\Phi_p$  above  $\alpha_p$  depends upon the extent of the separation occurring, which in turn is affected by the extent to which the injection angle departs from  $\alpha_p$ . The requirement for a high thrust augmentation is to achieve complete mixing and a uniform velocity profile while maintaining attached flow up to the diffuser exit plane. For the wall blowing ejector, a combination of primary nozzle h and  $\alpha$  exists which provides the best compromise between exit velocity profile uniformity and flow separation.

Figure 25 compares the trends in augmentation ratios for the fixed h and variable  $\alpha$  case from Figure 22 to that of the variable h and  $\alpha$  case from Figure 16. The peak augmentation ratio occurred at around 30 to 32 deg in both cases but the absolute value of  $\Phi_p$  was higher for the fixed height case ( $h = 0.375$



A

$$\begin{aligned} h &= 0.375 \text{ in} \\ \alpha &= 20 \text{ deg} \\ \Theta &= 41 \text{ deg} \\ \Phi &= 1.58 \end{aligned}$$



B

$$\begin{aligned} h &= 0.375 \text{ in} \\ \alpha &= 30 \text{ deg} \\ \Theta &= 41 \text{ deg} \\ \Phi &= 1.75 \end{aligned}$$

Figure 24. Effect of Injection Angle on Three-Dimensional Exit Velocity

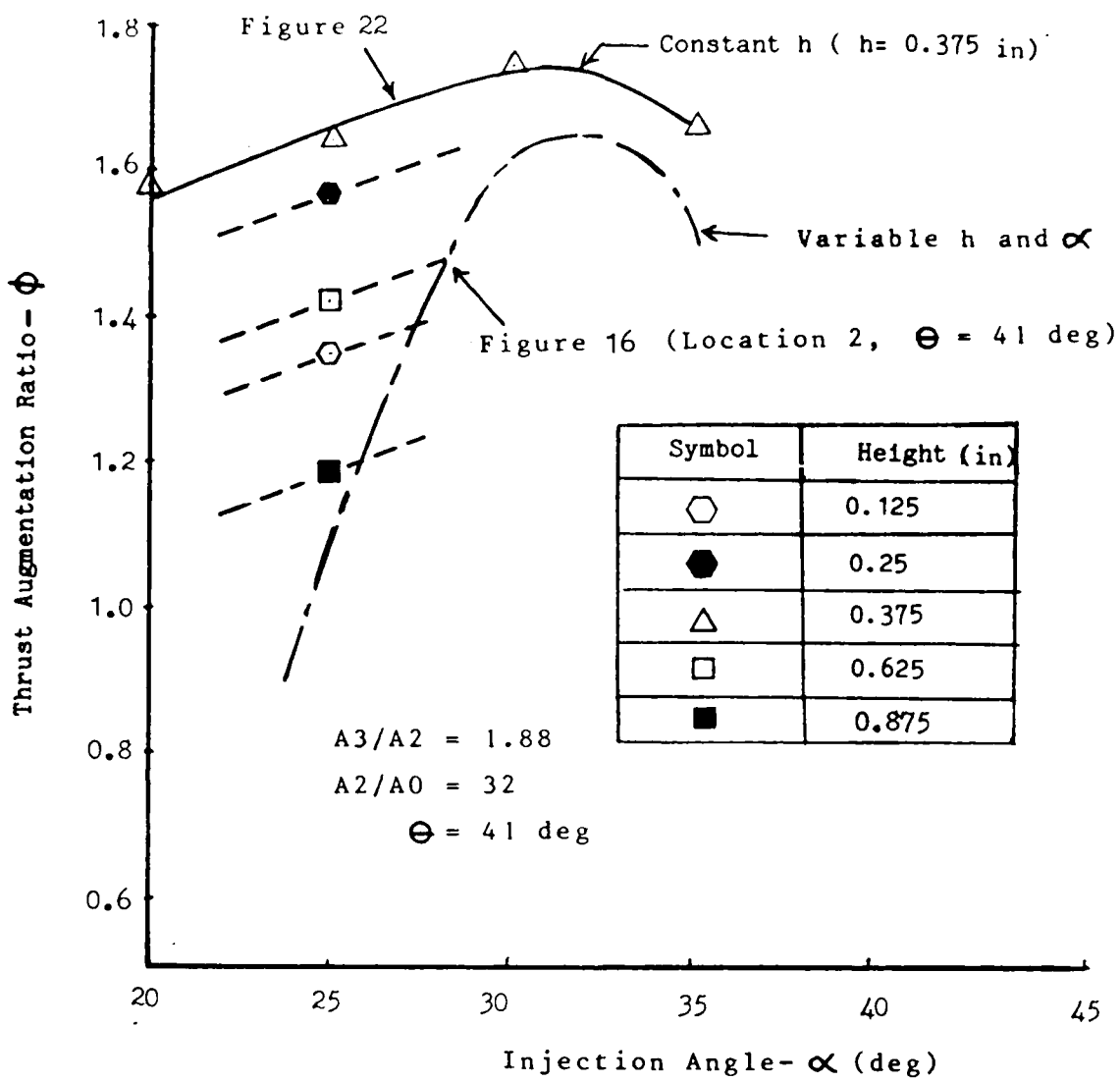


Figure 25. Comparison of Thrust Augmentation-Constant Nozzle Height vs Variable Nozzle Height and Injection Angle

in). The difference was due to the inability in the variable h and  $\alpha$  case to reach higher values of h due to the geometric limitation imposed by the method used in varying  $\alpha$  (hinged nozzle front legs). The height for the peak  $\phi$  obtained in the variable  $\alpha$  and h case was 0.25 in. Also, the slopes of the curves above and below  $\phi_p$  were significantly different. The slope for the variable h and  $\alpha$  case was considerably higher than the fixed h case. The decrease in  $\phi$  was more gradual on either side of  $\phi_p$  in the fixed h case. The steeper slope for the variable h and  $\alpha$  case was the result of the combined effects of h and  $\alpha$  on  $\phi$ , both of which are simultaneously occurring on this curve. The dotted lines show the predicted trends in  $\phi$  for various values of fixed heights.

The results of these experiments (i.e. constant h-variable  $\alpha$  and constant  $\alpha$ -variable h tests) confirm the findings of Unnever and Reznick on the importance of the injection angle on thrust augmentation ratio. The tests also extend their findings by establishing the criticality of the primary nozzle height in obtaining maximum thrust augmentation ratio.

### c. Effect of Alternating Injection Angles

In this experiment, an attempt was made to create a hypermixing jet arrangement similar to that tested in Ref 6. To avoid increasing the nozzle wetted perimeter and drag, the number of nozzles were kept at 8 throughout the duration of this test.

The results are shown in Figure 26 which shows the variation of  $\Phi$  with  $\alpha_o$  at discrete values of  $\alpha_e$ . For each fixed value of  $\alpha_e$ , peak  $\Phi$  occurred at  $\alpha_o = 30$  to 33 deg. In the vicinity of the peak  $\Phi$ , none of the alternating nozzle combinations provided a peak thrust augmentation ratio that was higher than the peak thrust augmentation ratio obtained when the nozzles were at uniform injection angles. The dotted line represents the case when all 8 nozzles were set at equal (uniform) injection angles. The bigger the difference between  $\alpha_e$  and  $\alpha_p$ , the lower the peak value of thrust augmentation. The alternating nozzle case showed considerable improvement in thrust augmentation over the uniform case at injection angles below  $\alpha_p$  however. In this region, the bigger the difference between  $\alpha_o$  and  $\alpha_e$ , the greater the improvement in thrust augmentation relative to the uniform  $\alpha$  case. This is attributed to the fact that as  $\alpha_e$  increased, half of the nozzles approached the optimum value of injection angle ( $\alpha_p = 32$  deg) for this nozzle location. The same trends were observed for nozzle location 1 ( $\Theta = 30$  deg) as shown in Figure 27. Figures 28A to 28F show the three dimensional exit velocity plots for  $\alpha_e = 29$  deg and increasing values of  $\alpha_o$ . The condition for  $\alpha_e = 29$  deg and  $\alpha_o = 14$  deg is shown in Figure 28A. The flow was characterized by highly irregular velocity peaks near the wall, a large unmixed region at the center and some localized flow separation. At  $\alpha_e = 29$  deg and  $\alpha_o = 26$  deg, the wall separation has disappeared but the profile retained the characteristic wall velocity height irregularities and unmixed region as shown in Figure 28B. The same irregular patterns were also

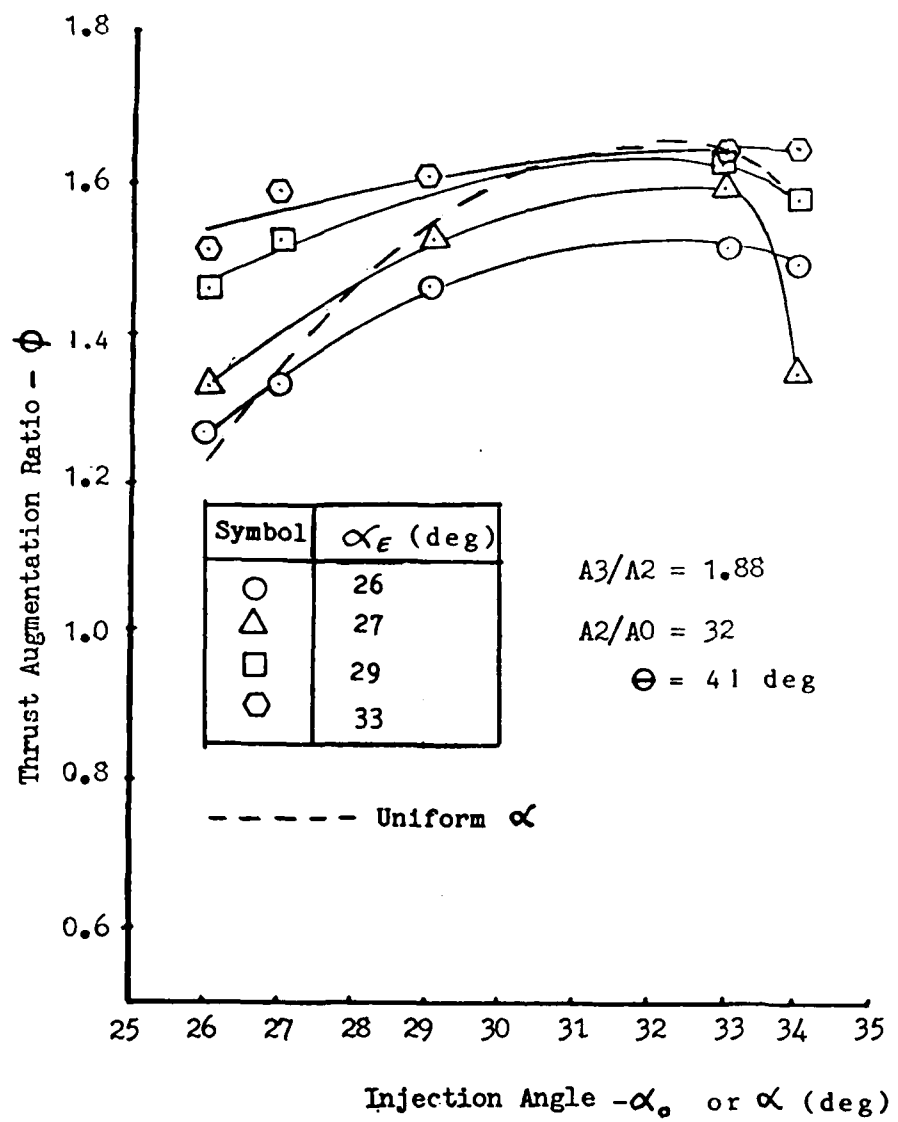


Figure 26. Effect of Alternating Injection Angles on Thrust Augmentation (Nozzle Location 2)

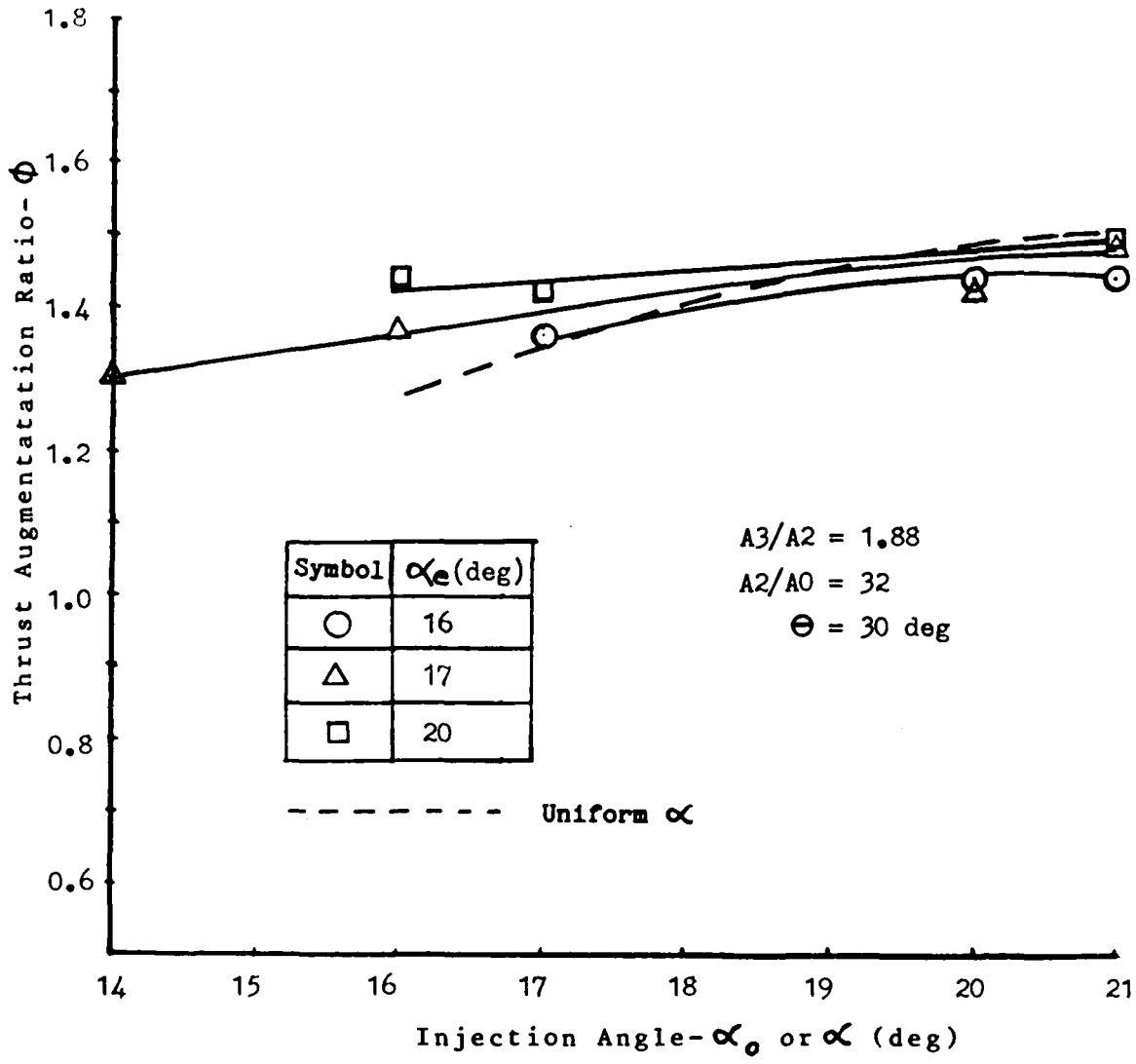
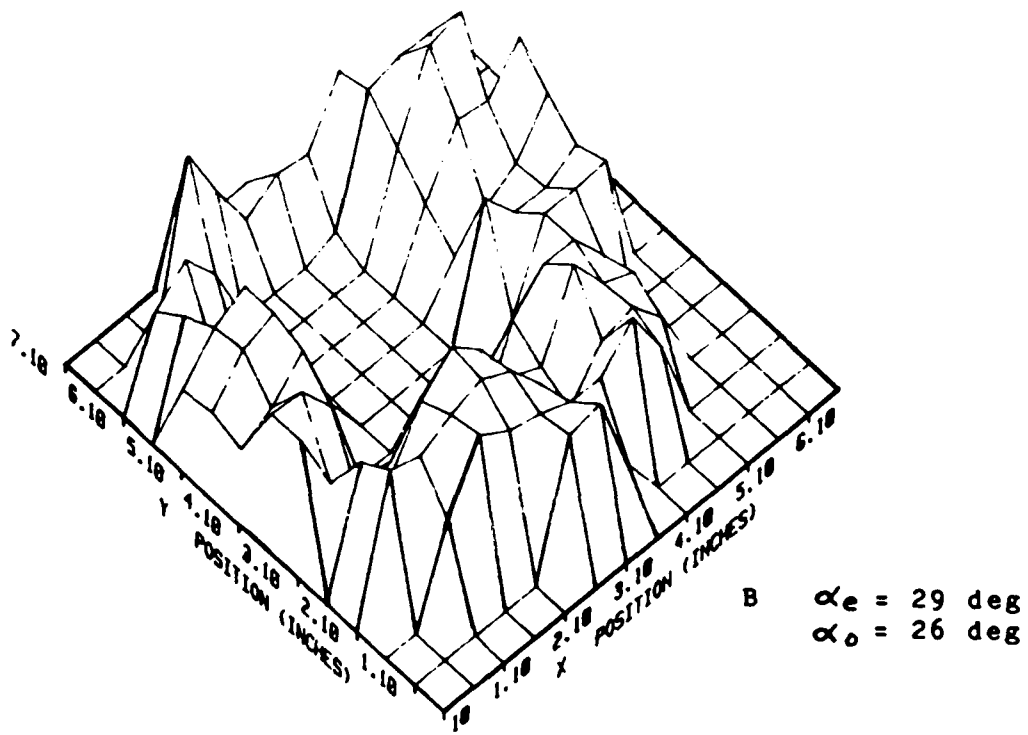
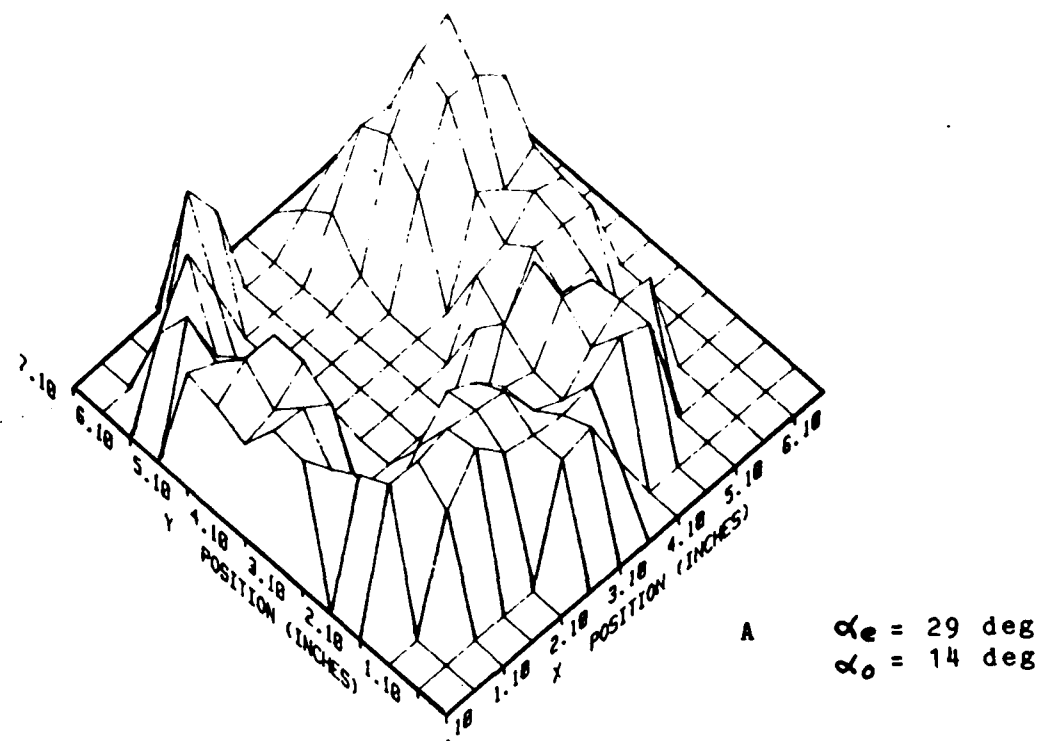


Figure 27. Effect of Alternating Injection Angles on Thrust Augmentation  
 (Location 1)



**Figure 28.** Effect of Alternating Injection Angles on Three-Dimensional Exit Velocity

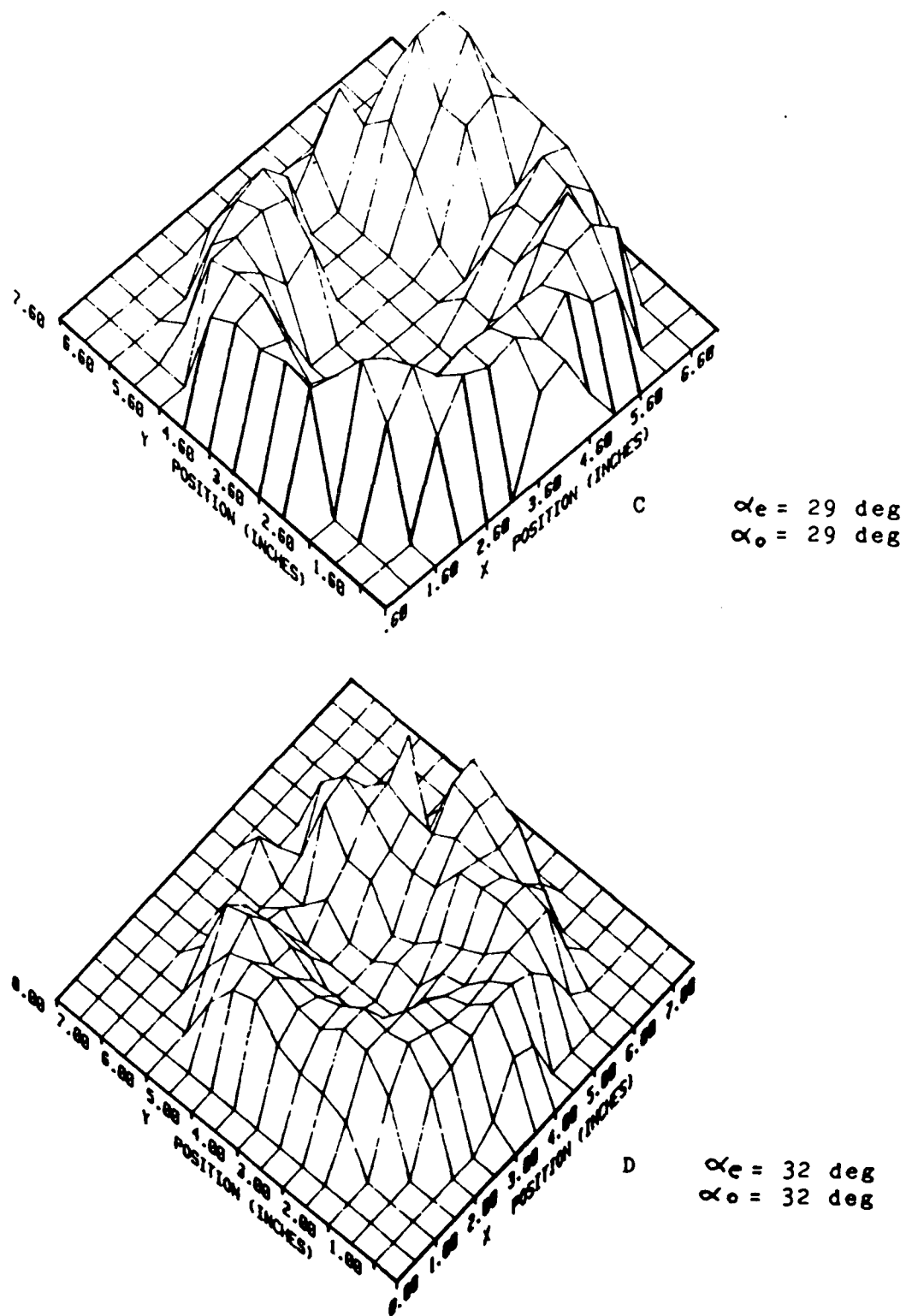


Figure 28. Effect of Alternating Injection Angles on Three-Dimensional Exit Velocity (Continued)

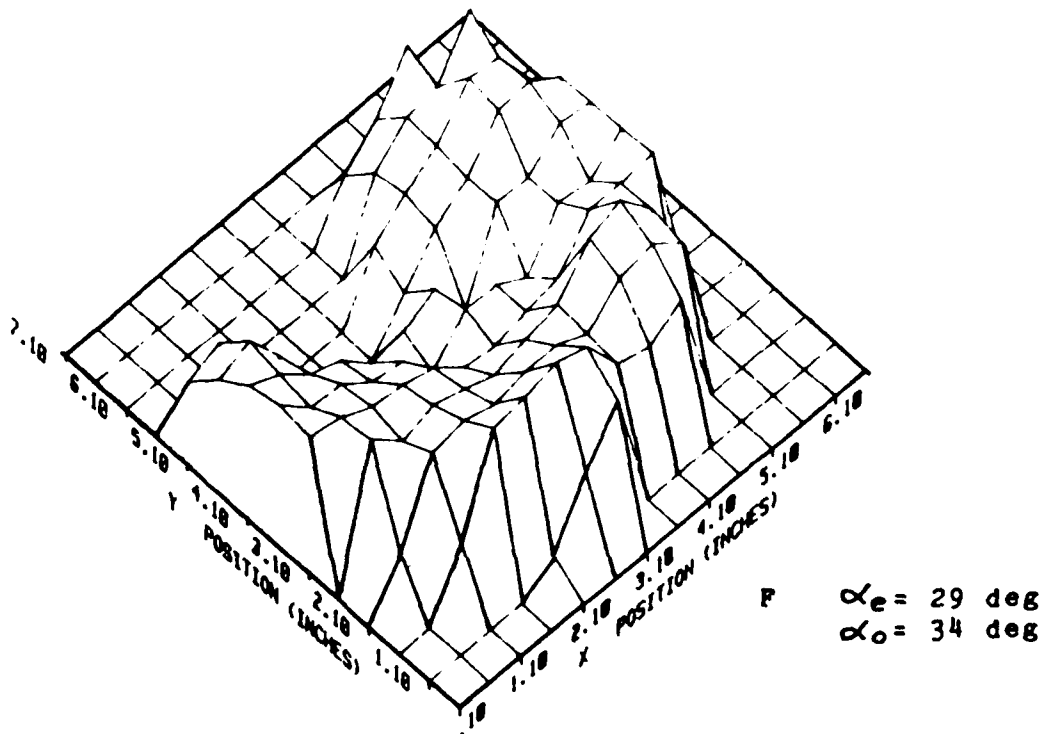
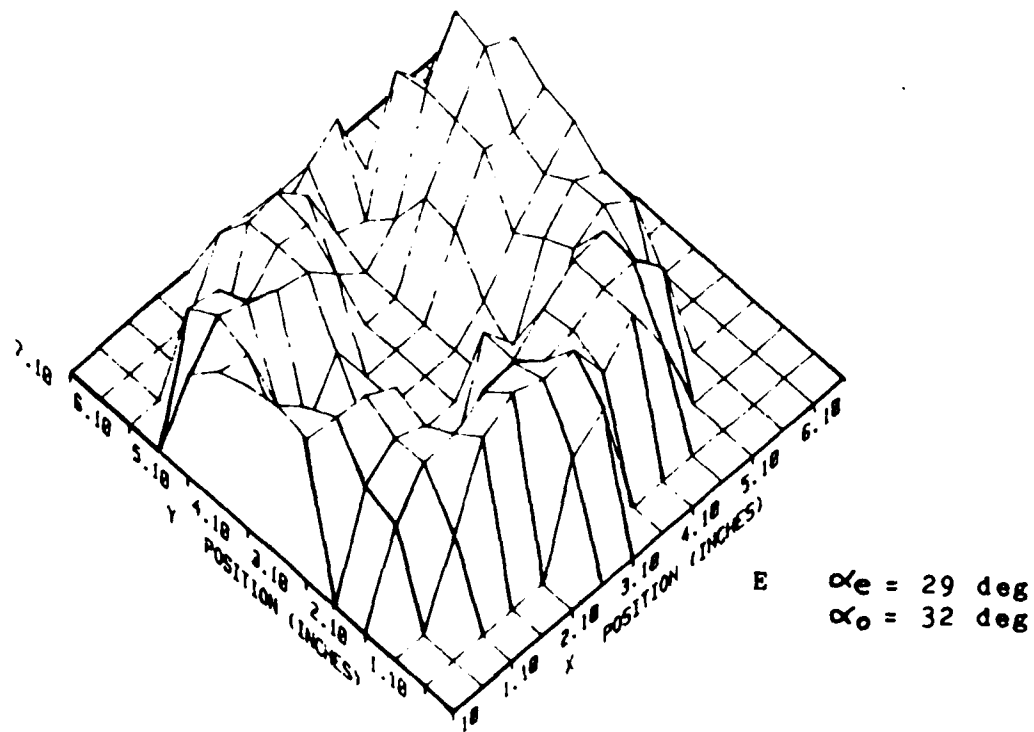


Figure 28. Effect of Alternating Injection Angles on Three-Dimensional Exit Velocity (Continued)

present for  $\alpha_e = 29$  deg and  $\alpha_o = 32$  deg as shown in Figure 28E. The area of the unmixed region in this case was slightly larger than that for the uniform  $\alpha = 32$  deg case shown in Figure 28D. At  $\alpha_e = 29$  deg and  $\alpha_o = 34$  deg, extensive separation occurred as shown in Figure 28F. This separation was more intensive than the separation observed in Ref 1 when all the nozzles were at a uniform injection angle of 34 deg.

Figure 29 compares the mass augmentation for the uniform  $\alpha$  case with the alternating  $\alpha$  case. At injection angles below 29 deg, mass augmentation with the use of the alternating pattern increased relative to the uniform pattern. The mass augmentation however remained relatively constant over the  $\alpha$  range that was tested and did not provide an improvement over the uniform  $\alpha$  case above  $\alpha_p$ .

The results of these tests have shown that the discrete nozzle alternating primary jet arrangement does not provide any more improvement in the maximum thrust augmentation ratio over that which can be obtained using a uniform pattern. The attainment of the highest thrust augmentation ratio for the circular ejector critically depends upon the formation and maintenance of a uniform and attached flow around the inlet area. Alternating the injection angles near the peak  $\phi$  could only result in incomplete mixing when some of the nozzles are set at injection angles less than  $\alpha_p$ , as shown in Figures 28D and 28E. It could also amplify localized separations which may exist in the inlet area when some of the nozzles are set above  $\alpha_p$ , as shown in Figure 28F.

As shown in Ref 2 and 3, the increase in drag caused by an increase in nozzle wetted perimeter necessary to create a mixing pattern had a strong influence in the decrease of thrust augmentation ratio relative to the thrust augmentation of the uniform injection angle nozzle arrangement. In addition however, an equally important factor for wall blowing ejectors using an alternating jet scheme is the inevitable loss of the smooth attached flow on the inlet due to the unfavorable interference between the wall and the turbulent

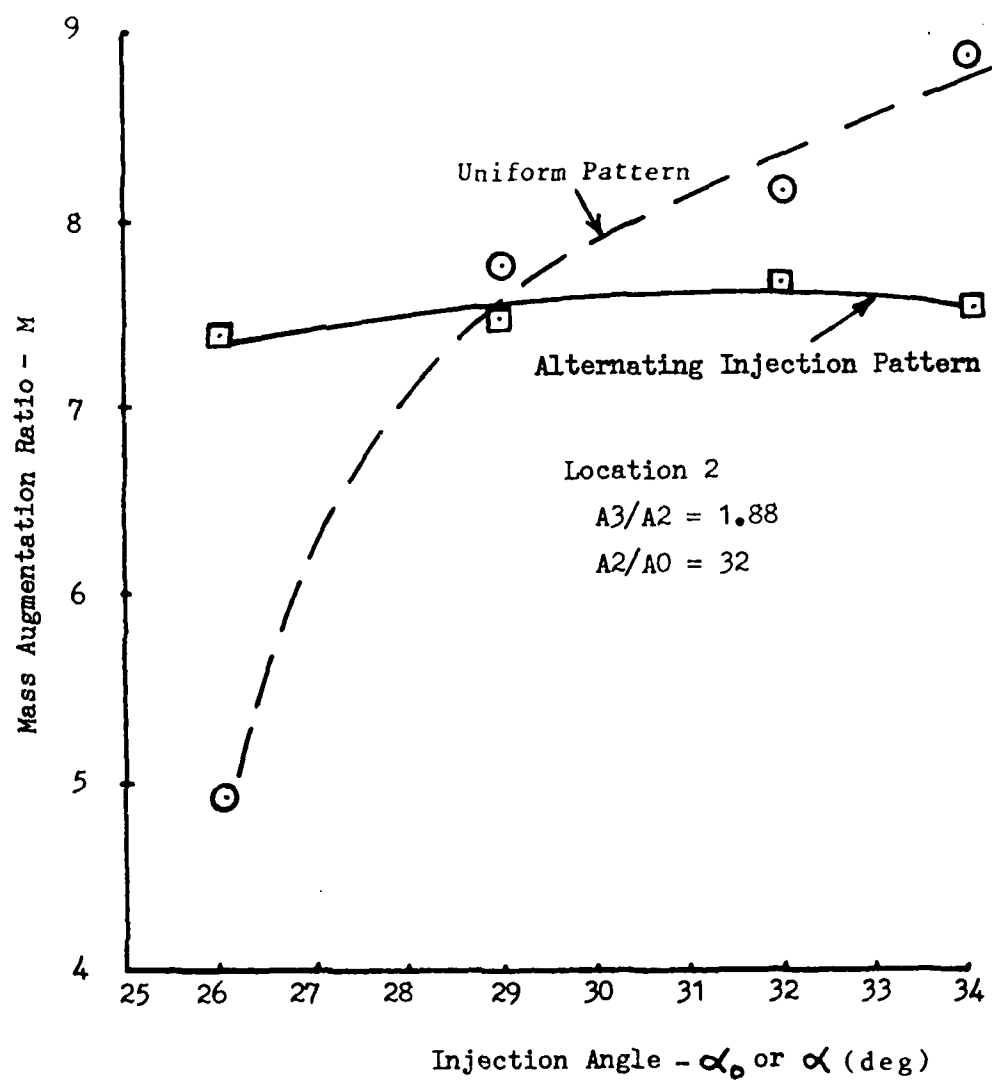


Figure 29. Effect of Alternating Injection Angles on Mass Augmentation

blowing pattern in close proximity to the wall. The success of the hypermixing nozzle tested in Ref 6 is attributed to its use in a center blowing ejector apparatus where the mixing pattern is less likely to interfere with the uniform attached flow on the inlet surface.

d. Effects of Diffuser Suction and Blowing

Diffuser Coanda blowing was investigated by Reznick (Ref 2) on a two dimensional ejector and was found to decrease thrust augmentation ratio. This portion of the study tested diffuser wall blowing and suction on the circular ejector to determine if the decrease in thrust augmentation ratio in the vicinity of  $\Phi_p$  could be delayed or prevented.

Effect of Diffuser Suction

For the suction test, the suction flow rate was fixed at 6% of the primary flow rate. Using a flowmeter, the measured flow rate was approximately 163 in<sup>3</sup>/sec. Suction was applied to the front and rear diffuser sections separately. Figure 30 shows the effect of rear diffuser suction on thrust augmentation for several nozzle locations. No substantial change in  $\Phi$  was observed at all locations. The same was true for suction in the front diffuser section as shown in Figure 31. A very slight increase in  $\Phi$  was observed for the rear diffuser suction at nozzle location 2. This small gain however would be diminished or totally offset when the energy required to generate the vacuum for suction and the thrust reduction caused by a reduction in the exit mass flow due to suction were taken into account.

A comparison of the exit velocity plots with and without suction in Figures 32A to 32 D and Figures 33A to 33F showed no significant differences between the two conditions. Figures 32A and 32B show the case for  $\Theta = 56$  deg and  $\infty = 45$  deg, with and without rear diffuser suction. The peak velocities around the exit perimeter and the low velocity regions at the center were very similar in shape.

Figure 34 shows the effect of rear diffuser suction when a significant amount of separation has occurred at the diffuser. In this case,  $h$  was 0.625 in,  $\Theta$  was 41 deg and  $\infty$  was 25 deg. With suction, a reattachment of the

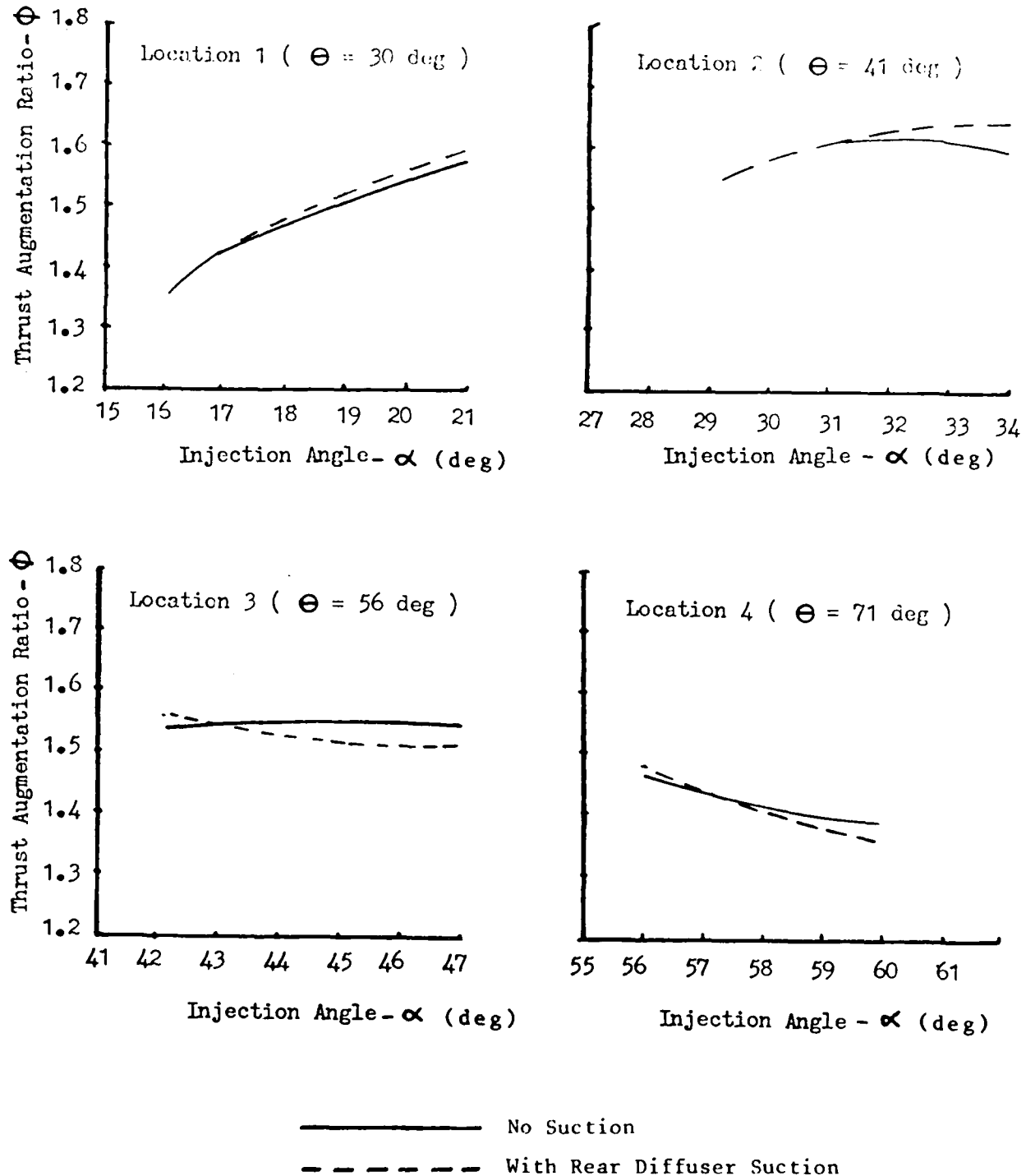


Figure 30. Effect of Rear Diffuser Suction on Thrust Augmentation

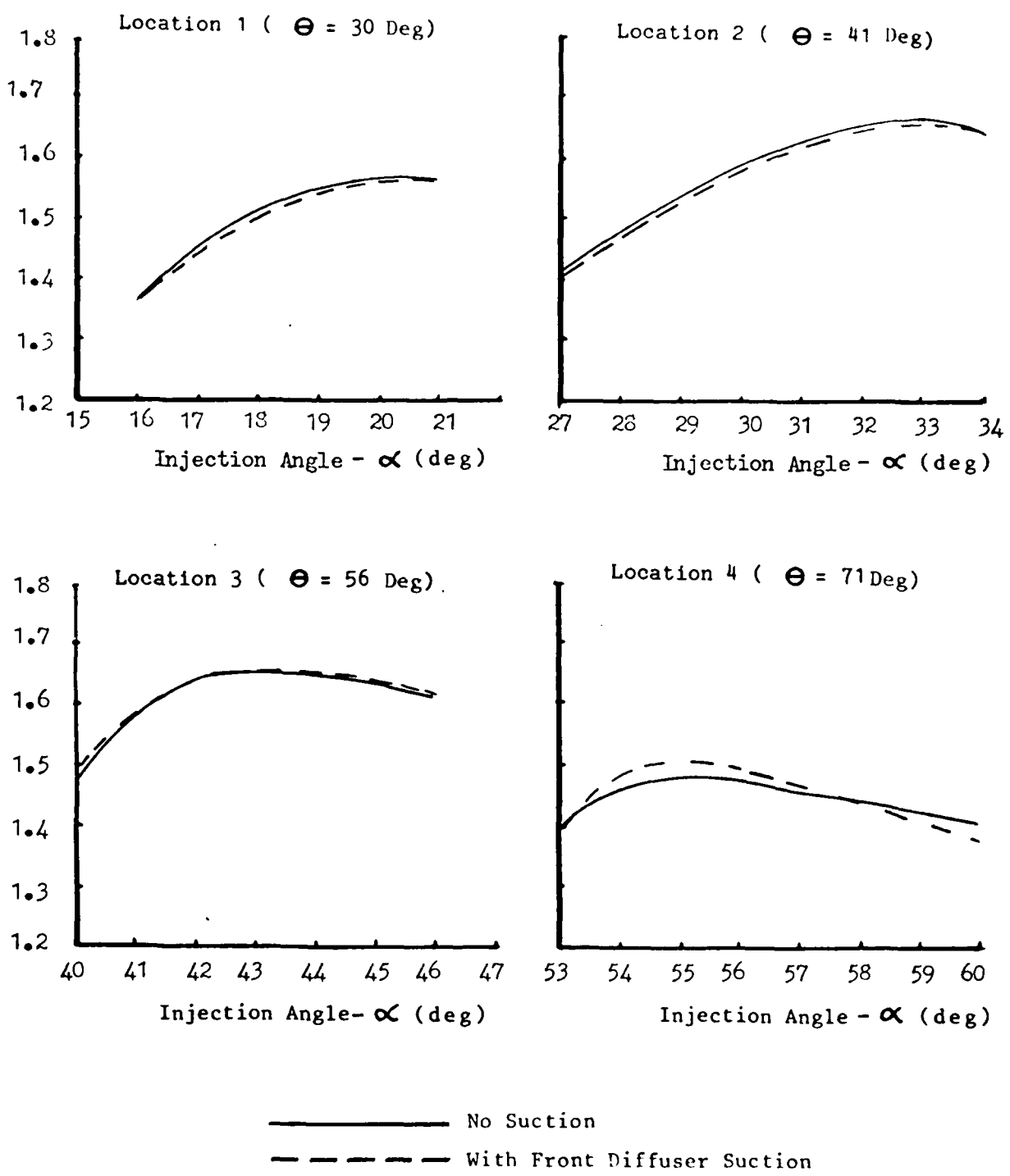


Figure 31. Effect of Front Diffuser Suction on Thrust Augmentation

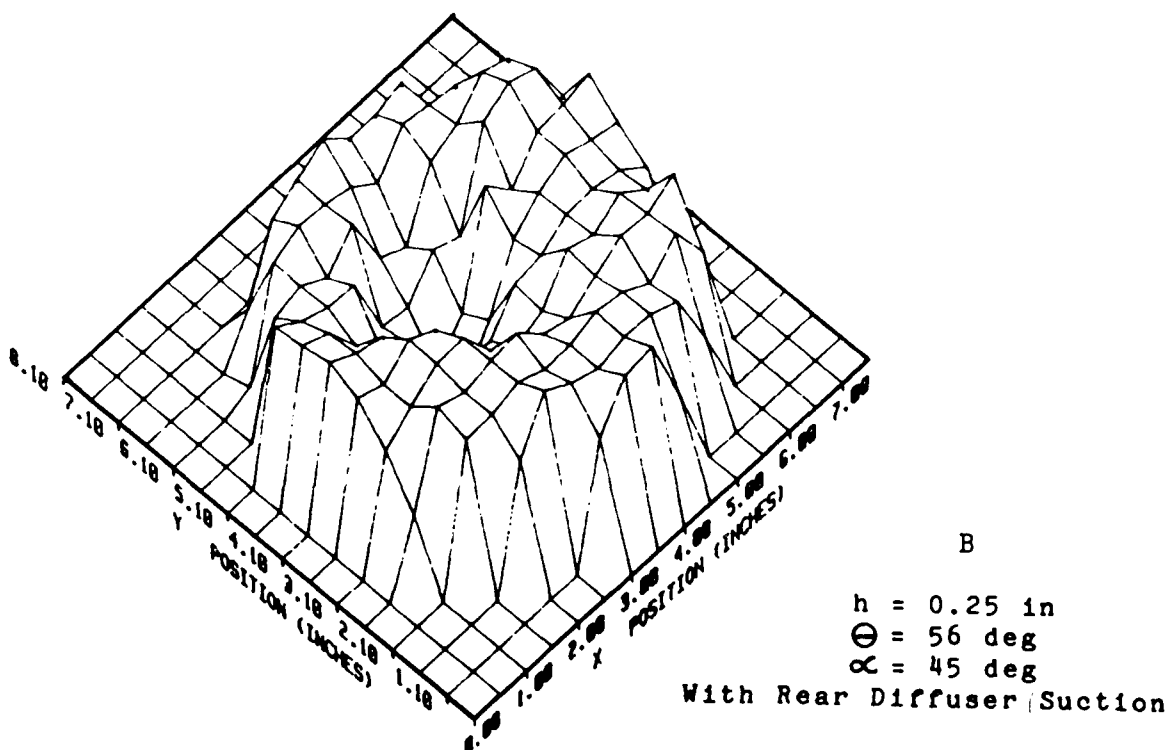
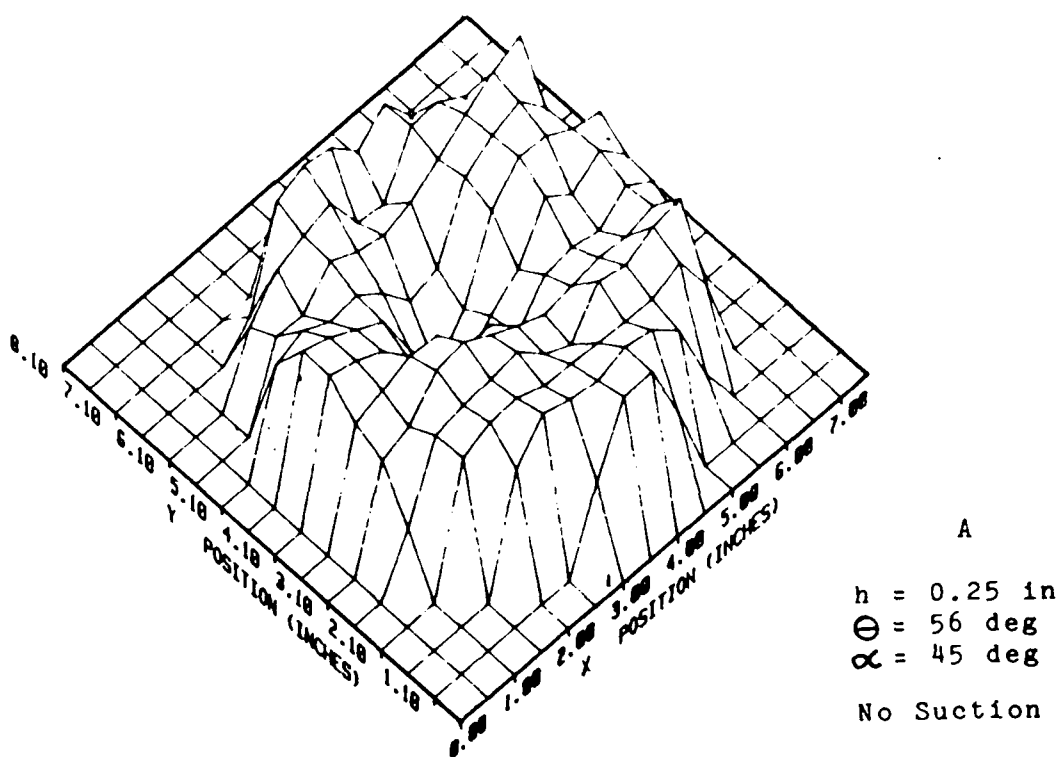


Figure 32. Effect of Rear Diffuser Suction on Three-Dimensional Exit Velocity

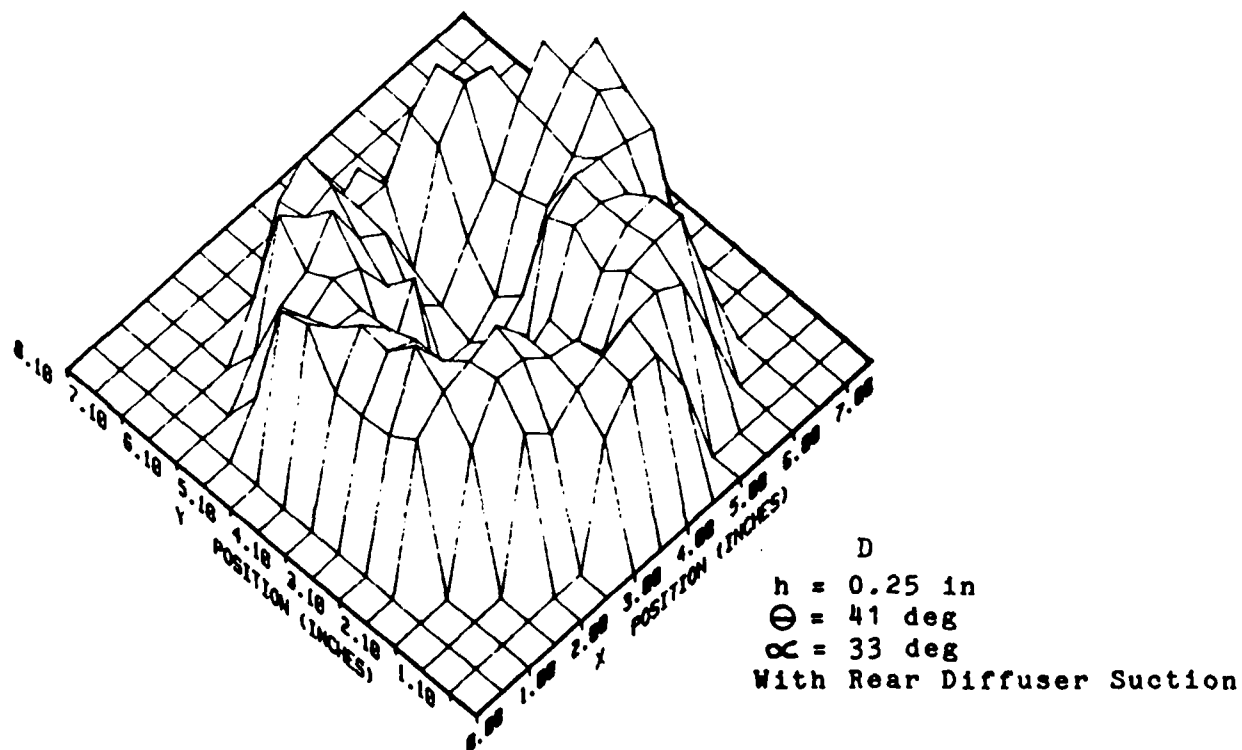
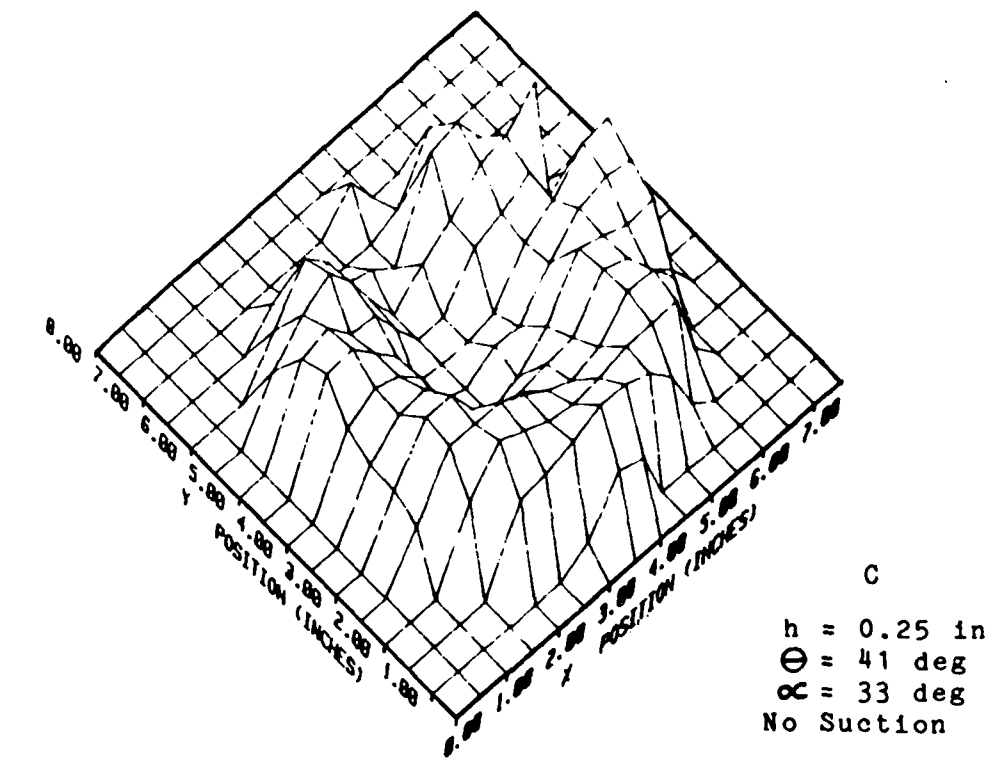


Figure 32. Effect of Rear Diffuser Suction on Three-Dimensional Exit Velocity (Continued)

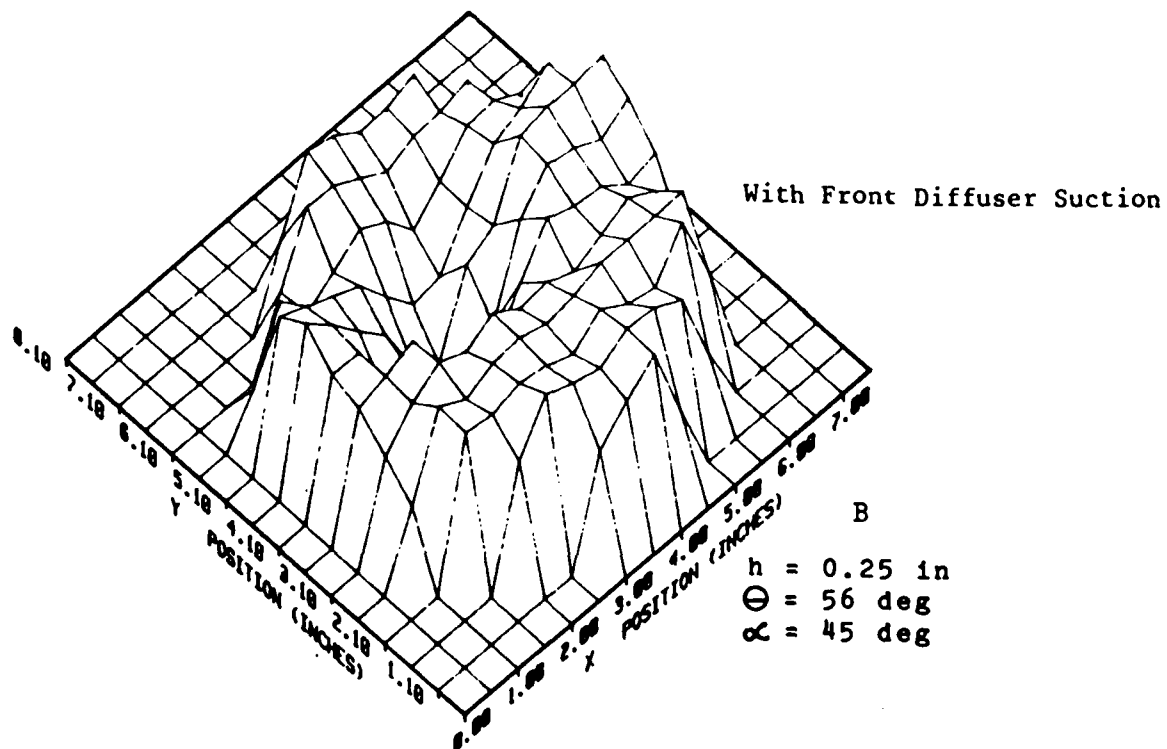
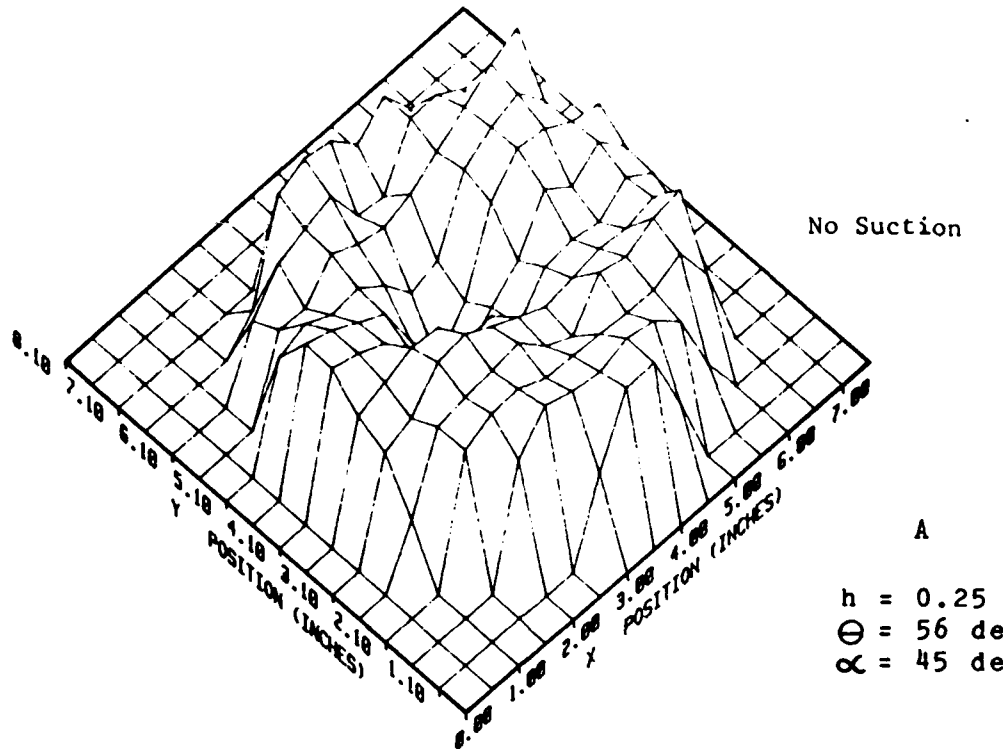


Figure 33. Effect of Front Diffuser Suction on Three-Dimensional Exit Velocity

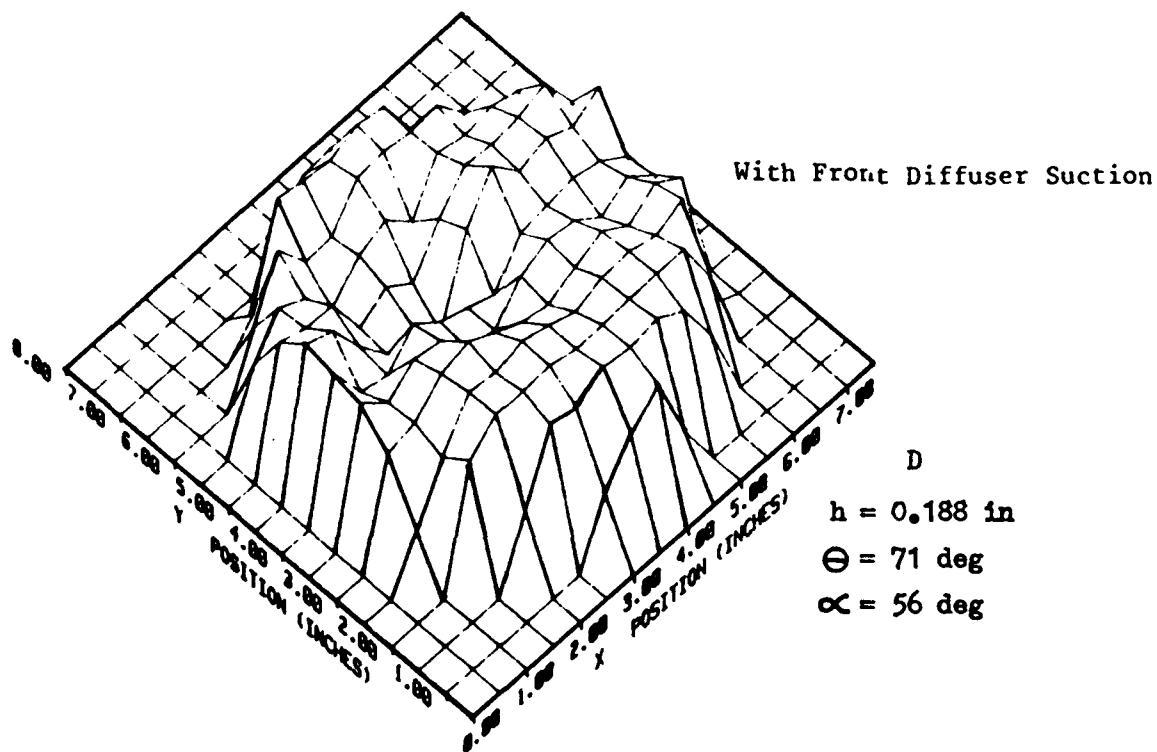
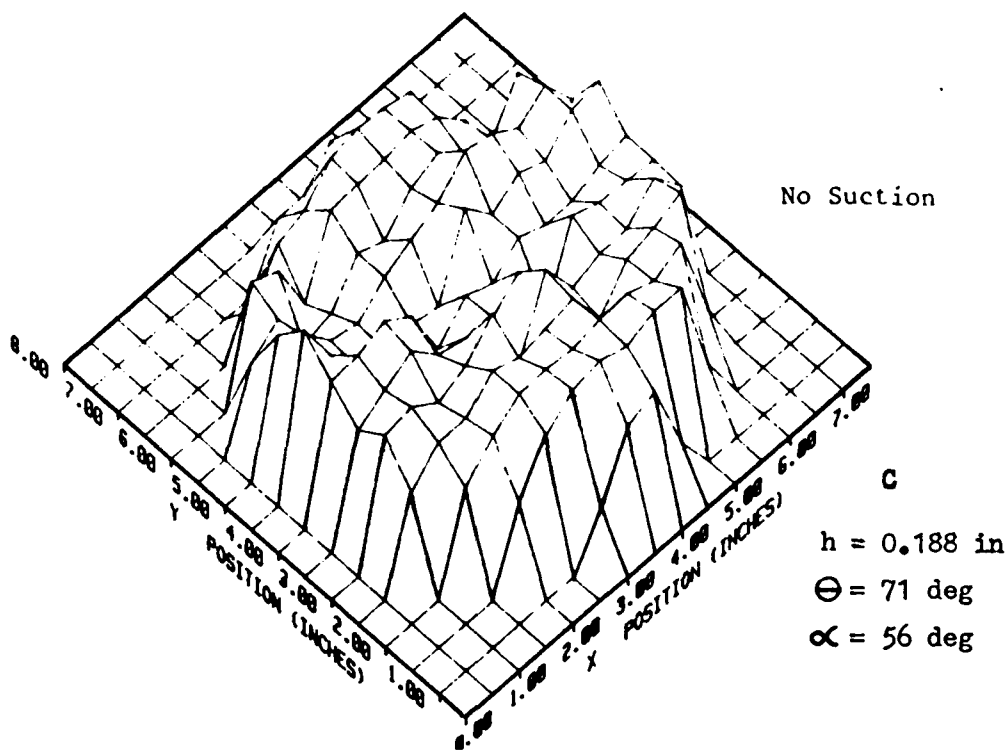


Figure 33. Effect of Front Diffuser Suction on Three-Dimensional Exit Velocity (Continued)

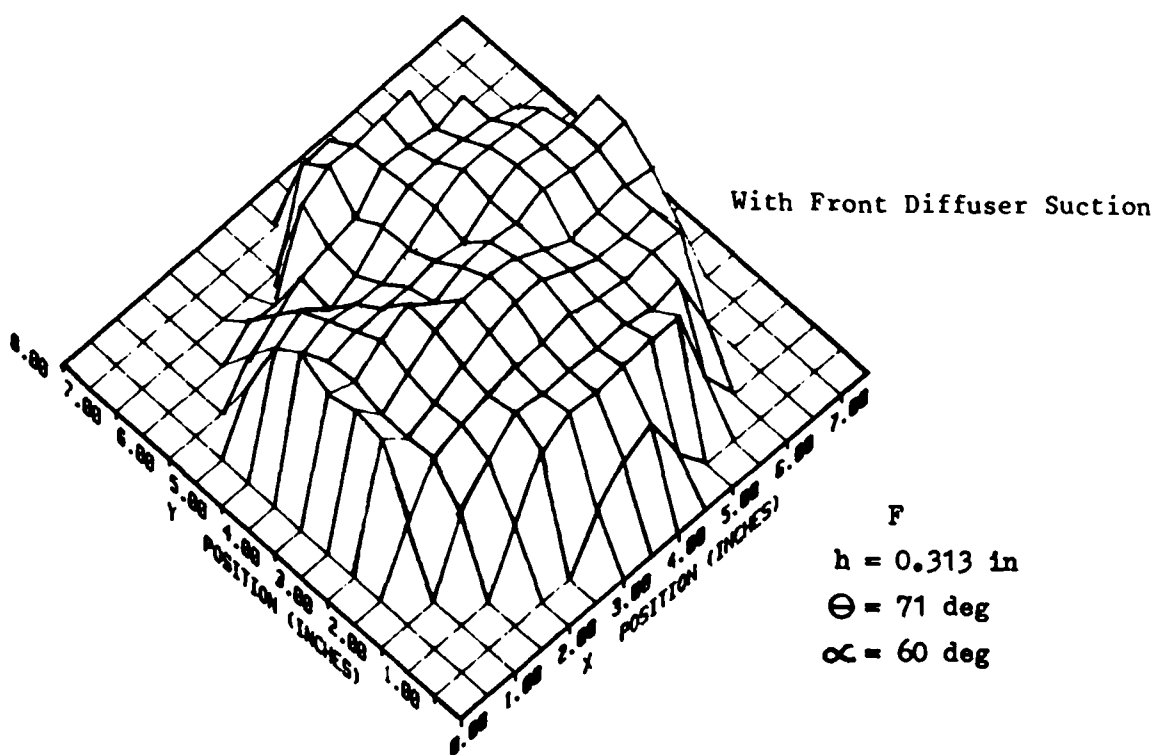
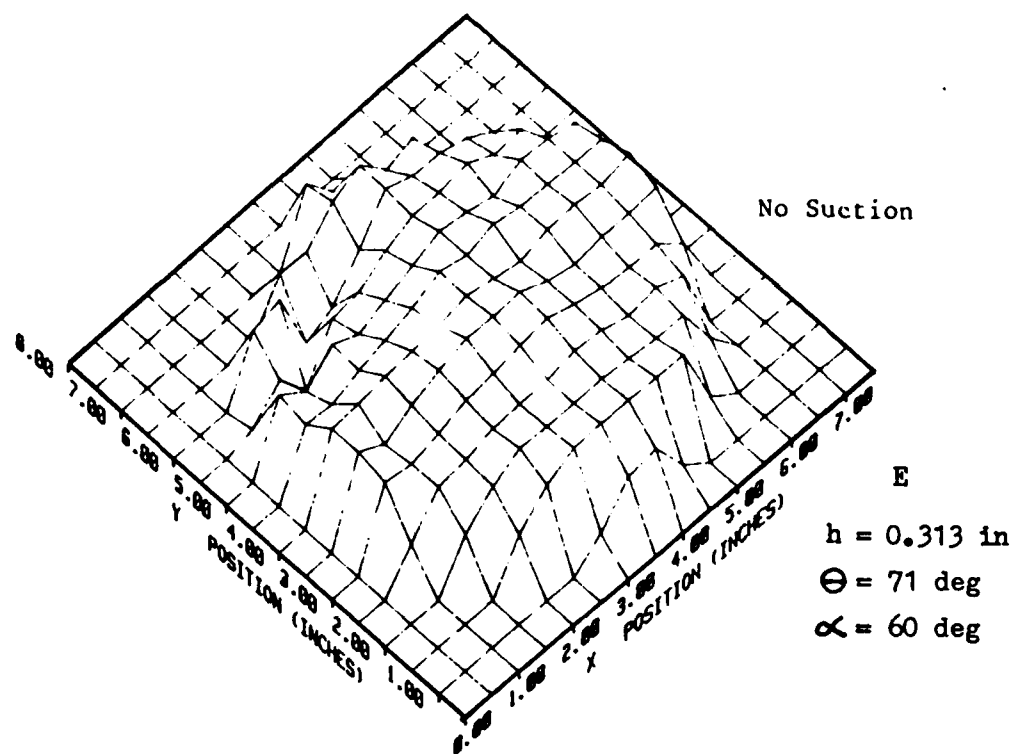


Figure 33. Effect of Front Diffuser Suction on Three-Dimensional Exit Velocity (Continued)

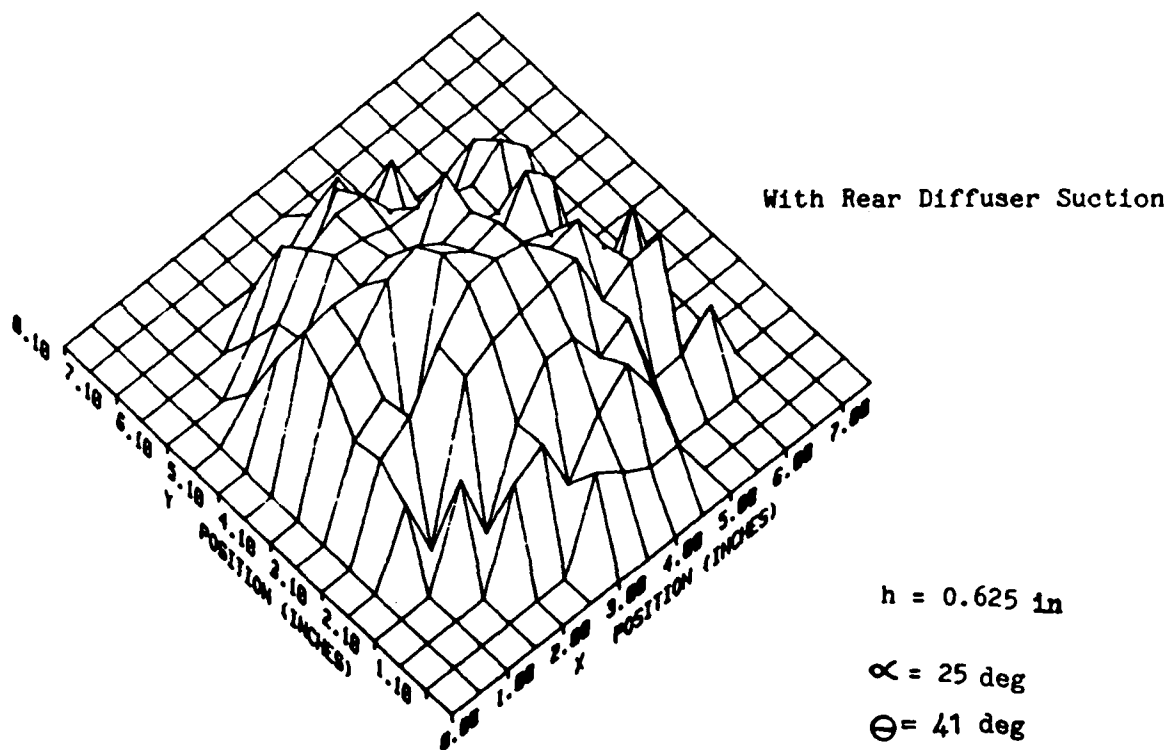
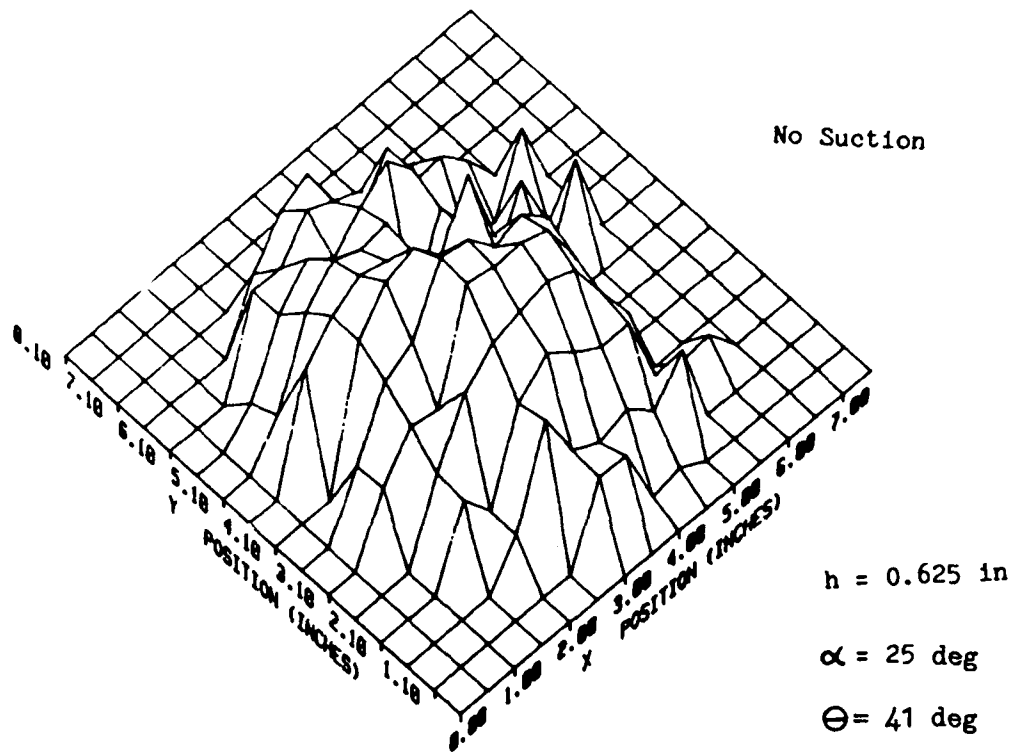


Figure 34. Effect of Rear Diffuser Suction on Three-Dimensional Exit Velocity (With Flow Separation)

flow in one sector of the exit plane was obtained.

Differences in the values of  $\phi$  without suction were observed during the front and rear diffuser suction experiments. The differences are attributed to the different levels of frictional losses caused by the use of tapes at two different locations on the diffuser wall during the experiments. For the rear suction tests, the front suction holes were taped over and vice versa. The results of the tests discussed above show the relative effects of diffuser suction on thrust augmentation.

The results of the tests show that the ejector diffuser area ratio chosen for this study did not cause an over expansion and normally provided a smooth attached flow at the diffuser for the range of injection angles that were tested. Thus, the decrease in thrust augmentation ratio at small injection angle increments above and below  $\alpha_p$  was not caused by severe diffuser stall but rather was the result of departures from the optimum combination of nozzle  $h$  and  $\alpha$  noted in the previous experiments, which relates to flow conditions at the inlet area. As a result, the use of boundary layer suction in the diffuser area was ineffective in maintaining a high  $\phi$  since severe flow separation has not yet propagated downstream to the diffuser as evidenced by the fully attached flows shown in Figures 32 and 33. The results of this tests suggest that a more effective method of controlling the sensitivity of  $\phi$  to small changes in  $\alpha$  and  $h$  in the vicinity of  $\alpha_p$  is to apply boundary layer control measures on the inlet surface near the primary nozzles in order to help maintain the smooth attached flow which is essential to the performance of this type of ejector. Only when a large separated region has propagated downstream to the diffuser area would diffuser suction be effective.

#### Effect of Diffuser Blowing.

For these tests, the flow rate for diffuser blowing was established

experimentally. Blowing pressure was fixed below the point where the blowing jets began to provide some measurable load cell thrust. At this point, the blowing flow rate measured was 53.3 in<sup>3</sup>/sec which was approximately 2% of the primary air flow rate.

Figure 35 shows the effect of blowing on thrust augmentation at three nozzle locations ( $\Theta = 30, 41$  and  $56$  deg). The values of  $\phi$  without blowing were generally lower than the baseline values presented in Figure 16. The decrease is attributed to higher friction losses due to increased roughness on the diffuser inner walls which resulted from the modifications necessary to install the blowing holes. Similar to the suction experiments, no substantial increase in thrust augmentation ratio was noted at all nozzle locations. At location 3, blowing resulted in a slight decrease in  $\phi$  at all injection angle settings. Figure 36 compares the velocity profiles with and without blowing at location 3 for  $\alpha = 44$  and  $46$  deg. No significant differences in the profiles were evident.

Similar to diffuser suction, diffuser blowing was also ineffective in preventing a decrease in thrust augmentation at small injection angle departures from  $\alpha_p$  since the diffuser was not over expanded. The decrease in thrust augmentation ratio was not the result of flow separation emanating from the diffuser area but rather by a departure from the best combination of nozzle  $\alpha$  and  $h$ . This method of preventing a decrease of thrust augmentation would be effective only when a condition of massive diffuser separation has occurred.

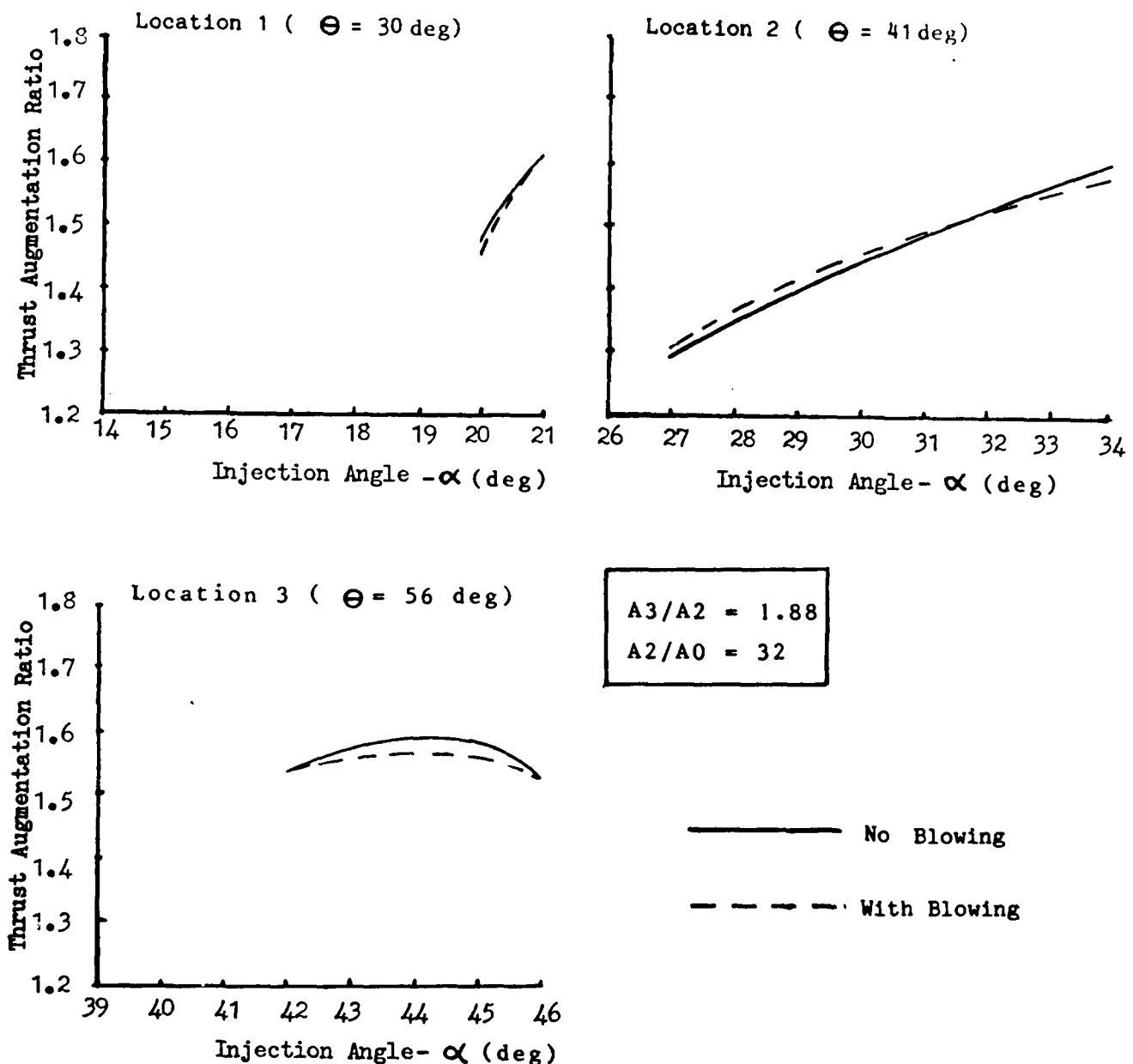


Figure 35. Effect of Diffuser Blowing on Thrust Augmentation

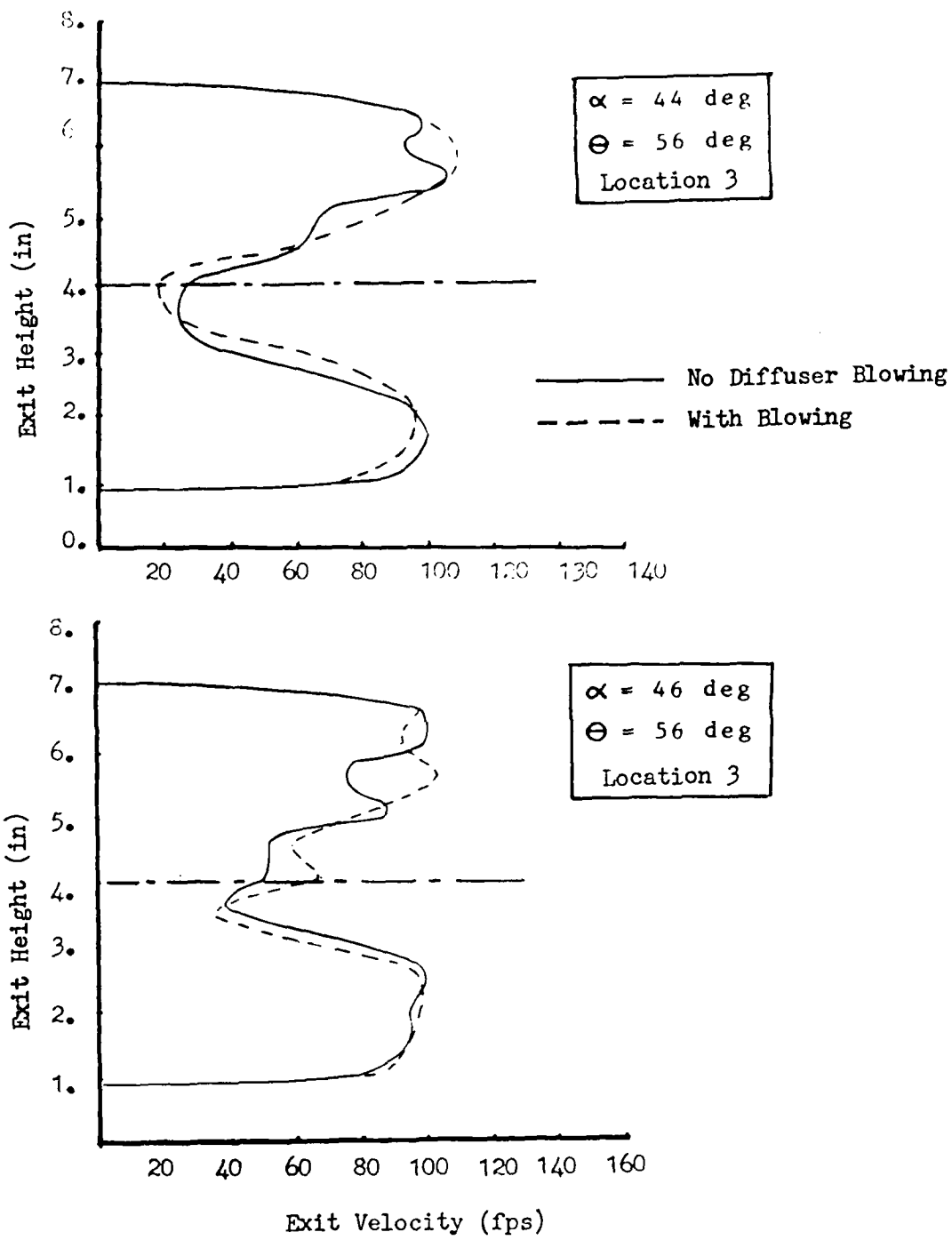


Figure 36. Effect of Diffuser Blowing on Exit Velocity Profiles

e. Effects of Inlet Cross Flow

In aircraft applications, cross flow in the inlet area may be introduced during the hovering mode with a slight forward velocity and with the ejector centerline pointed vertically downward. Also the presence of multiple propulsive units in close proximity and in ground effect could introduce recirculation and cross flow to the inlet of each individual unit. A look at the effect of a component of velocity perpendicular as well as inclined relative to the ejector centerline was made in this study.

For this test,  $\alpha$  was fixed at 32 deg,  $\Theta = 41$  deg and the nozzle heights were fixed at 0.25 in. Figure 37 shows the velocity distribution of the fan used in this experiment. The peak velocity measured using a total pressure probe was 23 fps which occurred at about 3 inches in front of the ejector inlet plane. This peak velocity was approximately 18 % of the peak velocity measured at the entrance to the ejector mixing chamber. Figure 38 shows the effect of the cross flow on thrust augmentation. An improvement in  $\phi$  was obtained in the presence of cross flow. The absolute value of  $\phi$  without the cross flow was higher than the value obtained under similar conditions in Figure 16. The difference is attributed to the presence of the fan in front of the ejector inlet plane which causes the ambient pressure in front of the inlet to be artificially lower than the surrounding area. A similar observation was reported in Ref 2. Figure 39 shows a comparison of the exit velocity profiles for the fan ON and fan OFF case. For the fan OFF case, the characteristic high wall velocities and the unmixed region near the center were present. In the fan ON case, the peak velocity on the lower wall shifted slightly towards the centerline resulting in a loss in symmetry. A reduction in the upper wall velocity also occurred, however, the low velocity unmixed region disappeared and no wall separation was evident. This is confirmed by the three dimensional exit velocity plot shown in Figure 40. A slight increase

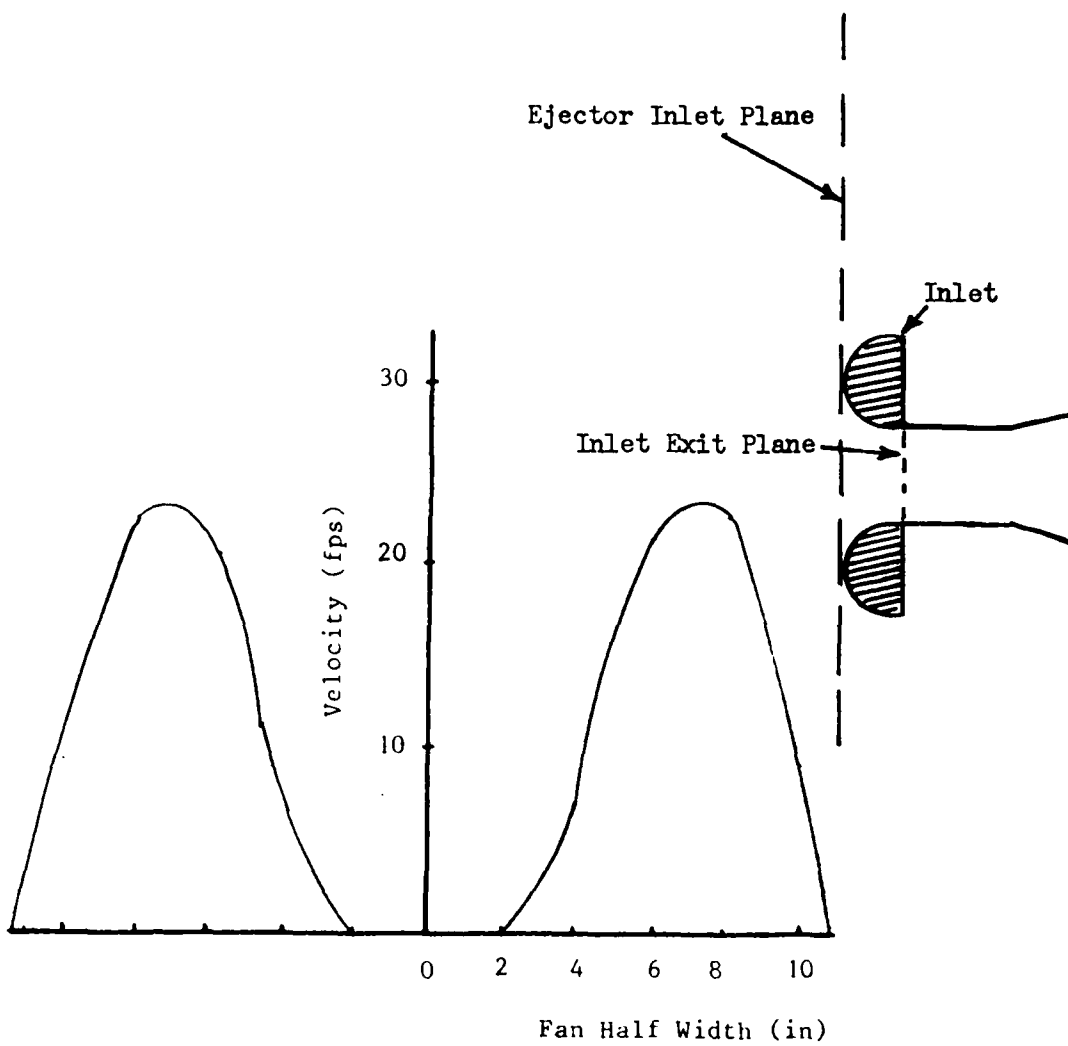


Figure 37 Cross Wind Velocity Profile

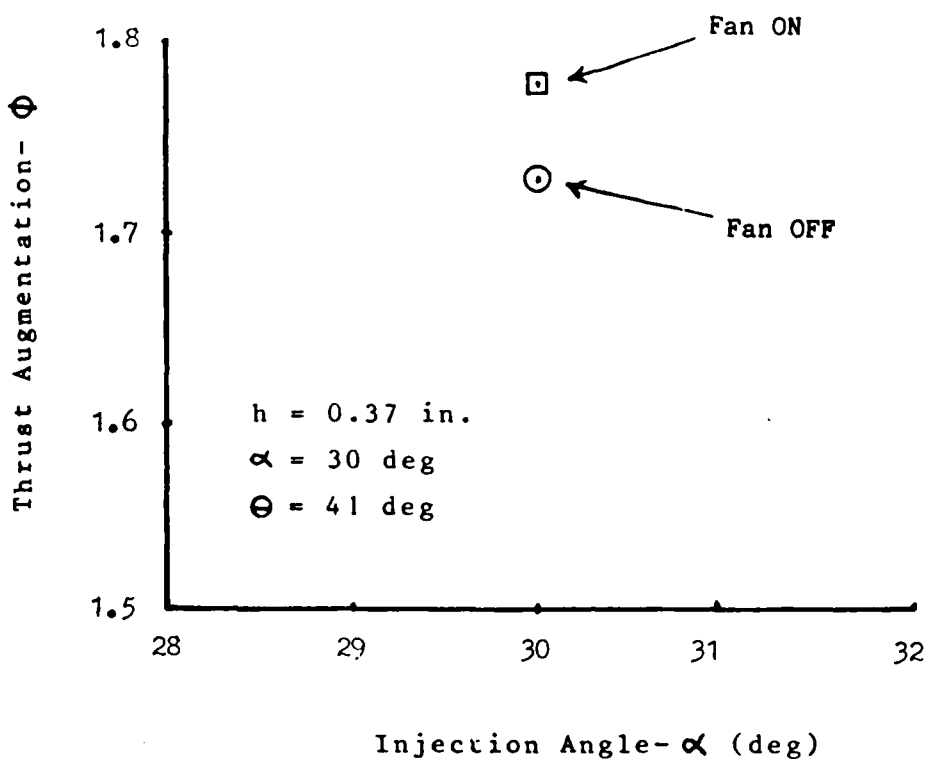


Figure 38. Cross Wind Effect on Thrust Augmentation

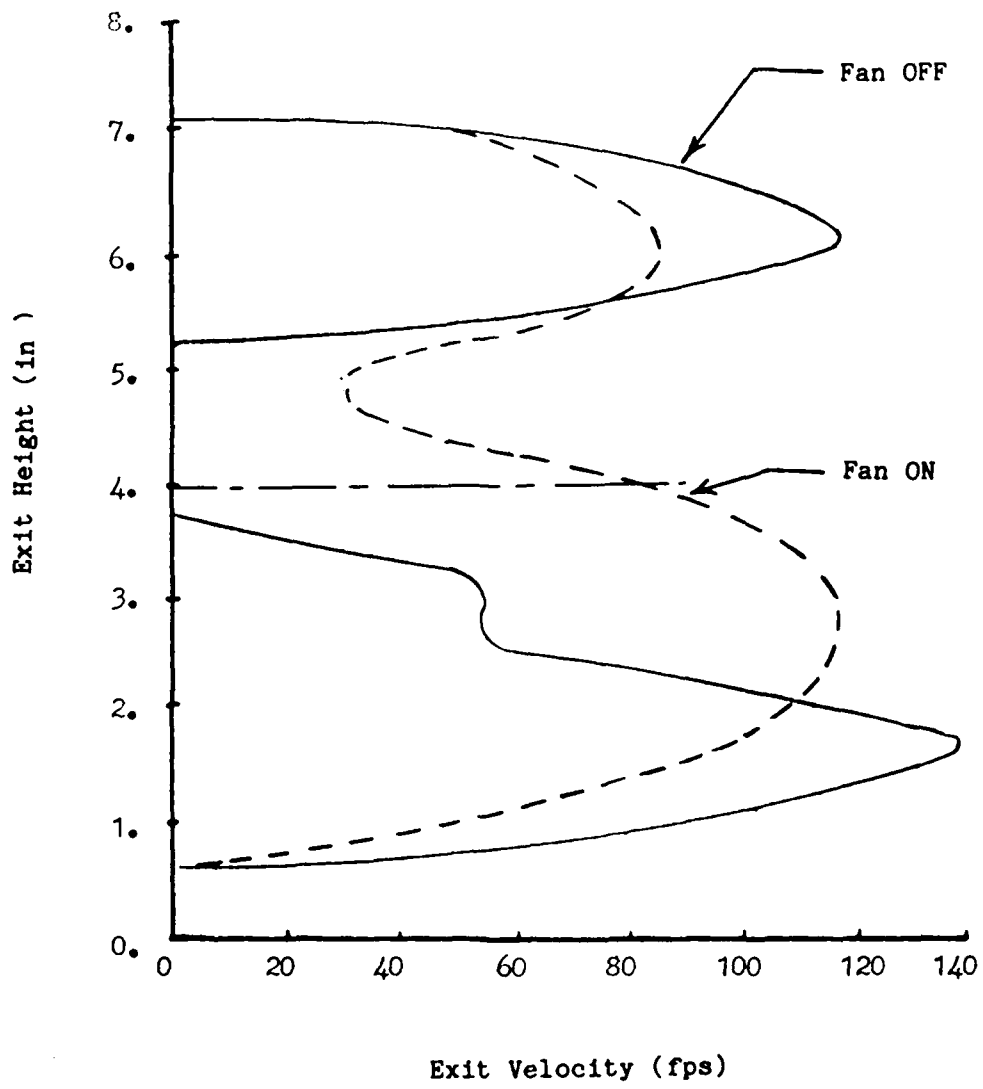


Figure 39. Cross Wind Effect on Exit Velocity Profile

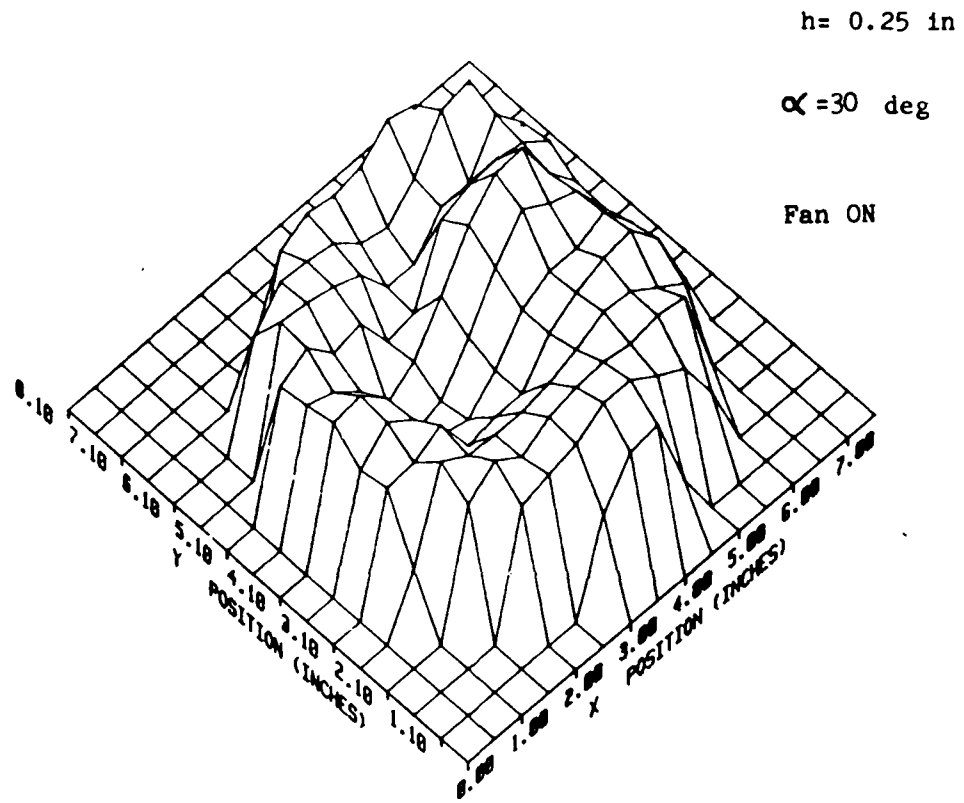


Figure 40. Three-Dimensional Plot of Exit Velocity with Cross Wind

in the peak velocity in one sector occurred while a smooth uniform velocity distribution was maintained around the remainder of the perimeter of the inlet.

Figure 41 shows a comparison of the velocity profiles measured at the entrance to the mixing chamber with and without cross flow. The profile for the fan ON case also exhibited asymmetry at this location.

The fan flow modified the direction of the inlet flow such that the velocity at the lower surface (windward) was increased while the velocity at the upper surface (leeward) was slightly retarded. This change may be the result of a shift in the local direction of the flow near the inlet area such that the direction in the windward side is more tangent to the inlet surface than on the leeward side.

The direction of the cross flow was modified using a deflector plate shown in Figure 42 to provide a direction other than normal to the ejector centerline. The plate span was 12.4 in and width was 6 in. The result is shown in Figure 43. The gain in thrust augmentation ratio due to cross flow gradually diminished as the plate deflection angle,  $\psi$ , was increased from 0 up to 45 deg. Above 45 deg, a crossover occurred and at 90 deg, thrust augmentation ratio was degraded considerably. In general, for the fan OFF case, the presence of the deflector plate reduced the thrust augmentation relative to the configuration without the plate. At  $\psi$  = 0 deg, when the plate is parallel to the centerline, only a slight decrease in  $\Phi$  relative to the no plate configuration occurred. At  $\psi$  = 90 deg, the loss in  $\Phi$  was considerable. The decrease in  $\Phi$  in the presence of the plate was caused by frictional losses which increased as the deflection angle increased up to a maximum of 90 deg. Figures 44A to 44C show a comparison of the velocity profiles with and without crossflow for  $\psi$  = 0, 45 and 90 deg at the diffuser exit plane and the entrance to the mixing chamber. At  $\psi$  = 0 deg, again

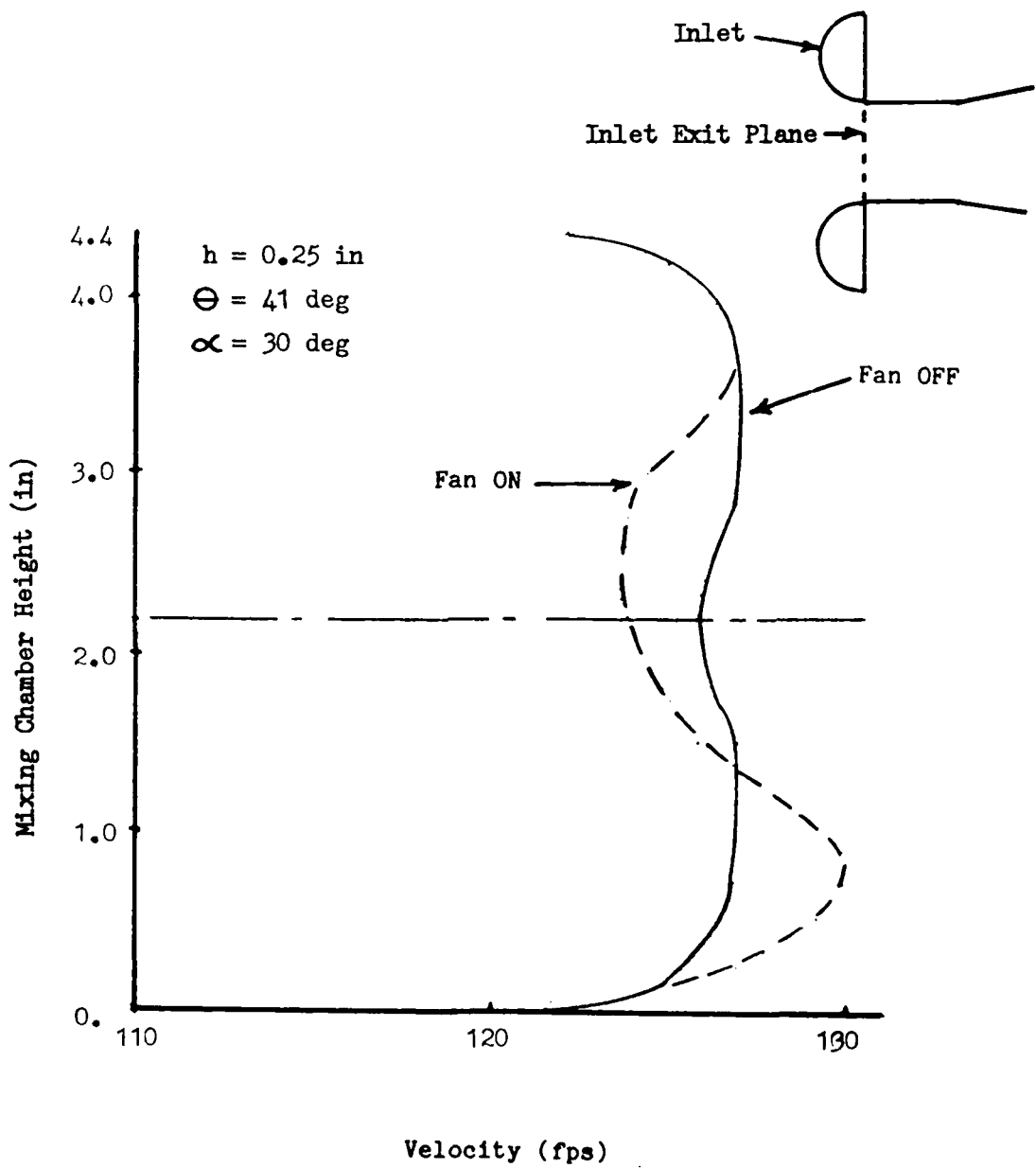


Figure 41. Velocity Profiles at the Inlet Exit Plane

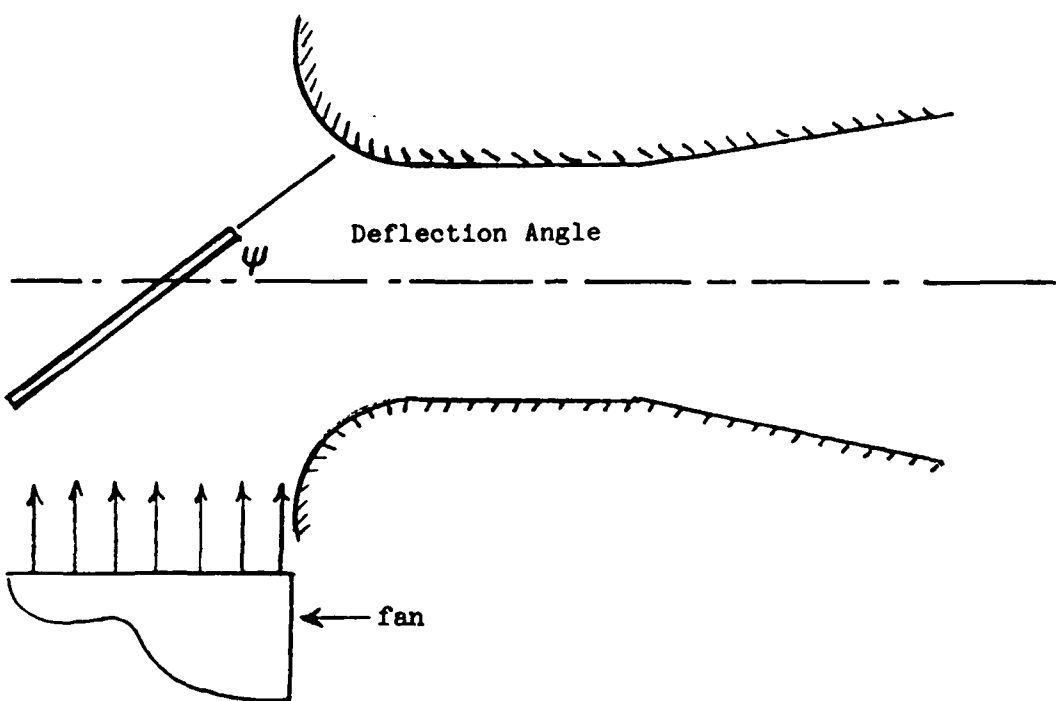


Figure 42. Inlet Flow Deflector Plate

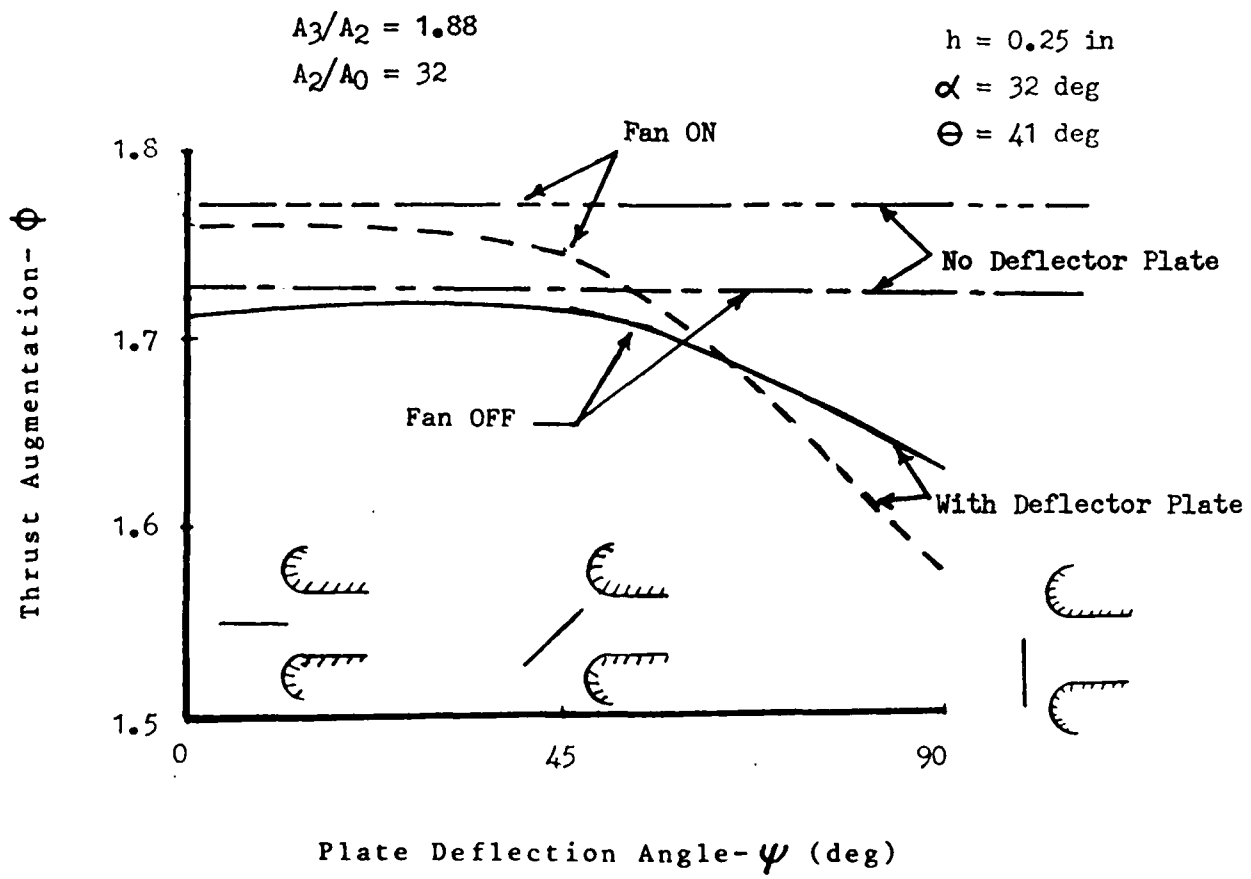
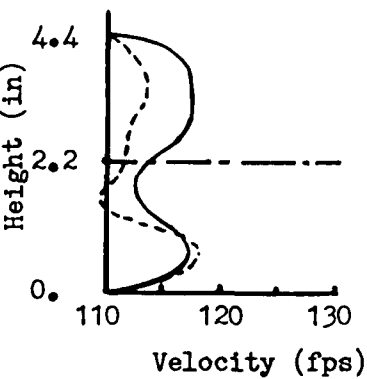
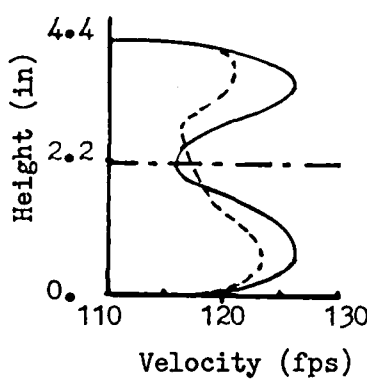
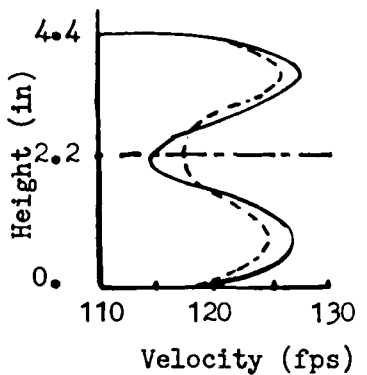
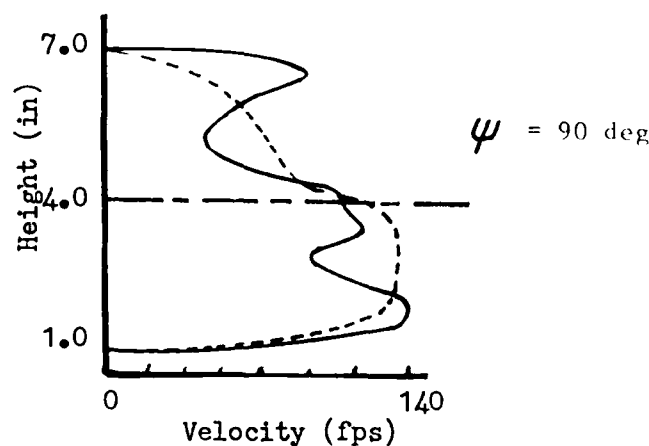
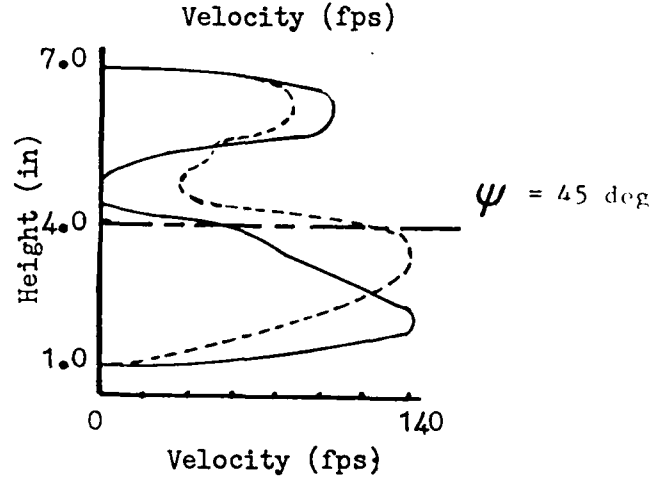
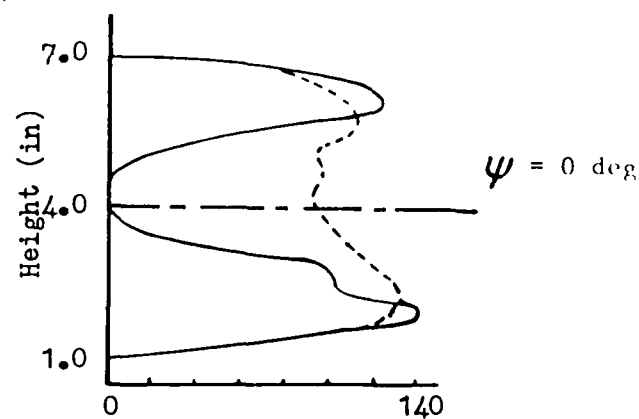


Figure 43. Effect of Deflector Plate Angle on Thrust Augmentation

Inlet Exit Plane  
(Entrance to Mixing Chamber)



Diffuser Exit Plane



$\alpha = 32$ deg
$\Theta = 41$ deg
$A_3/A_2 = 1.88$
$A_2/A_0 = 32$

— Fan OFF  
- - - - Fan ON

Figure 44. Effect of Deflector Plate on Exit Velocity Profiles

the profiles without cross flow were symmetric while those with cross flow had a slight asymmetry with the lower walls having slightly higher peaks than the upper walls. Mixing was greatly improved with cross flow and no separation was present. At  $\psi = 45$  deg, the asymmetry for the fan ON case increased but mixing again improved at both ejector stations. At  $\psi = 90$  deg, the fan ON case has lost all symmetry, the velocity at the mixing chamber entrance showed increased retardation on the upper lip and the exit velocity profile exhibited some separation on the leeward side.

It appears that as the deflection plate angle was increased in the presence of cross flow, the velocity on the inlet upper lip progressively decreased until it lost sufficient momentum which resulted in localized separation at the diffuser exit.

The results of this tests showed that a small amount of crosswind benefitted thrust augmentation by altering the inlet flow field and providing a favorable velocity direction on the windward section of the inlet surface which enhanced flow attachment and improved mixing. Also, the fan forced an increase in the mass flow rate of the secondary air flowing into the ejector thereby increasing the the mass and thrust augmentation. With the use of a deflector plate, this benefit diminished or was totally lost due to higher drag losses caused by the presence of the plate and due to velocity retardation which occurred at the leeward side of the inlet surface which caused separation to occur downstream at the diffuser.

f. Effect of Pt/Pa on Thrust Augmentation

Figure 45 shows the behavior of  $\phi$  with Pt/Pa at various nozzle locations at a height of 0.25 in. The change in thrust augmentation ratio was not the same for all locations for Pt/Pa over the range from 1.01 to 1.14. At  $\Theta = 30$  and 41 deg, decreasing Pt/Pa also caused the augmentation ratio to decrease whereas at  $\Theta = 56$  deg, the opposite trend was true. A comparison of the exit velocity profiles at 2 locations at Pt/Pa = 1.027 and h = 0.25 in is shown in Figure 46. The calculated primary nozzle exit velocity at this pressure ratio was approximately 217 fps. As  $\Theta$  increased, a slight increase in mixing occurred as shown by a decrease in the size of the unmixed region at the center of the profiles. This is confirmed in Figure 47 which shows the mass augmentation ratio for the three nozzle locations. Figure 48 compares the three-dimensional exit velocity plots for  $\Theta = 41$  and 56 deg at Pt/Pa = 1.027 and h = 0.25 in. Both plots show a smooth uniform flow around the exit perimeter with the area of the low velocity region for  $\Theta = 56$  deg being smaller than that for  $\Theta = 41$  deg.

The increase in thrust augmentation ratio at the low primary pressure to ambient pressure ratios is attributed to the lower nozzle exit velocities which allows the flow to remain attached over the curved inlet surface area at higher values of  $\Theta$ . The result is an increase in the effective mixing chamber length as the nozzle location is moved further out along the inlet surface thereby allowing a more thorough mixing of the primary and secondary flows before reaching the diffuser exit plane. The result is a higher thrust augmentation ratio.

Location	Sym	$\Theta$ (deg)	$\alpha$ (deg)
1	$\Delta$	30	20
2	$\circ$	41	32
3	$\square$	56	45

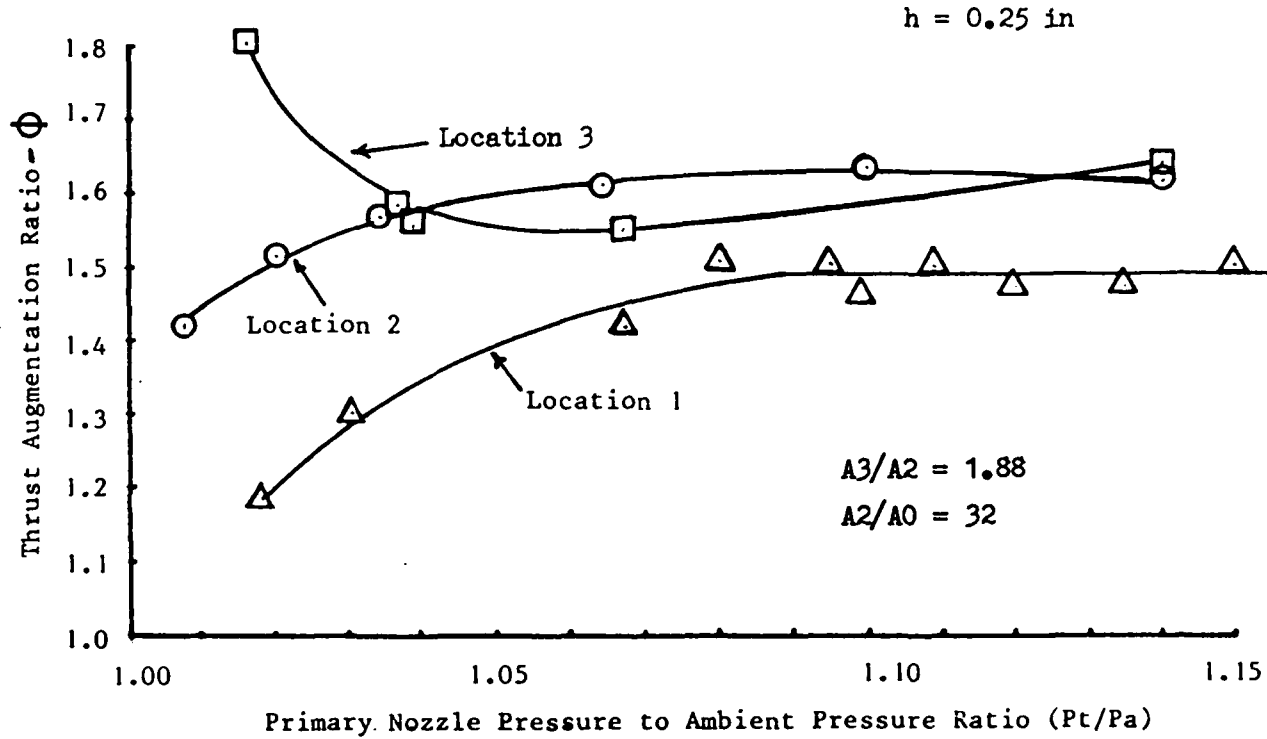


Figure 45. Effect of  $P_t/P_a$  on Thrust Augmentation Ratio ( $h = 0.25 \text{ in}$ )

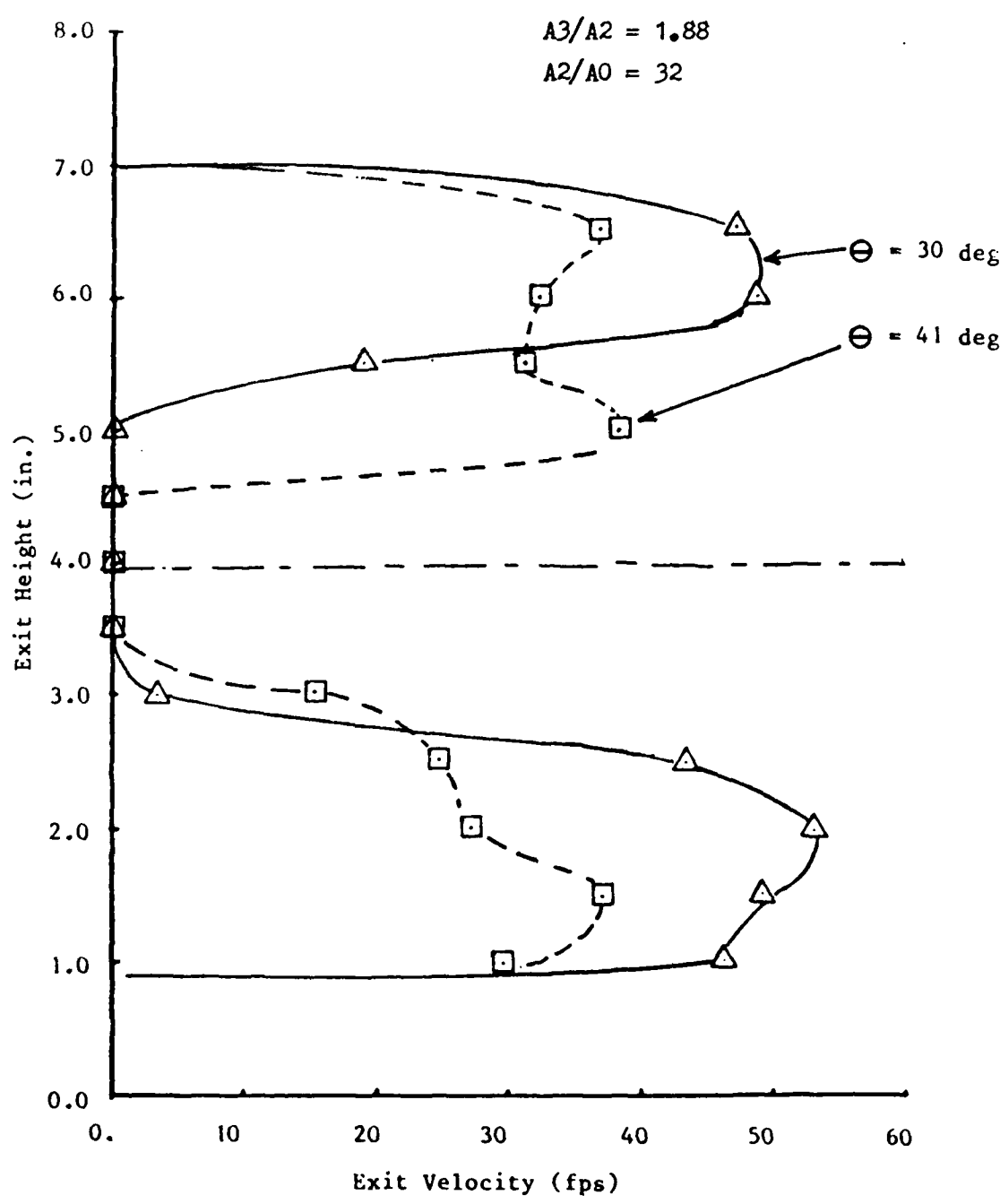


Figure 46. Effect of Nozzle Location on Exit Velocity Profile ( $P_t/P_a = 1.027$ )

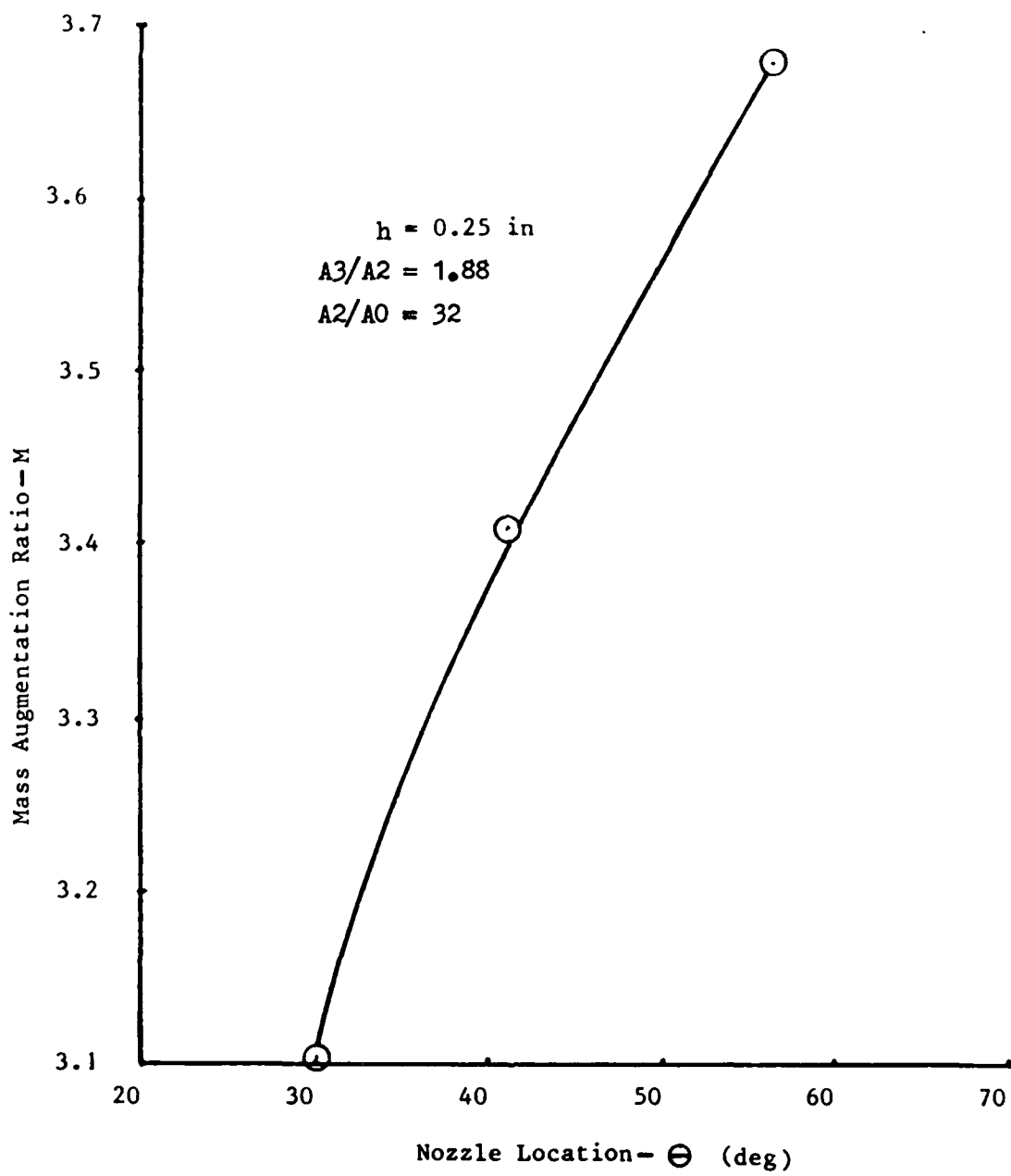


Figure 47. Effect of Nozzle Location on Mass Augmentation Ratio ( $P_t/P_a = 1.027$ )

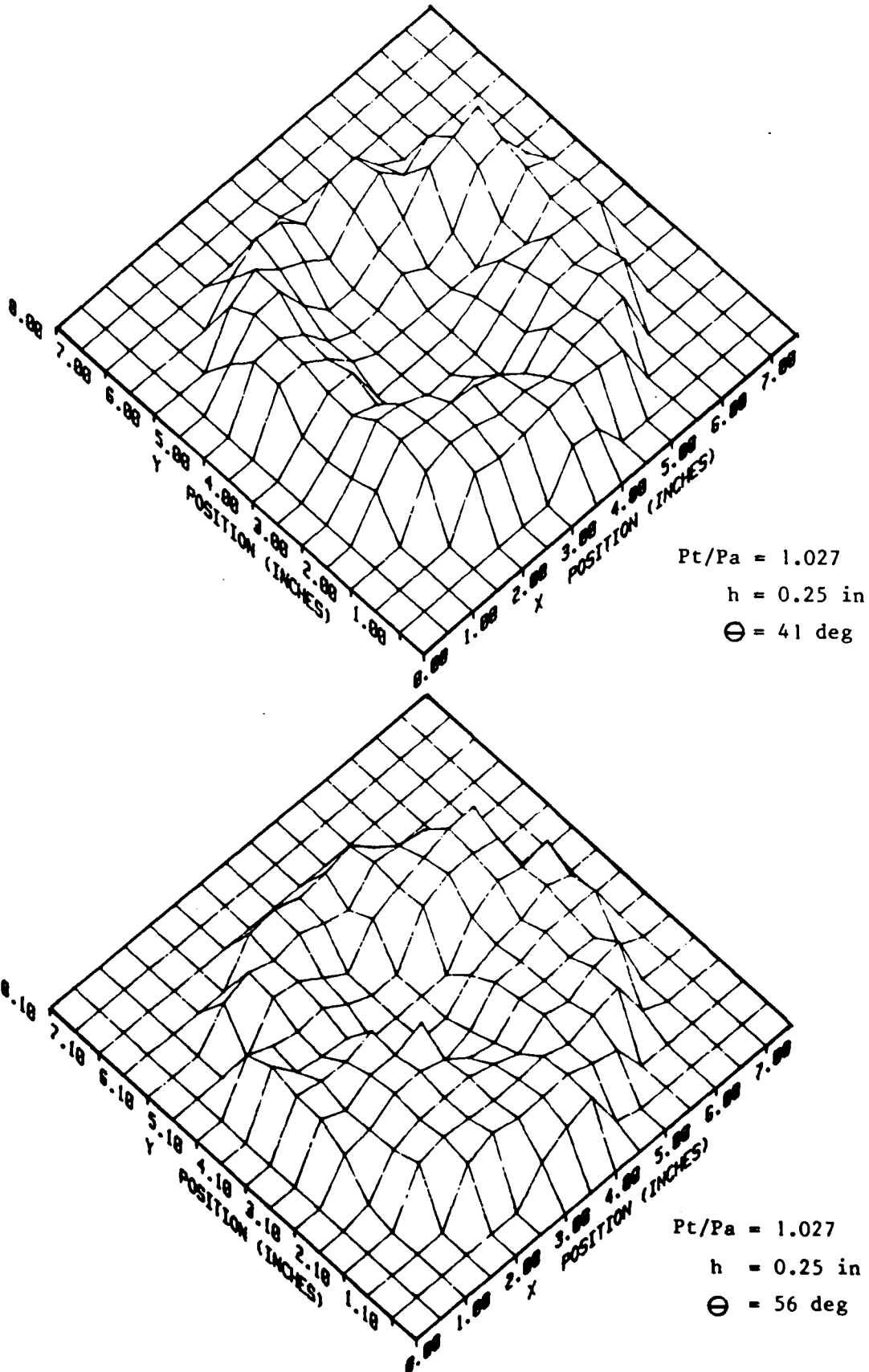


Figure 48. Effect of Nozzle Location on Three-Dimensional Exit Velocity  
 $(Pt/Pa = 1.027)$

## VI. CONCLUSIONS

Based on the results of this study, the following conclusions are made:

1. The maximum thrust augmentation ratio of the 4.4 in diameter circular ejector is critically dependent upon both the primary nozzle injection angle and height. An optimum combination of  $\alpha$  and  $h$  exists that provides the highest thrust augmentation ratio which represents the best compromise between exit flow uniformity and diffuser wall separation.

2. The use of alternating injection angles to create a mixing pattern to increase the maximum thrust augmentation is inferior to the uniform injection pattern for a wall blowing ejector. With an alternating pattern, jet interference with the wall results in incomplete mixing and prevents the formation of a uniform attached flow on the inlet and mixing chamber walls which is essential to the formation of a favorable wall pressure distribution necessary for thrust augmentation.

3. Diffuser blowing and suction are ineffective in preventing a decrease in thrust augmentation ratio at small injection angles above and below the  $\alpha$  where maximum thrust augmentation ratio occurs. The mechanism for the degradation of  $\Phi$  in this region is the departure from the optimum combination of injection angle and height and not due to a strong diffuser separation.

4. A low cross flow velocity component at the inlet will increase thrust augmentation due to an increase in the secondary mass flow rate and an improvement in the mixing. With cross flow, the uniformity of the velocity profile at the exit plane improves without diffuser separation. The use of a deflector plate to modify the direction of the cross flow relative to the ejector centerline does not provide any improvement in thrust augmentation relative to the configuration without the plate. The plate introduces drag losses and cause velocity retardation on the leeward side of the inlet surface

which can induce flow separation in the diffuser area.

5. At low primary nozzle pressure to ambient pressure ratios, thrust augmentation increases with nozzle location. The low primary nozzle exit velocities at low  $P_t/P_a$  values allow the flow to turn and remain attached to the curved inlet surface at higher values of  $\Theta$ . A higher  $\Theta$  increases the effective mixing chamber length of the ejector which then allows a more thorough mixing, resulting in a more uniform exit velocity and higher thrust augmentation ratio.

## VII. RECOMMENDATIONS

The following areas should be further investigated to continue the optimization and development of the design data base for thrust augmenting ejectors:

1. A study should be conducted to determine the effectiveness of blowing and suction applied on the inlet area in maintaining high thrust augmentation.
2. The cross flow study should be expanded to determine the sensitivity of both circular and rectangular ejectors to various levels of crosswinds.
3. A study should be conducted to determine the changes in thrust augmentation due to ground effects or the close proximity of other ejector units as in the case of multiple propulsive systems.
4. The effectiveness of aerodynamic fairings in reducing primary nozzle drag should be examined.
5. The use of a hypermixing pattern, introduced aft of the inlet area to circumvent the loss of a smooth attached flow on the inlet area should be studied.

## VIII. BIBLIOGRAPHY

1. Lewis, William D. An Experimental Study of Thrust Augmenting Ejectors, AFIT Thesis, 1983.
2. Reznick, Steven G. An Experimental Study of Circular and Rectangular Thrust Augmenting Ejectors, AFIT Thesis, 1980.
3. Unnever, G. An Experimental Study of Rectangular and Circular Thrust Augmenting Ejectors, AFIT Thesis, 1981.
4. Von Karman, T. "Theoretical Remarks on Thrust Augmentation", Contributions to Applied Mechanics, Reissner Anniversary Volume, Ann Arbor, Michigan, 1949, pp 461-468.
5. Alperin, M. and Wu, J.J. "High Speed Ejectors", Flight Dynamics Research Corporation, AFFDL-TR-79-3048, May 1979.
6. Bevilaqua, P.M. "An Evaluation of Hypermixing for Thrust Augmenting Ejectors", Journal of Aircraft, Vol 11, No. 6, June 1974, pp. 348-354.
7. Jane's All The World's Aircraft, 1983-1984.
8. Alperin, M. and Wu, J.J. "The Alperin Jet Diffuser Development, Testing and Performance Verification Report", Naval Weapons Center, California, NWL TP 5863, 1976.
9. Bean, Howard S. Fluid Meters, Their Theory and Application (Sixth Edition). New York: ASME, 1971.
10. Reznick, S.G. and Franke, M.E. "Inlet and Diffuser Effects on the Thrust Augmentation of Circular and Rectangular Ejectors", AIAA Paper 81-1680, 1981.
11. Franke, M.E. and Unnever, G.E. "Performance Characteristics of Rectangular and Circular Thrust Augmenting Ejectors", AIAA Paper 85-1344, AIAA/SAE/ASME/ASEE Joint Propulsion Conference, Monterey, California, July 1985

## IX. APPENDIX

### 1. Procedures for Varying Injection Angle or Height.

The templates used to independently vary the nozzle  $h$  and  $\alpha$  are shown in Figures 10 and 11. The procedures used to independently vary these two parameters are discussed in the following paragraphs.

#### a. Procedure for Varying Nozzle $h$ at a Fixed Value of $\alpha$ .

Figure 10 shows the template when used to vary  $h$  at a fixed value of  $\alpha$  for a given nozzle location. The template edge along a constant  $\Theta$  line was marked at 0.125 in increments. The constant  $\alpha$  lines (parallel lines) were scribed on the template starting along the constant  $\Theta$  edge. To set the nozzles to the desired value of  $h$ , a straight edge was taped on the template, coincident with a constant  $\alpha$  line which was 0.125 in higher than the line with the desired value of  $h$ . The straight edge was used as a guide to set the primary nozzle flat upper surface approximately parallel with the constant  $\alpha$  lines. This is illustrated in Figure A-1. The primary nozzle thickness was 0.125 inch which placed the nozzle chin to the desired value of  $h$ .

#### b. Procedure for Varying Nozzle $\alpha$ at a Fixed Value of $h$ .

The same templates used in the constant  $\alpha$ -variable  $h$  experiments were used in the constant  $h$ -variable  $\alpha$  experiments. As shown in Figure 11, at a given nozzle location and a fixed value of  $h$ , radial lines corresponding to different values of  $\alpha$  were scribed on the template. The radial lines were used as guides to set the nozzle injection angles using a straight edge in a manner similar to the constant  $\alpha$ -variable  $h$  experiments. The origin of the radial lines was located at a value of  $h$  which was 0.125 in higher than the desired value of  $h$  as shown in Figure A-2, in order to allow for the thickness of the nozzle which was 0.125 in.

### 2. Diffuser Modifications for the Boundary Layer Control Experiments.

For the boundary layer control experiments, the diffuser was provided

with two plenum chambers. The chambers were installed aft of the front flanges of each diffuser section and extended 1.75 in rearwards from the flanges. Each chamber was provided with two 0.375 in diameter copper tubing supply ports located 180 degrees apart in the three and nine o'clock positions. The chamber dimensions were selected to provide the maximum possible volume within the constraints imposed by the existing section mating flanges. Perforated sheet metal diffuser plates were installed in the plenum chambers beneath the supply ports in order to distribute the supply air evenly around the perimeter of the plenum chambers.

On the inner diffuser walls, beneath the plenum chambers, two sets of suction holes were initially installed for the suction experiments. The holes were drilled circumferentially around the walls. Both sets of holes were located 0.25 in aft of the diffuser section flange mating surfaces. The front hole diameters were 0.125 in and were spaced at 0.375 in intervals while the rear hole diameters were 0.125 in and were spaced at 0.25 in intervals. The diameters and spacing were selected to provide the highest number of holes possible without weakening the diffuser wall structure.

In order to fabricate blowing holes with the air jets as close a tangent to the wall as possible, 0.125 in diameter holes were first drilled on the inner wall with the hole centerlines being parallel with the ejector centerline. The resulting area of each hole when projected perpendicular to the diffuser wall was elliptical in shape and appeared excessive. In order to reduce the normal area and to minimize the component of the jet efflux perpendicular to the ejector wall, tape was used to partially cover the elliptical areas. The resulting blowing area, when projected on a plane perpendicular to the ejector centerline was semi-circular in shape. This modification is shown in Figure 15.

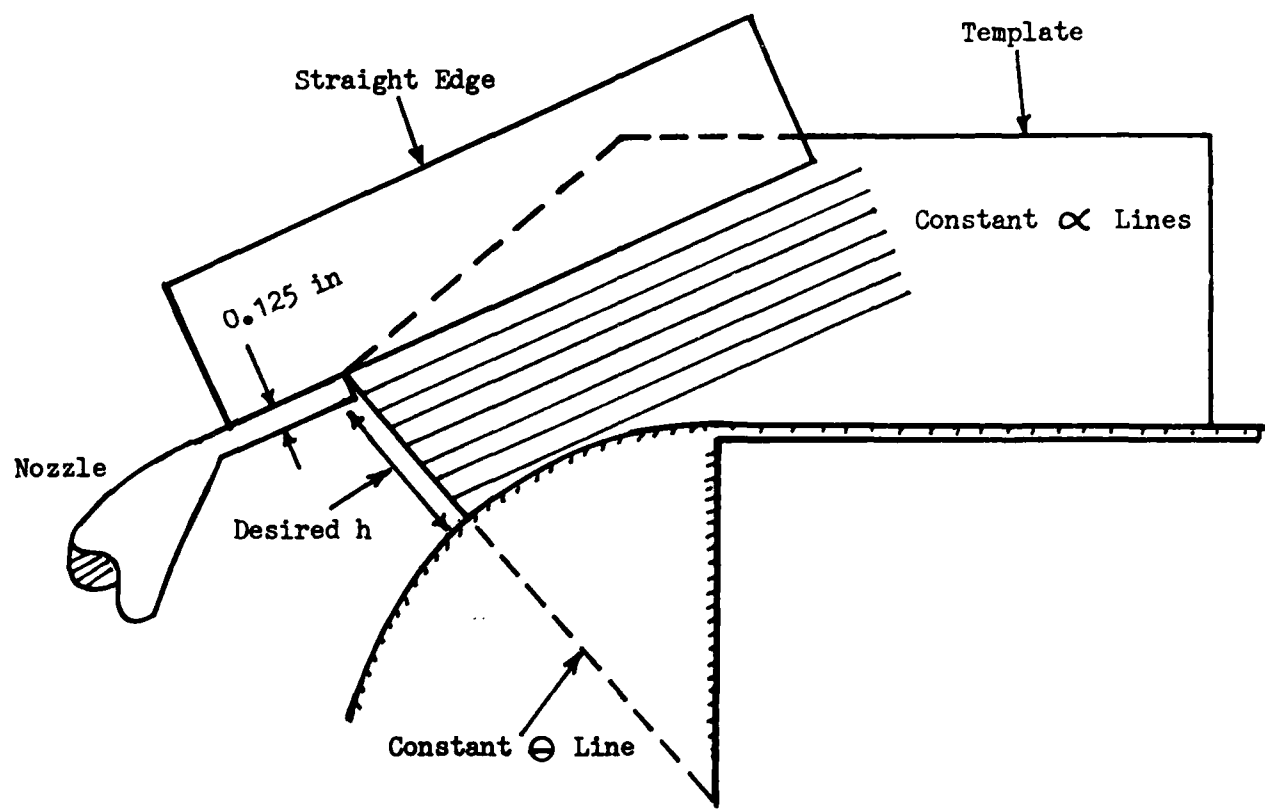


Figure A-1. Procedure for Varying Nozzle  $h$  at a Fixed Value of  $\alpha$ .

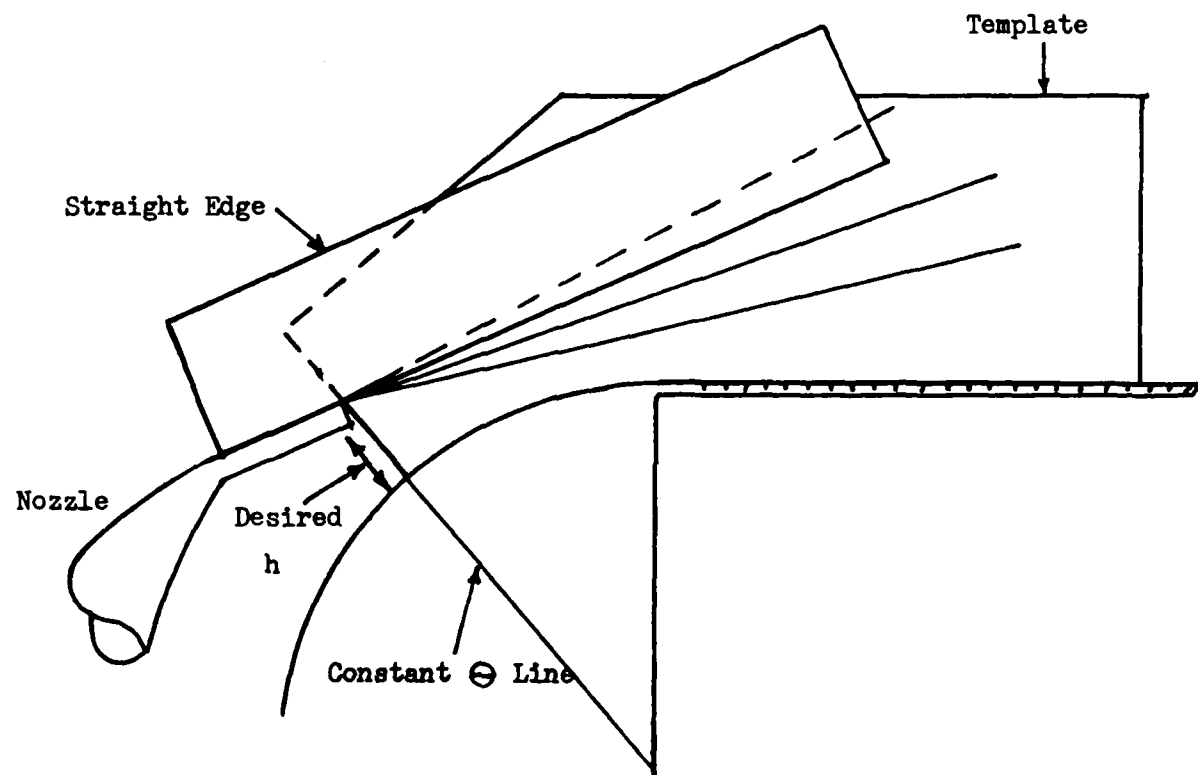


Figure A-2. Procedure for Varying Nozzle  $\alpha$  at a Fixed Value of  $h$ .

VITA

Captain Generoso C. Uhuad [REDACTED]

[REDACTED]. After graduating from [REDACTED], [REDACTED] in 1967, he attended FEATI University, Manila, graduating with a B.S. in Aeronautical Engineering in 1971. He enlisted in the USAF in 1972 and was assigned to the Ground Radio Communications School, Keesler AFB, Biloxi, Mississippi. Following completion of radio maintenance training, he was stationed at the 766 Radar Squadron, Caswell Air Force Station, Limestone, Maine. In January 1976, he was reassigned to the 503 Medium Bombardment Wing/1916 Communications Squadron, Pease Air Force Base, New Hampshire. In February 1977, he attended the Air Force Officer Training School, Lackland AFB, Texas and received his commission as a Second Lieutenant in May 1977. He was then assigned to the Air Force Flight Dynamics Laboratory, W-PAFB, Ohio where he served as a development engineer and aerodynamicist for the X-29 Forward Swept Wing program. In October 1982, he was assigned to the Propulsion SPO/Aeronautical Systems Division, W-PAFB, where he served as a project engineer for the T-56 Engine Model Derivative Program, Integrated Turbine Engine Monitoring System and Product Verification testing of the F110 engine. He is currently serving as a propulsion engineer supporting the F-15 STOL Demonstrator Aircraft program.

Permanent Address: [REDACTED]  
[REDACTED]

UNCLASSIFIED

SECURITY CLASSIFICATION OF THIS PAGE

A1723%

## REPORT DOCUMENTATION PAGE

1a. REPORT SECURITY CLASSIFICATION UNCLASSIFIED		1b. RESTRICTIVE MARKINGS	
2a. SECURITY CLASSIFICATION AUTHORITY		3. DISTRIBUTION/AVAILABILITY OF REPORT Approved for public release; distribution unlimited	
2b. DECLASSIFICATION/DOWNGRADING SCHEDULE			
4 PERFORMING ORGANIZATION REPORT NUMBER(S) AFIT/GAE/AA/86M-3		5. MONITORING ORGANIZATION REPORT NUMBER(S)	
6a. NAME OF PERFORMING ORGANIZATION School of Engineering	6b. OFFICE SYMBOL (If applicable) AFIT/EN	7a. NAME OF MONITORING ORGANIZATION	
6c. ADDRESS (City, State and ZIP Code) Air Force Institute of Technology Wright-Patterson AFB, Ohio 45433		7b. ADDRESS (City, State and ZIP Code)	
8a. NAME OF FUNDING/SPONSORING ORGANIZATION	8b. OFFICE SYMBOL (If applicable)	9. PROCUREMENT INSTRUMENT IDENTIFICATION NUMBER	
8c. ADDRESS (City, State and ZIP Code)		10. SOURCE OF FUNDING NOS.	
		PROGRAM ELEMENT NO.	PROJECT NO.
11. TITLE (Include Security Classification) See Block 19		TASK NO.	
		WORK UNIT NO.	
12. PERSONAL AUTHOR(S) Generoso C. Uhuad, B.S., CPT, USAF		13a. TYPE OF REPORT MS Thesis	
		13b. TIME COVERED FROM 85 Jan 2 TO 85 Dec 6	14. DATE OF REPORT (Yr., Mo., Day) 1985 December
16. SUPPLEMENTARY NOTATION		15 PAGE COUNT 101	
17. COSATI CODES		18. SUBJECT TERMS (Continue on reverse if necessary and identify by block number) Ejector Thrust Augmentation V/STOL Mass Flow Augmentation	
19. ABSTRACT (Continue on reverse if necessary and identify by block number)  Title: An Experimental Investigation of a Circular Thrust Augmenting Ejector  Thesis Advisor: Milton E. Franke, PhD  A 4.4 in diameter circular ejector was tested to determine the effect on thrust augmentation ratio of the primary nozzle height and injection angle. Also tested were the effects of alternating primary nozzle injection angles, diffuser blowing and suction, inlet cross flow and low primary nozzle exit velocities on thrust augmentation. The results showed that both the primary nozzle injection angle and height affect the maximum thrust augmentation ratio attainable. A small amount of cross flow at the inlet increased the maximum thrust augmentation. The alternating primary nozzle injection angle arrangement did not increase the maximum thrust augmentation above that which was obtained using uniform primary nozzle injection angles. Diffuser blowing or suction did			
20. DISTRIBUTION/AVAILABILITY OF ABSTRACT UNCLASSIFIED/UNLIMITED <input checked="" type="checkbox"/> SAME AS RPT. <input type="checkbox"/> DTIC USERS <input type="checkbox"/>		21. ABSTRACT SECURITY CLASSIFICATION UNCLASSIFIED	
22a. NAME OF RESPONSIBLE INDIVIDUAL Milton E. Franke, PhD		22b. TELEPHONE NUMBER (Include Area Code) 513-255-2362	22c. OFFICE SYMBOL AFIT/EN

UNCLASSIFIED

SECURITY CLASSIFICATION OF THIS PAGE

Block #19

not provide an improvement in the maximum thrust augmentation above that which was obtained without diffuser boundary layer control. Finally, at low primary nozzle exit velocities, thrust augmentation increase as the nozzles were moved out along the inlet surface. The increase in thrust augmentation is attributed to the ability of the flow to remain attached to the inlet surface at low primary nozzle exit velocities thereby increasing the ejector effective mixing chamber length.

UNCLASSIFIED

SECURITY CLASSIFICATION OF THIS PAGE